Three Essays on Equity, Volatility and Commodity Derivatives

Yahua Xu

A thesis presented for the degree of
Doctor of Philosophy

Auckland University of Technology
Department of Finance
Faculty of Business and Law
New Zealand

December, 2016

Abstract

The options market is one of the most important derivatives markets. It plays a significant role in risk management. The importance of the options market is essentially due to the fact that an option is a financial contract that gives its holder the right, but not the obligation, to buy or sell another asset, called the underlying, at a specified price over a specific time. The underlying asset can be any financial product. The variety of options is wide, some of them can have a very complicated structure, creating a real challenge for academics and practitioners. This thesis focuses on three types of options which differ in terms of underlying assets. It will consider options written on equity and volatility Leverage Exchange Traded Funds (LETFs), options written on the VIX index and options written on USO (an ETF related to crude oil).

The first essay contributes to the understanding of the pricing of options written on a set of LETFs which track the same index. A parametric perspective is used which employs a stochastic volatility framework for the dynamics of the underlying LETFs, each one having a specific leverage ratio. Closed-form pricing formulas are obtained by adopting a Fast Fourier Transform (FFT) approach. Jump risk is also incorporated into the volatility model and a sensitivity analysis of prices is carried out. As all the LETFs track the same underlying index, the option pricing framework developed is therefore consistent.

The second essay analyzes the higher-order moment risk premiums of the volatility market by utilizing VIX options that are the most liquid volatility derivatives. Both variance and skew risk premiums are considered and a nonparametric point of view is

adopted. This essay is the first study to discuss higher-order moment risk premiums for volatility market. The empirical findings underline the specifics of the volatility market and novel results are provided.

The third essay extends the study of higher-order moment risk premiums to the crude oil market by considering USO options. There are several contributions in this essay. Firstly, it is the first study to analyze higher-order moment risk premiums of the crude oil market as both variance and skew risk premiums are incorporated. Secondly, the risk premiums are decomposed, conditional on the direction of market movements, to take into account the assumption that the upward and downward market fluctuations carry asymmetric information. The empirical results suggest that, compared to their undecomposed counterparts, the decomposed risk premiums are more informative in predicting future market returns. The decomposition of the risk premiums is proved to be essential in obtaining significant results and as the third order moment (i.e. the skew) is also considered this work constitutes a general and important contribution to the financial commodity literature.

Contents

List of Figures

List of Tables

List of Abbreviations

CBOE Chicago Board Options Exchange

NYMEX New York Mercantile Exchange

ATM At the Money

ITM In the Money

OTM Out of the Money

ETFs Exchange Traded Funds

LETFs Leveraged Exchange Traded Funds

ETNs Exchange Traded Notes

VIX CBOE Volatility Index

VXX iPath S&P 500 VIX Short Term Futures ETN

SVJ Stochastic Volatility with Jumps in Price

SVCJ Stochastic Volatility with Contemporaneous Jumps in Price and Volatility

LRSV Logarithmic Model with Stochastic Volatility

SPX S&P 500 Index

SPXU Proshares UltraPro Short S&P 500 ETF

SDS Proshares UltraShort S&P 500 ETF

SH	Proshares Short S&P 500 ETF
SPY	SPDR S&P 500 ETF
SSO	Proshares Ultra S&P 500 ETF
UPRO	Proshares UltraPro S&P 500 ETF
SVXY	Proshares Short VIX Short-Term Futures ETF
VIXY	Proshares VIX Short-Term Futures ETF
UVXY	Proshares Ultra VIX Short-Term Futures ETF
FFT	Fast Fourier Transform
SDEs	Stochastic Differential Equations
TRTH	Thomson Reuters Ticker History
CAPM	Capital Asset Pricing Model
USO	United States Oil Fund

List of Symbols

s_t Time-t Price of an Equity ETF

ω Brownian Motion

Q Risk-neutral Probability Measure

P Physical Probability Measure

l_t Time-t Price of an Equity LETF

V_t Time-t Price of an Unleveraged Volatility ETF

x_t Time-t Price of a Volatility LETF

$c(t, l_0, v_0)$ Time-t Price of A European Call Option on an Equity LETF

$p(t, l_0, v_0)$ Time-t Price of A European Put Option on an Equity LETF

$c(t, x_0, v_0)$ Time-t Price of A European Call Option on a Volatility LETF

$p(t, x_0, v_0)$ Time-t Price of A European Put Option on a Volatility LETF

$C_{t,T}(K)$ Time-t Price of A European Call Option with Maturity T and Strike K on VIX

$P_{t,T}(K)$ Time-t Price of A European Put Option with Maturity T and Strike K on VIX

$F_{t,T}$ Time-t Price of A Future Contract with Maturity T

$r_{t,T}$ Log Return of Forward $F_{t,T}$

Var	Risk-neutral Variance Extracted from VIX Options
$rVar$	Realized Variance Extracted from VIX Futures
$Skew$	Risk-neutral Skewness Extracted from VIX Options
$rSkew$	Realized Skewness Computed from VIX Daily Returns
$xVar$	Variance Risk Premium on Volatility Market
$xSkew$	Skew Risk Premium on Volatility Market
$B_{t,T}$	Time-t Price of Zero-coupon Bond with Maturity T
xm^{USO}	USO Market Excess Return
$C_{t,T}^{USO}(K)$	Time-t Price of A European Call Option with Maturity T and Strike K on USO
$P_{t,T}^{USO}(K)$	Time-t Price of A European Put Option with Maturity T and Strike K on USO
iv	Risk-neutral Variance from USO Options
iv^u	Upside Risk-neutral Variance from USO Options
iv^d	Downside Risk-neutral Variance from USO Options
is	Risk-neutral Skewness from USO Options
is^u	Upside Risk-neutral Skewness from USO Options
is^d	Downside Risk-neutral Skewness from USO Options
rv	Realized Variance from USO Daily Returns
rv^u	Upside Realized Variance from USO Daily Returns
rv^d	Downside Realized Variance from USO Daily Returns
rs	Realized Skewness Computed from USO Daily Returns

rs^u	Upside Realized Skewness from USO Daily Returns
rs^d	Downside Realized Skewness from USO Daily Returns
vp	Variance Risk Premium on Crude Oil Market
vp^u	Upside Variance Risk Premium on Crude Oil Market
vp^d	Downside Variance Risk Premium on Crude Oil Market
sp	Skew Risk Premium on Crude Oil Market
sp^u	Upside Skew Risk Premium on Crude Oil Market
sp^d	Downside Skew Risk Premium on Crude Oil Market

Attestation of Authorship

I hereby declare that this submission is my own work and that, to the best of my knowledge and belief, it contains no material previously published or written by another person (except where explicitly defined in the acknowledgments), nor material which to a substantial extent has been submitted for the award of any other degree or diploma of a university or other institution of higher learning.

Signed:

Date:

Acknowledgements

I would like to acknowledge a number of people without whom it would not have been possible for me to complete this thesis. First and foremost, I would like to express my special thanks and appreciation to my Ph.D. primary supervisor, Dr. José Da Fonseca, for his continuous support, motivation, simulation and encouragement. It was a great honour to be his first Ph.D. student, and his joy and enthusiasm for research was contagious and inspirational for me. His specialization and deep understanding of the research field guided me through all the time of my Ph.D. journey, during which I met several obstacles and could not move on without his insightful comments. The thesis would not have been completed without his supervision, and therefore it is difficult to state how much appreciation and gratitude I owe him. I would like to express special thanks to my second supervisor, Associate Professor Peiming Wang, and additional supervisor, Professor Alireza Tourani-Rad, who have always been there to support and encourage me. I gratefully acknowledge the financial support from Auckland University of Technology, which enabled me to concentrate on my research and complete my Ph.D. work, as well as allowing me to present my research findings in international conferences and accomplish the progress I made during these three years.

My time at Auckland University of Technology was enjoyable largely due to my colleagues in the Finance Department as they contributed by building a pleasant working environment. I am particularly indebted to Ivan, Adrian, Marinela, Helena and Angela with whom I could escape from the research stress temporarily through our group activities. I am grateful for the time we spent together, for dinners, for the movie nights and for the weekend outings, which refreshed my brain when it refused to function. I would also like to especially thank my office mate, Tu C. Ho, for the constant chatting we have had, for setting a good example of how to handle difficulty in life. Special thanks to my friends who cannot all be named here: Tzu-En, Jiahao, Tongtong, Mona, Sisi, Xiaoyou, Bian, and Binghong, for the continuous support through the entire Ph.D. journey. I wish you all a bright future.

Finally, my sincere thanks goes to my parents, especially my mother, who has provided endless support to me. To them, I dedicate this thesis.

Auckland, December 2016.

Chapter 1

Introduction

It is well known that options market is a significant component of the overall derivatives markets. Options provide several advantages such as cost efficiency and/or hedging risk opportunities. However, the large variety of option markets and the sophisticated structures of options bring challenges to researchers. Part of the complexity of options arises from the fact that they can be written on any financial asset as essentially the option is a financial contract that gives the holder the right to buy or sell an underlying asset at a specified price over a specific time. New option products written on complicated underlyings are regularly introduced in the market as a result of investors' changing demands.

Chapter 2 serves as a starting point for the thesis, and it presents a primer on the option market. The chapter starts with a description of Leveraged Exchange Traded Funds (LETFs) and their derivative market. A brief literature review about research on LETFs and their options is also given, all of which is oriented toward the S&P 500 LETF market. This chapter also explains the importance of the volatility market and the need for further research on this new and fast growing market. Even though the first volatility index, the VIX, is developed upon a set of S&P 500 options, the popularity and proliferation of volatility products make the volatility an asset class by itself. Most of the literature so far focuses on VIX options and but this research is the first to focus on the pricing of volatility LETF options. It not only focuses on addressing the pricing of sophisticated structured options such as LETF options, it also employs a nonparametric methodology to extract market information from Out of the Money (OTM) options. A literature review of parametric and nonparametric methodologies is given in this chapter.

In Chapter 3, pricing frameworks are developed for options on two sets of LETFs, tracking the daily performance of the S&P 500 index and VIX index, respectively, by employing stochastic volatility models. The key for a given set of LETFs targeting the same underlying is the set of leverage ratios. These LETFs differ from each other in leverage ratios, while they are connected to the same source of randomness, which is the underlying. Chapter 3 proposes a stochastic volatility framework for the LETFs and further develops the pricing of options on LETFs on the S&P 500 index by employing Fast Fourier Transform (FFT). This framework was originally proposed by Zhang (2010). We extend this framework by incorporating jumps risk and show how the option pricing can be developed. A sensitivity analysis of price curves is performed to illustrate the impact of the model parameters on the prices. Using Bao et al. (2012) as a starting point, we develop a novel and consistent pricing framework for options written on volatility LETFs. The whole discussion of Chapter 3 is based on the dynamics proposed for the LETFs, and therefore it constitutes a parametric approach to the option pricing problem.

In contrast to Chapter 3, which is based on a parametric approach, Chapters 4 and 5 exploit a nonparametric methodology to build higher-moment risk premiums from volatility and crude oil option prices. This approach allows the extraction of market information by using option data in a model-free way. There is a strand of literature examining the information role of derivative markets, e.g., An et al. (2014) and Johnson and So (2012), which argues that forward-looking information is contained in option markets and it is slowly incorporated into the stock market. Therefore, the thesis focuses on providing a comprehensive study of option market, from both parametric and nonparametric perspectives.

Chapter 4, more specifically, employs the nonparametric methodology proposed by

Kozhan et al. (2013) to extract variance and skew risk premiums from VIX options. So far, most of the previous research is limited to the variance risk premium and mostly to the equity (index) option market. This chapter presents the first study on variance and skew risk premiums for the volatility market and explains how they are related to VIX index returns as well as to S&P 500 index returns. What is more, the results obtained for this market contrast with those in Kozhan et al. (2013) for the equity index option market. The results further confirm that the volatility market has its own specific aspects and highlights the importance of such research on the volatility market.

Chapter 5 extends the study of higher moment risk premiums to the crude oil market, one of the most important commodity markets. Moreover, the risk premiums are decomposed conditional on the market return sign following the strategy proposed by Kilic and Shaliastovich (2015). One key finding is that the decomposed risk premiums contain more predictive information about market excess returns. Also, both the upside and downside variance risk premiums are negative in the crude oil market, while Kilic and Shaliastovich (2015) show that the upside variance risk premium is positive and the downside variance risk premium is negative in the equity market. Compared to Kilic and Shaliastovich (2015), this thesis considers not only the variance risk premium but also the skew risk premium along with the conditional decompositions.

Overall, this thesis provides a comprehensive study on option markets, with a focus on LETF options, VIX options and USO options. The research is carried out using both parametric and nonparametric frameworks. The empirical results for VIX options and USO options reveal some differences compared to equity index options, often used in previous studies, and underline the necessity of analyzing these new markets. To conclude, Chapter 6 provides a summary of key findings and suggests certain new directions for future research.

Chapter 2

A Primer on Options Market

This part gives a brief introduction and explanation of related financial markets and literature for the whole thesis.

2.1 LETFs and their derivative market

Exchange Traded Funds (ETFs) have gained tremendous popularity due to the advantages they offer, such as easy diversification, low costs, tax efficiency and transparency. A Leveraged ETF (LETF) is a specific type of ETF that is designed to provide a multiple of the daily return of a given underlying ETF or index. In order to complete this goal, fund managers need to rebalance the components of the holding portfolio on a daily basis. The multiple is often called the leveraged ratio. Options written on LETFs are available as well. Typically, an LETF has a very liquid underlying ETF, and there can be options traded on both the LETFs and the underlying ETF. Trading options on LETFs offers investors several advantages over trading the underlying LETF itself. The LETF option is a powerful vehicle to trade on the market because of its potential for large gains or its uses for hedging risk. The LETF option also provides an additional tool for speculation. LETFs and their corresponding derivatives market are quite new compared with other traditional financial assets.

As stated in Zhang (2010), there can be LETFs with various leverage ratios tracking the same underlying ETF or index; therefore, the pricing of LETFs is connected by the leverage ratios and the dynamics of the underlying. Zhang (2010) also points out that the leverage can only be maintained in the short term, which is the key of a leveraged product, as the leverage decays quite fast in the long run. Specifically, this thesis focuses on LETFs tracking two prominent market indices, namely, the S&P 500 and the VIX index.

2.2 Research on LETFs and their options

So far, limited research has been carried out on LETFs and their related derivative market, which can be explained by the fact that the LETF option market is relatively new. The first theoretical work is carried out by Zhang (2010), which analyzes a sextet of LETFs tracking the S&P 500 index and proposes using the Heston model to price options written on these LETFs. Ahn et al. (2015) extend the work of Zhang (2010) by considering the role of jumps by analyzing the performance of stochastic volatility with jumps in price (SVJ) model and stochastic volatility with contemporaneous jumps in price and volatility (SVCJ) model. Deng et al. (2014) provide an analysis of options of LETF along with some results on the impact of the leverage ratio on the shape of the volatility smile. Note that all the previous works consider options written on LETFs tracking the S&P 500 equity index.

2.3 The volatility derivative market

Since the Global Financial Crisis, the role of volatility products in portfolio risk management, such as diversifying and hedging by incorporating volatility products, has become increasingly significant, especially in turbulent markets. Even though the VIX index is derived from S&P 500 options, the volatility index and its derivatives have evolved into an asset class itself and have specific properties that are different from the traditional assets, such as equities. The need for a better understanding and modelling of equity volatility and the pricing of its derivatives has increased dramatically.

The VIX index, which is well known as "the fear index", was introduced in the market by the Chicago Board Options Exchange (CBOE) in 1993. As VIX has become an asset class of its own, it can act as a benchmark or underlying for a host of futures, options and ETFs. For example, futures on VIX were introduced in March, 2004 and options on VIX were launched in February, 2006. Both VIX futures and options can provide investors with access to diversified investment portfolios by incorporating a volatility risk factor. The trading of volatility exchange traded products/funds (ETPs/ETFs) has also been booming, as traders look for profit opportunities during market fluctuations. According to Bloomberg News on September 15, 2016, the total transaction volume of volatility-related ETPs amounted to $4.3 billion in 2016, in sharp contrast to almost nothing less than a decade ago.

However, institutional investors such as pension funds are not allowed to take direct positions in VIX futures and options. The proliferation of volatility-related ETPs/ETFs provides these investors with direct exposure to market volatility. One such ETF is the volatility LETF which aims to track a certain multiple of the underlying VIX futures index. Options written on these volatility LETFs are also available. So far, research on LETF options has mainly focused on the options written on LETFs tracking S&P 500 index, and none has been carried out on options written on LETFs tracking the VIX index. The underlying index for the LETFs is the S&P 500 VIX Short-Term Futures Index, rather than the VIX index itself. As the VIX futures index has a close connection with the VIX, previous works on VIX modelling can be a good reference for the modelling of the volatility of LETFs.

2.4 Research on volatility options

So far, the majority of the literature on the volatility index and its derivatives is on VIX futures and options. A brief discussion on the modelling of VIX dynamics and pricing of VIX derivatives is presented here. One prominent feature of VIX options is that the implied volatility surface exhibits a positive volatility skew, while the volatility skew is negative in the case of equity index options. Sepp (2008) reasons that since out-of-money (OTM) call options on the VIX provide a protection against market crash, extra compensation for taking risk should be charged. Sepp (2008) also suggests incorporating stochastic volatility into the VIX dynamics to model the feature of positive skew in VIX options, and this strategy is consistent with what was done for the equity (index) option market to which stochastic volatility models have been applied extensively. [1]

Detemple and Osakwe (2000) propose a mean-reverting logarithmic process for the volatility dynamics. Kaeck and Alexander (2010) find that modelling the dynamics of the log value of the VIX index is superior to the direct modelling of that of the volatility level, so they propose a stochastic volatility model for the logarithm of the VIX. Bao et al. (2012) adopt the model of Kaeck and Alexander (2010) for the dynamics of iPath S&P 500 VIX Short Term Futures ETN (VXX) and derive a pricing formula for options written on the VXX. Mencía and Sentana (2013) find that modeling the log of VIX with a mean reverting process combined with a stochastic volatility leads to a satisfactory model to price VIX futures and options. Gehricke and Zhang (2014) propose a model for VXX, focusing on the time-varying mean behavior of the VXX. Branger et al. (2016) propose parametric models for VIX options, and the empirical analysis demonstrates that a stochastic central tendency is of importance for the pricing of VIX futures while a stochastic volatility-of-volatility contributes to match the prices of VIX options. Bardgett et al. (2017) also deal with VIX and S&P 500 options using a parametric approach and they find that VIX

[1] Stochastic volatility works well to characterize the negative skew observed in the equity option market, except for short-dated data for which jumps are needed (see Heston (1993) and Bates (1996)).

option market provides information about the variance of S&P 500 returns which is not spanned by the S&P 500 market. So far, no research on the pricing of options on volatility LETF has been carried out. To build a framework of pricing options on volatility LETFs, the research of Bao et al. (2012) will be used, as the VXX is essentially a volatility LETF with a leverage ratio of one.

2.5 Relation between equity and volatility markets

As stated previously, the first volatility index, namely, the VIX, is computed by using a set of S&P 500 options and represents the market's 30-day forward expectation of S&P 500 market volatility. The methodology used to build the VIX is nonparametric as no model is involved in the computations. It is widely acknowledged that the VIX index works well as a barometer of investor sentiment and market volatility. The introduction of VIX derivatives such as options and futures makes volatility trading available to investors. Moreover, the Global Financial Crisis made investors aware of the necessity to hedge investments by incorporating volatility products.

Apart from the VIX index, which is based on the S&P 500 index, there are also volatility indices on other equity market indices such as the Russell 2000 index, interest rates, commodity-related ETFs, currency-related ETFs, and volatility of VIX. For example, OVX is the volatility index built from USO options (the USO is an ETF tracking the WTI light sweet crude oil) and EVZ stands for the EuroCurrency ETF volatility index. Derivatives on these volatility indices, such as futures and options, are available as well. As a result, the rapid growth of volatility products has turned the volatility into an asset class in itself but it has some unique properties compared to the much more mature equity and equity option markets.

2.6 Parametric and nonparametric approaches

In this thesis, both parametric and nonparametric approaches are utilized to analyze the option market. Specifically, Chapter 3 relies on parametric models to analyze both equity and volatility LETFs and options written on these LETFs; Chapters 4 and 5 rely on a nonparametric methodology to investigate higher moment risk premiums for the volatility and crude oil markets. A brief explanation of the differences between these two approaches is given in this section.

The parametric methodology relies on the specification of a dynamic model and its parameters. In terms of option pricing, the stochastic volatility model is the most popular pricing framework, which assumes the volatility term follows a stochastic process. As mentioned previously, the stochastic volatility model proposed by Heston (1993) achieved great popularity for its capability to generate the volatility smiles observed in the equity index option market. One shortcoming of Heston's (1993) model is that it does not work well for short-dated options. Bakshi et al. (1997) conjecture that jumps in volatility may be necessary as stochastic volatility model can not fully explain the short-term volatility smile. There are many works in the literature focusing on adding jumps to stochastic volatility models. Among these works, Duffie et al. (2000) find that the inclusion of jumps into volatility leads to a more pronounced smirk for both short and long maturities. Eraker et al. (2003) confirm strong evidence for jumps in both volatility and returns and emphasize that jumps play a greater role than stochastic volatility in the periods of market downturns.

The nonparametric method is also called the model-free method. Carr and Wu (2009) are the first to propose a direct and model-free approach for quantifying the variance risk premium for financial assets. They synthesize the risk-neutral variance of an asset by utilizing a particular linear combination of options written on that asset. Furthermore, by taking the difference between this risk-neutral variance and the ex-post realized variance of the asset, they can measure its variance risk premium. Based on Carr and Wu (2009), Kozhan et al. (2013) propose a generalized approach to quantify the risk premium for the third order moment, i.e., the skew risk premium. They show that a risk premium for a given moment order is equivalent to a swap contract, where the fixed leg is the risk-neutral moment, the floating leg is the realized moment, and the expected profit from the trading strategy is the risk premium of the moment. Moreover, there is a strand of literature documenting that financial markets react differently to positive and negative shocks (For this aspect, refer to Barndorff-Nielsen et al. (2008) and Patton and Sheppard (2015).). The different impacts of positive and negative market movements on economic fundamentals lead Kilic and Shaliastovich (2015) to decompose the variance risk premium, and further demonstrate that decomposed variance risk premiums are more informative for future stock market returns.

In all, parametric and nonparametric methodologies are complementary. The former enables a concise description of the asset dynamics, as the model parameters give an easy-to-understand impact on the option prices and the calibration or estimation can be more robust to outliers. In contrast, nonparametric methodology allows one to obtain very general conclusions on key financial variables (such as risk premiums) without making any model assumptions. Even though at first sight the model-free methodology looks very appealing, this generality comes at a price as it can be quite sensitive to outliers. Both approaches have pros and cons, so the best strategy is to use them both as this work will show.

2.7 Variance and Skew Swap Contracts

A variance swap is an over-the-counter contract which allows speculation on or hedging risks associated with volatility of the underlying product, such as equity index and exchange rate. Payoff for the receiver of the floating leg, who is the payer of the fixed leg at the same time, is the difference between the realized variance and the variance swap rate which actually represents the risk-neutral variance. Carr and

Wu (2009) first demonstrate that the variance swap rate can be synthesized by a particular linear combination of option prices. The methodology is normally called model-free as it does not rely on any pricing model to measure the variance swap rate.

The variance risk premium is actually the payoff for a variance swap contract initiated at time t with maturity T

$$\underbrace{\text{realized variance}}_{\text{received at time } T} - \underbrace{\text{risk-neutral variance}}_{\text{paid at time } t},$$

where the fixed leg of the variance swap contract stands for the risk-neutral variance and the floating leg of the variance swap contract stands for the realized variance.

An any-order moment risk premium is proposed by Kozhan et al. (2013), who developed a general trading strategy so that a swap contract based on any-order moment can be synthesized. Correspondingly, an any-order moment risk premium is the payoff of the moment swap contract initiated at time t with maturity T

$$\underbrace{g(r_{t,T})}_{\text{received at time } T} - \underbrace{E_t^Q[g(r_{t,T})]}_{\text{paid at time } t}, \tag{2.1}$$

where $r_{t,T}$ stands for the log return of the underlying asset from t to T, P stands for the physical measure and Q stands for the risk-neutral measure.

Regarding different order moment swaps, the key is the specific form of payoff function g in Equation (2.1). According to Kozhan et al. (2013), payoff for the variance swap contract is

$$g^v(r) = 2\left(e^r - 1 - r\right),$$

where r is daily log return of the underlying asset.

Payoff for the skew swap contract is

$$g^s(r) = 6\left(2 + r - 2e^r + re^r\right).$$

The specific expressions of variance and skew swap risk premiums will be further discussed in Chapter 4.

Chapter 3

A Study of Options on Equity and Volatility LETFs

3.1 Introduction

A leveraged exchange traded fund (LETF) is a specific type of ETF that is designed to track multiple daily returns of a given ETF or index. Options written on LETFs are provided as well. Since the LETFs with various leverage ratios are tracking the same underlying ETF or index, the pricing of LETFs is connected by the leverage ratios and the dynamics of the underlying, as in Zhang (2010). Moreover, as options on different LETFs share the same source of risk, which is the underlying ETF, then their prices are determined by the leverage ratio and the dynamics of the underlying asset. This thesis focuses on LETFs related to two prominent market indices, namely, the S&P 500 and the VIX, and the pricing of options on these LETFs. For simplicity, an LETF tracking a multiple daily return of the S&P 500 Index is named an equity LETF and an LETF tracking a multiple daily return of the S&P 500 VIX Short Term Futures Index is named a volatility LETF.

This thesis focuses on two sets of LETFs here. The first is the set of equity LETFs, namely, SPXU (-3), SDS (-2), SH (-1), SPY (+1), SSO (+2) and UPRO (+3).

Options on these equity LETFs were introduced in the market in 2011. The second is the set of volatility LETFs, namely, VIXY (+1), UVXY (+2) and SVXY (-1), which are issued by ProShares. Options written on these volatility LETFs are also available in the market. [1]

So far, limited research has been carried out on LETFs and their related derivative market. Avellaneda and Zhang (2010) are the first to systematically investigate equity LETFs tracking the S&P 500 and their option pricing from a theoretical perspective. Other studies include Lu et al. (2009), Ahn et al. (2015), Deng et al. (2014), and Leung et al. (2014). Lu et al. (2009) analyze the evolution of Ultra ETF (+2) and UltraShort ETF (-2) from the ProShares family, which finds that the long term returns of both LETFs deviate from the leverage ratios, emphasizing the fact that LETFs are designed to track the short term multiple returns of the underlying. By studying a sextet of LETFs tracking S&P 500 index, Deng et al. (2014) show that the Heston model can reproduce the crooked smiles generated by LETF options and the curvature of volatility smiles can be affected by leverage ratios. Ahn et al. (2015) analyze the consistent pricing of options on LETFs, by comparing several stochastic volatility models, which also point out the model-dependency of LETF option prices.

This thesis also analyzes the set of volatility LETFs and consider the pricing of options on these assets. So far, no research on a dynamic model of the volatility LETFs and their derivative pricing has been proposed. We develop an analysis of the volatility LETF market by specifying a proper model for the underlying asset and the pricing of the options. The focus is volatility products as volatility has grown into a new asset class as a result of the increasing popularity and demand for volatility trading. So far, most literature is on VIX modelling and its option pricing. Note that the underlying index for the LETFs is the S&P 500 VIX Short-Term Futures Index, rather than the VIX index itself. Therefore, pricing options

[1] The set of equity LETFs, namely, SPXU (-3), SDS (-2), SH (-1), SPY (+1), SSO (+2) and UPRO (+3), are tracking the S&P 500 index. The number in the brackets is the corresponding leverage ratio designed to target. The set of volatility LETFs, namely, VIXY (+1), UVXY (+2) and SVXY (-1), are designed to track the S&P 500 VIX Short-Term Futures Index.

on volatility LETFs is closely related to pricing VIX options, but the difference can not be neglected.

Jump is another concern that features the volatility smile observed in the option market. There is an extensive body of research on the impacts of jumps on option pricing. For example, Bates (1996) is the first to add jumps into the stochastic volatility model for pricing foreign exchange rate options. Other papers about combining jumps and stochastic volatility include, among others, Duffie et al. (2000), Eraker (2004) and Broadie et al. (2007). Moreover, the specification of jump intensity is another issue worth of concern. Indeed, Bates (1996) and Duffie et al. (2000) introduce jump risk with constant intensity while other researchers, such as Bates (2000) and Eraker (2004), assume the jump risk is time varying. In this thesis, the jump term is added into the pricing models of both equity and volatility LETFs. In addition, the jump risk will be analyzed under two situations, namely, the constant jump intensity and the stochastic jump intensity. The corresponding option pricing formula will be further derived by using Fourier Inversion techniques. To the author's knowledge, no research on pricing LETF options by combining the stochastic volatility and jump risk has been carried out so far.

This chapter is organized as follows. Section 2 presents the stochastic volatility models for pricing options on both equity and volatility LETFs. In Section 3, the option pricing formulas are computed via Fourier Transform. Section 4 provides the asymptotic expansions for option pricing. Section 5 gives a brief data description. Section 6 presents the numerical results. Section 7 provides an analytical extension of option pricing models by incorporating jumps. Section 8 concludes.

3.2 The stochastic volatility models

In this part, the thesis focuses on the feature of volatility skew observed in the LETF option market, namely, the negative volatility skew implied by equity LETF option data and the positive volatility skew implied by volatility LETF option data, respectively. Introducing stochastic volatility into the option pricing model can be an effective way to characterize this feature. Prominent examples include Heston (1993) and Hull and White (1987). In fact, Heston model is adopted in this thesis for the dynamics of equity LETFs and a logarithmic model with stochastic volatility (LRSV) for the dynamics of volatility LETFs.

Regarding options on equity LETFs with different leverage ratios, which share the same source of randomness, namely, the underlying ETF, therefore, pricing options written on the set of LETFs is related. This important property was explained in Zhang (2010) who provides a unifying framework to value these options within the Heston model

The S&P 500 VIX Short-Term Futures Index has a close connection with the VIX, and previous work on VIX modeling can be a good reference for the modeling of volatility LETFs. As one prominent feature of VIX options is that the implied volatility surface exhibits positive volatility skew, Sepp (2008) suggests incorporating stochastic volatility into the VIX dynamics to capture this feature. Detemple and Osakwe (2000) propose a mean-reverting logarithmic process for the volatility dynamics. Kaeck and Alexander (2010) find that modelling the dynamics of the log value of the VIX index is superior to the direct modelling of that of its level. Bao et al. (2012) adopt the model of Kaeck and Alexander (2010) for the dynamics of VXX, which is an ETN issued by iPath Barclays that tracks the daily performance of the S&P 500 VIX Short-Term Futures Index, and perform the pricing of options on this asset. The work of Bao et al. (2012) only focuses on the dynamics of the unleveraged ETF and pricing of corresponding options. We aim to provide a consistent pricing framework for options on volatility LETFs, based on the framework of Bao et al. (2012).

3.2.1 Equity index LETFs

In this part, the dynamics of equity LETFs are discussed and a consistent pricing framework for all the LETF options is provided. The underlying asset of equity LETFs is denoted by s_t, which may qualify as a stock. Then the dynamics of s_t can be given by the set of stochastic differential equations (SDE in the sequel) under the risk-neutral probability

$$ds_t = (r-q)s_t dt + \sqrt{v_t} s_t dw_t^1, \tag{3.1}$$

$$dv_t = \kappa(\theta - v_t)dt + \sigma\sqrt{v_t} dw_t^2, \tag{3.2}$$

In the above system, $(w_t^1, w_t^2)_{t\geq 0}$ is a two-dimensional Brownian motion with correlation structure $corr(d\omega_t^1, d\omega_t^2) = \rho$, r is the risk-free rate, q is the dividend yield, κ is the mean-reverting speed, θ is the long-term mean of variance and σ is the volatility of volatility. This model is the classical Heston model and belongs to the affine class. It means that the moment generating function of the log-stock $\ln s_t$, denoted by y_t, and the integrated volatility are known in closed form. Indeed, this function is given by the following proposition.

Proposition 1 *Let (y_t, v_t) be a vector with $y_t = \ln s_t$ where $(s_t, v_t)_{t\geq 0}$ is given by Equation (3.1) and Equation (3.2), then its moment generating function is given by*

$$G(t, z_1, z_2, y, v) = E^Q[e^{z_1 y_t + z_2 \int_0^t v_u du} | y_0 = y, v_0 = v] = e^{a(t)+b(t)v_0+z_1 y_0}, \tag{3.3}$$

where

$$a(t) = \frac{2\kappa\theta}{\sigma^2}\left(t\lambda_- - \ln\left(\frac{\lambda_+ - \lambda_- e^{-\sqrt{\Delta}t}}{\lambda_+ - \lambda_-}\right)\right) + (r-q)z_1 t, \tag{3.4}$$

$$b(t) = \frac{(z_1^2 - z_1 + 2z_2)}{2}\frac{1 - e^{-\sqrt{\Delta}t}}{\lambda_+ - \lambda_- e^{-\sqrt{\Delta}t}}, \tag{3.5}$$

and

$$\lambda_{\pm} = \frac{(\kappa - z_1\rho\sigma) \pm \sqrt{\Delta}}{2}, \tag{3.6}$$

$$\Delta = (\kappa - z_1\rho\sigma)^2 - \sigma^2(z_1^2 - z_1 + 2z_2), \tag{3.7}$$

the proof of which can be found in Appendix 3.9.

A leveraged exchange traded fund l_t provides a multiple, denoted by m, of the daily return of the underlying ETF $(s_t)_{t\geq 0}$. It was shown in Avellaneda and Zhang (2010) that these two assets are related through the following relation

$$\frac{dl_t}{l_t} = m\frac{ds_t}{s_t} + (1-m)rdt,$$

with the initial value l_0 known and r denotes the risk-free interest rate. It can be seen that both l_t and s_t share the same source of randomness.

Using Itô's Lemma, it can be deduced that

$$l_t = l_0 \left(\frac{s_t}{s_0}\right)^m e^{\left(\frac{m-m^2}{2}\right)\int_0^t v_u du + (1-m)rt}. \tag{3.8}$$

Obviously, if $m = 1$ then $l_t = s_t$. For a connection between the leveraged asset and the Constant Proportion Portfolio Insurance (CPPI) strategy proposed by Black and Perold (1992), see Bertrand and Prigent (2003). Following Avellaneda and Zhang (2010), other papers for example Haugh (2011) and Jarrow (2010) also focused on this relation indicated by Equation (3.8). Taking the logarithm of Equation (3.8), this equation can be rewritten as

$$\ln l_t - \ln l_0 = m(\ln s_t - \ln s_0) + \frac{m-m^2}{2}\int_0^t v_u du + (1-m)rt. \tag{3.9}$$

This equation illustrates that l_t provides a multiple of the stock return, and also underlines the presence of a bias due to volatility. As $m \in \{-3, -2, -1, 2, 3\}$ the volatility contribution will be negative. Thus whatever the sign of m is, it will reduce the return of the LETF compared to the stock return. Both options on $(s_t)_{t\geq 0}$ and $(l_t)_{t\geq 0}$ are available, and it is therefore of interest to focus on the consistent pricing of options on these assets.

3.2.2 Volatility index LETFs

It is assumed that the underlying asset price V_t of volatility LETFs follows the logarithmic model with stochastic volatility (LRSV) with instantaneous variance v_t, which is discussed in Kaeck and Alexander (2010) and Bao et al. (2012)

$$d\ln V_t = \kappa(\theta - \ln V_t)dt + \sqrt{v_t}d\omega_t^1, \tag{3.10}$$

$$dv_t = \kappa_v(\theta_v - v_t)dt + \sigma_v\sqrt{v_t}d\omega_t^2, \tag{3.11}$$

where the initial value V_0 is known, the initial value of v_0 is unknown as it is a latent variable, $(\omega_t^1, \omega_t^2)_{t\geq 0}$ is a Brownian motion with correlation coefficient ρ, r is risk-free interest rate, κ is the mean-reverting speed of the log-value of V_t, θ is the long-term mean of the log-value of V_t, v_t is the stochastic volatility of V_t, κ_v is the mean-reverting speed of the stochastic volatility v_t, θ_v is the long-term mean of the stochastic volatility v_t and σ_v is the volatility of volatility.

Remark 2 *First, let us stress the fact that our objective is to show that within the framework proposed by Bao et al. (2012) the pricing of options on volatility LETF is feasible, it does not mean that their framework is the most relevant one. Certainly, taking into account the recent contribution of Gehricke and Zhang (2014) will lead to a more realistic model.*

Proposition 3 *Let (y_t, v_t) be a vector with $y_t = \ln V_t$ where $(V_t, v_t)_{t\geq 0}$ is given by Equation* (3.10) *and Equation* (3.11)*, then its moment generating function is given by*

$$G(t, z_1, z_2, y, v) = E^Q[e^{z_1 y_t + z_2\int_0^t v_u du}|y_0 = y, v_0 = v] = e^{A(t)+B(t)v_0+C(t)y_0}, \tag{3.12}$$

with $A(t)$, $B(t)$ and $C(t)$ solving the set of ordinary differential equations (ODEs)

$$\begin{aligned}
\frac{\partial A}{\partial t} &= \kappa_v \theta_v B(t) + \kappa \theta C(t), \\
\frac{\partial B}{\partial t} &= z_2 + \frac{1}{2} C^2(t) + \left(\rho \sigma_v C(t) - \kappa_v\right) B(t) + \frac{1}{2} \sigma_v^2 B^2(t), \\
\frac{\partial C}{\partial t} &= -\kappa C(t),
\end{aligned}$$

with initial conditions $A(0) = 0$, $B(0) = 0$ and $C(0) = z_1$. Therefore, we have $C(t) = z_1 \exp(-\kappa t)$. The function $B(t)$ is a Riccati equation with time-dependent coefficients, and can be solved by applying a numerical method such as Runge-Kutta. The function $A(t)$ can also be solved by utilizing the Runge-Kutta method. The proof can be found in Appendix 3.9.

For a volatility LETF with leverage ratio m, its price x_t is based on the underlying price V_t as follows

$$\frac{dx_t}{x_t} = m \frac{dV_t}{V_t} + (1-m) r dt,$$

with the initial value x_0 known and r denotes the risk free interest rate. We can see that both V_t and x_t share the same source of randomness.

By applying Itô's Lemma, the dynamics of the log-price $\ln x_t$ with instantaneous variance v_t is given by

$$d \ln x_t = m d \ln V_t - \left(\frac{m^2 - m}{2} \right) v_t dt + (1-m) r dt, \tag{3.13}$$

with the known initial value $\ln x_0$,

Equation (3.13) further implies that

$$x_t = x_0 \left(\frac{V_t}{V_0} \right)^m e^{-\left(\frac{m^2-m}{2}\right) \int_0^t v_u du + (1-m) r t}. \tag{3.14}$$

Equation (3.13) demonstrates the compounding effects, which means that returns over periods longer than one day will deviate from the target return, as documented by Zhang (2010). The deviation depends on the volatility of the underlying and the leverage ratio.

3.3 Option pricing on LETFs

3.3.1 Option on equity LETFs

The pricing of options on LETF was originally presented in Zhang (2010) using the Heston model. A slightly different approach was proposed by Ahn et al. (2015) for the Heston model with jumps on the stock. Other papers focusing on option pricing are Deng et al. (2014) based on the Heston model; Leung et al. (2014) where the stock follows a non affine dynamic process and option price approximations are given using expansions based on the fast mean reverting decomposition of the volatility process. For the sake of completeness, the pricing of these products is presented below.

Considering a European call option on an LETF with strike price K and maturity time t, using standard arguments, it can be proved that

$$\begin{aligned} c(t, l_0, v_0) &= e^{-rt} E^Q \left[(l_t - K)_+ \right] \\ &= e^{-rt} E^Q \left[\left(l_0 \left(\frac{s_t}{s_0} \right)^m e^{\left(\frac{m-m^2}{2} \right) \int_0^t v_u du + (1-m)rt} - K \right)_+ \right] \\ &= e^{-rt} E^Q \left[(l_0 e^{x_t} - K)_+ \right] \\ &= e^{-rt} \int_{-\infty}^{+\infty} (l_0 e^x - K)_+ f(x) dx, \end{aligned} \tag{3.15}$$

where $f(x)$ is the density of $x_t = \ln\left(\frac{l_t}{l_0}\right) = m \ln\left(\frac{s_t}{s_0}\right) + \left(\frac{m-m^2}{2}\right) \int_0^t v_u du + (1-m)rt$.

By $\varphi(t, z) = E^Q \left[e^{izx_t} \right]$ the characteristic function of x_t is denoted and

$$\begin{aligned} c(t, l_0, v_0) &= \frac{e^{-rt}}{2\pi} \int_{-\infty+i\gamma}^{+\infty+i\gamma} \varphi(t, z) \int_{-\infty}^{\infty} (l_0 e^x - K)_+ e^{-izx} dx dz \\ &= \frac{e^{-rt}}{2\pi} \int_{-\infty+i\gamma}^{+\infty+i\gamma} \varphi(t, z) \frac{K^{1-iz} l_0^{iz}}{iz(iz-1)} dz, \end{aligned}$$

where $\gamma = \Im(z) < -1$.

Defining $k_0 = \ln\left(\frac{K}{l_0}\right)$, the above equation can be simplified to

$$c(t, l_0, v_0) = \frac{Ke^{-rt}}{\pi} \int_{0+i\gamma}^{+\infty+i\gamma} e^{-izk_0} \frac{\varphi(t, z)}{iz(iz-1)} dz. \tag{3.16}$$

The characteristic function of $(l_t)_{t\geq 0}$ in Equation (3.16) is linked to the moment generating function Equation (3.12) as follows

$$\begin{aligned} \varphi(t, z) = E^Q\left[e^{izx_t}\right] &= E^Q\left[e^{iz(m \ln \frac{s_t}{s_0} + \frac{m-m^2}{2}\int_0^t v_u du + (1-m)rt)}\right] \\ &= e^{i(1-m)zrt} G\left(t, izm, iz\frac{m-m^2}{2}, 0, v_0\right). \end{aligned}$$

If we wish to relax the assumption on $\Im(z)$, then we can firstly consider a put minus a cash position. The Fourier transform of this function is

$$\int_{-\infty}^{+\infty} \left((K - l_0 e^x)_+ - K\right) e^{-izx} dx = \frac{Ke^{-iz \ln \frac{K}{l_0}}}{iz(iz-1)}. \tag{3.17}$$

Equation (3.17) implies that the constraint $\Im(z) \in [-1, 0]$ and the call option price can be obtained by using the call-put parity relation. The proof can be found in Appendix 3.9. Numerically, the option pricing is performed using the FFT following the exposition made by Carr and Madan (1999).

3.3.2 Option on volatility LETFs

The price of a European call option written on the LETF with leverage ratio m having strike K and time to maturity t, or equivalently maturity t if the current time is $t = 0$, is

$$\begin{aligned} c(t, x_0, v_0) &= e^{-rt} E^Q\left[(x_t - K)_+\right] \\ &= e^{-rt} x_0 \int_{-\infty}^{\infty} \left(e^y - e^{k_0}\right)_+ f(y) dy, \end{aligned}$$

where $y_t = \ln \frac{x_t}{x_0}$, $k_0 = \ln\left(\frac{K}{x_0}\right)$ and $f(y)$ is the probability density function of the random variable y_t.

The pricing formula above indicates that the option value actually depends on the probability density function $f(y)$. In fact, the computation of $f(y)$ can be easily and effectively performed by inverting the characteristic function via Fourier Transform.

By $\phi_X(t,z) = E^Q\left[e^{izx_t}\right]$ the characteristic function of x_t is denoted and

$$\begin{aligned} c(t,x_0,v_0) &= \frac{e^{-rt}}{2\pi}\int_{-\infty+i\gamma}^{+\infty+i\gamma}\phi_X(t,z)\int_{-\infty}^{\infty}\left(x_0e^x - K\right)_+ e^{-izx}dxdz \\ &= \frac{e^{-rt}}{2\pi}\int_{-\infty+i\gamma}^{+\infty+i\gamma}\phi_X(t,z)\frac{K^{1-iz}x_0^{iz}}{iz(iz-1)}dz, \end{aligned}$$

where $\gamma = \Im(z) < -1$.

The call option pricing formula can be expressed as

$$c(t,x_0,v_0) = \frac{Ke^{-rt}}{\pi}\int_0^{\infty}\Re\left[\phi_X(t,z)e^{-izk_0}\frac{1}{iz(iz-1)}\right]dz_R, \tag{3.18}$$

where $z = z_R + z_I i$ is a complex number with $i = \sqrt{-1}$ and $z_R \in \mathbb{R}$, $z_I \in \mathbb{R}$. The above integral is limited to $z_I < -1$, the proof of which can be found in Appendix 3.9. For the corresponding price of the put option denoted by $p(t,x_0,v_0)$, which has exactly the same time to maturity t, strike price K and the underlying LETF with leverage ratio m, the price is obtained via put-call parity.

More precisely, the price of a European put option written on the LETF with leverage ratio m having strike K and time to maturity t, or equivalently with maturity t if the current time is $t = 0$, is

$$p(t,x_0,v_0) = c(t,x_0,v_0) - x_t + Ke^{-rt}. \tag{3.19}$$

Carr and Madan (1999) applied the FFT algorithm to compute Equation (3.18), and this thesis follows this strategy.

3.4 Short term asymptotic expansions of implied volatility

Consider the Heston model

$$
\begin{aligned}
ds_t &= (r-q)s_t dt + \sqrt{v_t} s_t dw_t^1, \\
dv_t &= \kappa(\theta - v_t)dt + \sigma\sqrt{v_t} dw_t^2,
\end{aligned}
$$

with correlation structure $corr(d\omega_t^1, d\omega_t^2) = \rho$.

Referring to Forde and Jacquier (2009), the short-time asymptotic implied volatility $I(p)$ has the following expansion around $p = 0$

$$
I(p) = \sqrt{v_0}\left[1 + \frac{1}{4}\rho z + (\frac{1}{24} - \frac{5}{48}\rho^2)z^2 + O(z^3)\right], \tag{3.20}
$$

where $z = \frac{\sigma p}{v_0}$.

Equation (3.20) indicates that when the moneyness p is close to zero, the implied volatility is determined by the initial instantaneous volatility of variance v_0, the correlation coefficient ρ and z which is the ratio between instantaneous volatility of the underlying σp and v_0. Based on the short term asymptotics of implied volatility shown by Equation (3.20), the small-time asymptotic implied volatility of LETFs is further explored.

The dynamic system of an LETF l_t with leverage ratio m is given by the following set of stochastic differential equations (SDE in the sequel) under the risk-neutral probability

$$
dl_t = (R-Q)l_t dt + l_t\sqrt{Y_t} dw_t^1, \tag{3.21}
$$

$$
dY_t = \kappa^Y(\theta^Y - Y_t)dt + \sigma^Y\sqrt{Y_t} dw_t^2, \tag{3.22}
$$

with $(w_t^1, w_t^2)_{t\geq 0}$ a two-dimensional Brownian motion with correlation structure

$corr(d\omega_t^1, d\omega_t^2) = \rho$.

Corresponding to the dynamic system of the underlying asset s_t, the coefficients have the following relationship

$$\begin{aligned}
R &= r, \\
Q &= mq, \\
y_0 &= m^2 v_0, \\
\kappa^Y &= m^2\kappa, \\
\theta^Y &= \theta, \\
\sigma^Y &= m\sigma, \\
\rho^Y &= sgn(m)\rho.
\end{aligned}$$

with $sgn(m) = 1$ if $m \geq 0$ and $sgn(m) = -1$ if $m < 0$.

As a result, the short-time asymptotic implied volatility $I^m(p)$ for the LETF with leverage m has the following expansion around $p = 0$

$$I^m(p) = \sqrt{y_0}\left[m + \frac{1}{4}sgn(m)\rho z + (\frac{1}{24} - \frac{5}{48}\rho^2)\frac{z^2}{m^2} + O(z^3)\right], \tag{3.23}$$

where $z = \frac{\sigma p}{y_0}$.

Equation (3.23) indicates that the implied volatility depends only on the leverage ratio and correlation coefficient; the higher the absolute value of leverage ratio, the larger the implied volatility. Also, for a pair of LETFs with opposite leverage ratios, the sign of leverage has an impact on the asymptotic implied volatility, and therefore the asymptotic values of volatility are different.

3.5 Data description

3.5.1 Equity index LETFs

There is a rich dataset which contains the prices of options on a sextet of LETFs tracking the daily performance (or a multiple) of the S&P 500 index. The dataset spans from March 24, 2011 to February 16, 2015, which is the overlapping period that option data on all the six LETFs are available. The underlying LETFs are issued by the ProShare company, which is a division of the ProFunds Group and offers many different ETFs in terms of asset class besides the equity LETFs. The detailed information of the LETFs targeting S&P 500 is reported in Table 3.1.

Table 3.1: Equity LETFs ticker and ratio

Fund Name	Ticker Name	Leverage Ratio
Proshares UltraPro Short S&P 500 ETF	SPXU	-3
Proshares UltraShort S&P 500 ETF	SDS	-2
Proshares Short S&P 500 ETF	SH	-1
SPDR S&P 500 ETF	SPY	+1
Proshares Ultra S&P 500 ETF	SSO	+2
Proshares UltraPro S&P 500 ETF	UPRO	+3

Note: Equity LETFs tracking the S&P 500 Index, complete names as well as the ticker names along with the associated leverage ratios.

Moreover, Figure 3.1 shows the 5-day evolution of the equity LETF prices, from June 1, 2011 to June 7, 2011. The price curve of an LETF and that of its corresponding reverse product are "mirror images". In contrast, Figure 3.2 reveals the 1-year evolution of the equity LETF prices, from June 1, 2011 to June 1, 2012. The price curves of a pair of LETFs with opposite leverage ratio are no longer symmetric to each other, indicating that the negative correlation between them decays over time. The above phenomenon is called "correlation decay", with the details given by Zhang (2010).

Figure 3.1: 5-day evolution of equity LETF prices

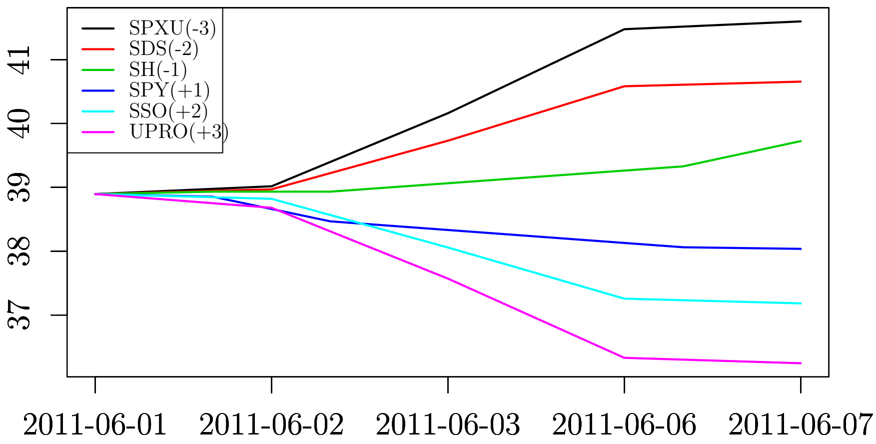

Note: Times series for equity LETF prices from 2011/06/01 to 2012/06/01.

Figure 3.2: 1-year evolution of equity LETF prices

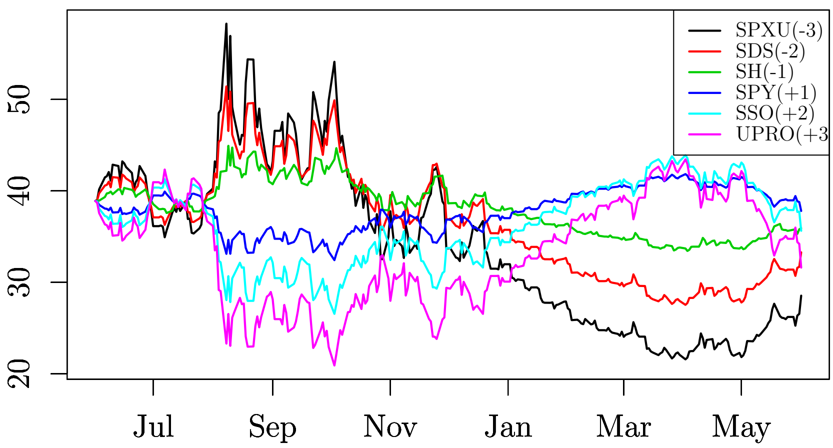

Note: Times series for equity LETF prices from 2011/06/01 to 2012/06/01.

The option data are provided by DataStream. The option prices are the daily closing bid-ask mid prices. The option volatility is obtained by using Cox-Rubinstein Binomial model and the option market price. The number of options increases over time, indicating that more and more investors are attracted to this market. For example, at the beginning sample date there were 462 options on SSO while at the end date there were 702 options, which is an indication of the fast growth of this option market. Regarding the calibration of options, this thesis restricts the analysis to October 24, 2011 and to a certain range of option moneyness that increases as the absolute value of the leverage ratio increases to be consistent with the relation Equation(3.9). Table 3.2 reports the number of options, the smallest and the largest maturity available as well as the moneyness range for each LETF.

Table 3.2: Properties of options on equity LETFs

	Number opt.	Smallest mat.	Largest mat.	Moneyness range
SPXU	135	0.071	1.241	$[0.5, 2.5]$
SDS	144	0.071	1.241	$[0.5, 2.0]$
SH	126	0.071	1.241	$[0.8, 1.5]$
SPY	722	0.071	1.241	$[0.8, 1.3]$
SSO	211	0.071	1.241	$[0.5, 1.4]$
UPRO	181	0.071	0.819	$[0.3, 1.6]$

Note: Options of equity LETF properties for the day 2011/10/24.

Not surprisingly options are more numerous for options on SPY (+1), which is the ETF tracking the S&P 500. More options are available for positive leverage ratios although the results depend on the range of moneyness selected. Note that compared to Ahn et al. (2015) and Leung and Sircar (2015) the range of moneyness in this thesis is quite large which translates into volatility smiles that display more curvature. Also, the LETF SH, with ratio -1, that is not considered in both Ahn et al. (2015) and Leung and Sircar (2015) is considered here. The following figures are the implied volatility smiles exhibited by options written on various equity LETFs. Specifically, Figure 3.3 shows the volatility smile generated by SDS options; Figure 3.4 shows the volatility smile generated by SH options; Figure 3.5 shows the volatility smile generated by SPY options, and Figure 3.6 shows the volatility smile generated by SSO options.

Figure 3.3: Volatility smile for SDS(-2)

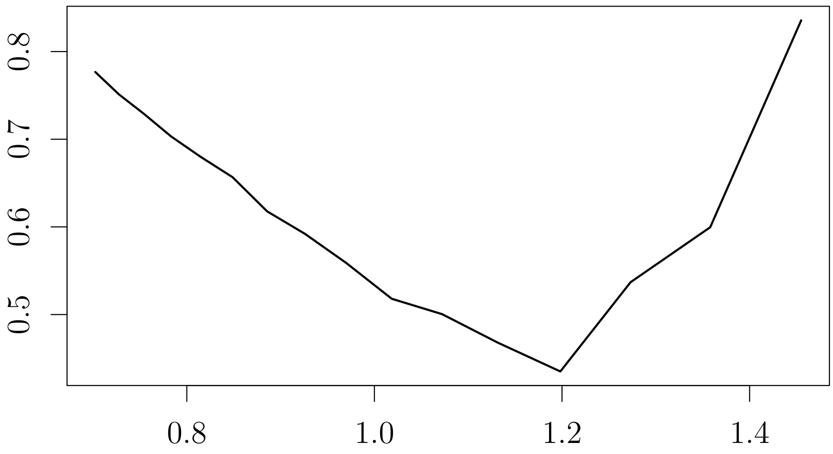

Note: Smile of the options with maturity 0.14, options on equity LETF SDS(-2) for 2011/10/24.

Figure 3.4: Volatility smile for SH(-1)

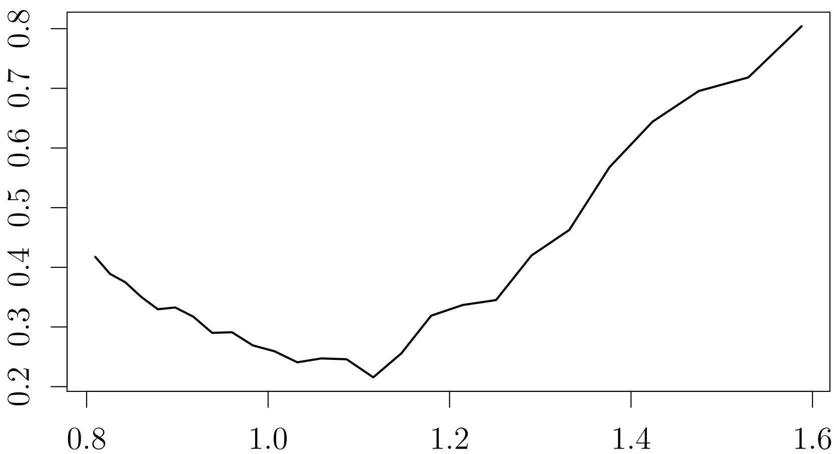

Note: Smile of the options with maturity 0.14, options on equity LETF SH(-1) for 2011/10/24.

Figure 3.5: Volatility smile for SPY(+1)

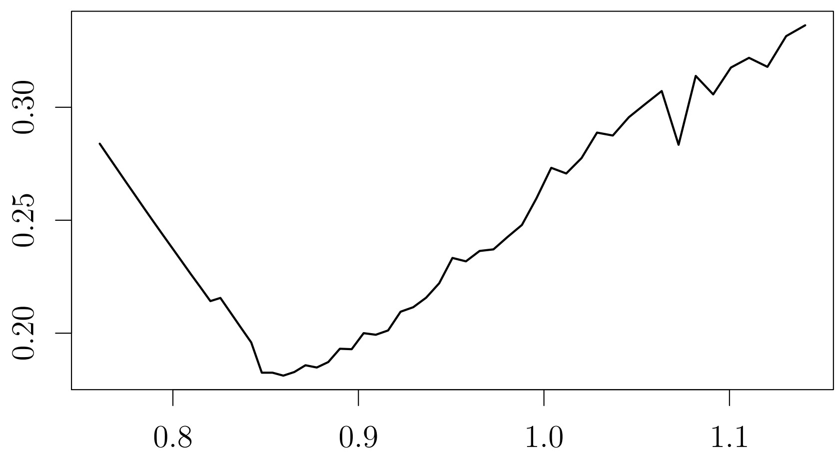

Note: Smile of the options with maturity 0.14, options on equity LETF SPY(+1) for 2011/10/24.

Figure 3.6: Volatility smile for SSO(+2)

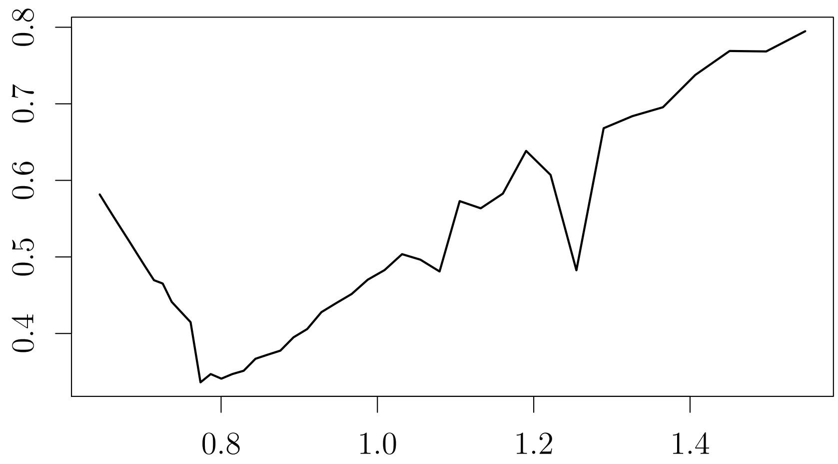

Note: Smile of the options with maturity 0.14, options on equity LETF SSO(+2) for 2011/10/24.

3.5.2 Volatility index LETFs

A dataset that contains the prices of options on a set of volatility LETFs is now available. Note that the underlying index is the VIX futures index, rather than the VIX itself, even though the two variables are highly correlated. The dataset spans from March 19, 2012 to October 31, 2014, which is the overlapping period for which option data on all the three volatility LETFs are available, and therefore use can be made of the information contained in the set of volatility LETFs. The underlying volatility LETFs are issued by the ProShare company, which is a division of the ProFunds Group and offers many categories of ETFs with regard to asset classes such as volatility, equity and currency. The detailed information of the volatility LETFs is reported in Table 3.3.

Table 3.3: Volatility LETF ticker and ratio

Fund Name	Ticker Name	Leverage Ratio
Proshares Short VIX Short-Term Futures ETF	SVXY	-1
Proshares VIX Short-Term Futures ETF	VIXY	+1
Proshares Ultra VIX Short-Term Futures ETF	UVXY	+2

Note: Volatility LETFs tracking the S&P 500 VIX Short-Term Futures Index, gives the complete name as well as the ticker name along with the associated leverage ratio.

In the above table, UVXY (+2) is designed to track twice the daily return of the S&P 500 VIX Short-Term Futures Index, before fees and expenses. The target returns are achieved by daily rebalance. VIXY (+1) is actually an unleveraged ETF but it can be treated as an LETF with leverage ratio 1 here for the purpose of consistency.

Moreover, a comparison of the short-term and long-term price curves of a volatility LETF and their reverse counterpart is made. Figure 3.7 shows 5-day price curves of VIXY(+1) and SVXY(-1), which are symmetric to each other, indicating a -1 correlation between them. In contrast, 1-year price curves of VIXY(+1) and SVXY(-1) represented by Figure 3.8 are no longer symmetric, suggesting that the correlation decays over time, as discussed in Zhang (2010).

The option data are provided by Thomson Reuters Ticker History (TRTH). The

Figure 3.7: 5-day evolution of volatility LETF prices

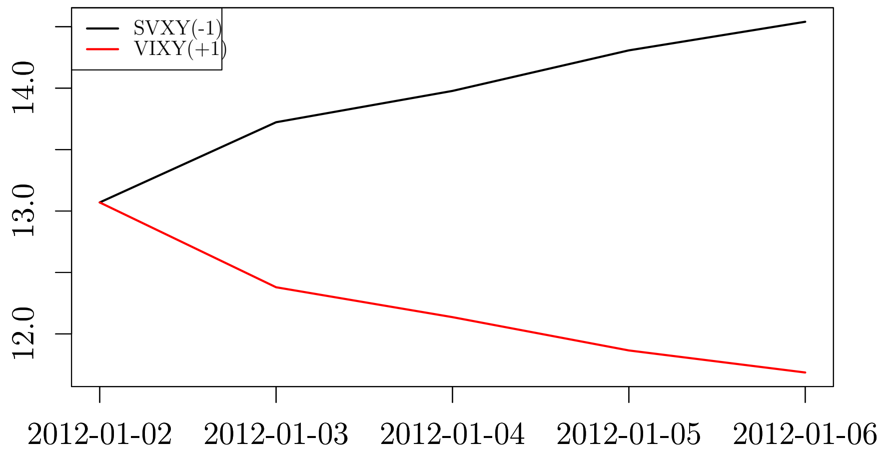

Note: Times series for volatility LETF prices from 2012/01/02 to 2012/01/06.

Figure 3.8: 1-year evolution of volatility LETF prices

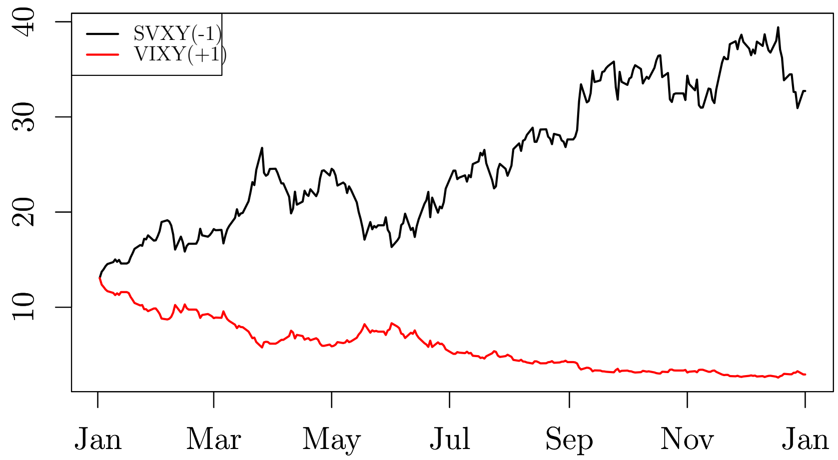

Note: Times series for volatility LETF prices from 2012/01/02 to 2013/01/02.

option prices are the daily closing bid-ask mid prices. The number of options increases with time. For example, at the beginning sample date there were 138 options on VIXY while at the end date there were 311 options on VIXY, which is an indication of the fast growth of the option market on volatility LETFs. Regarding the options, the analysis here is restricted to March 30, 2012. Table 3.4 exhibits the number of options, the smallest and the largest maturity available as well as the moneyness range for each LETF.

Table 3.4: Properties of options on Volatility LETF

	Number opt.	Smallest mat.	Largest mat.	Moneyness range
SVXY	144	0.060	0.482	$[0.5, 1.3]$
VIXY	150	0.060	0.482	$[0.5, 1.5]$
UVXY	114	0.060	0.482	$[0.5, 1.5]$

Note: Options of volatility LETF properties for 2012/03/30.

Figure 3.9: Volatility smile for SVXY(-1)

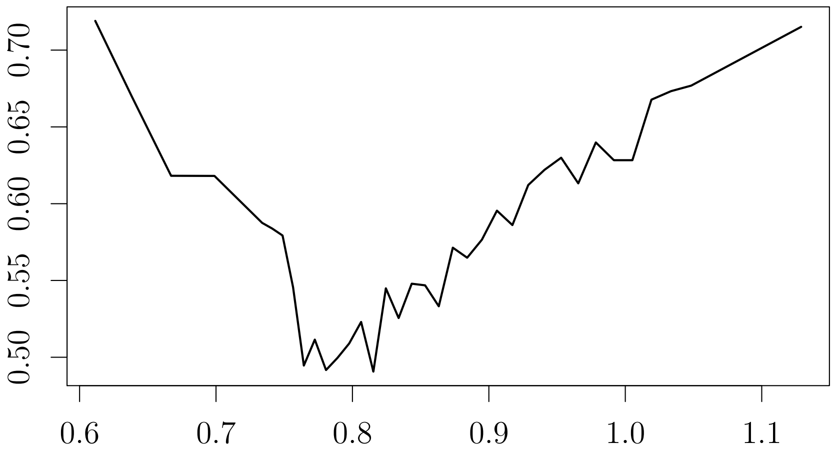

Note: Smile of the options with maturity 0.14, options on volatility LETF SVXY(-1) for 2014/10/01.

The volatility smile implied by the option price of a specified day is also plotted. In contrast to the equity LETF options, the numbers of options available for various leverage ratios are quite close. As Figure 3.9, Figure 3.10 and Figure 3.11 indicate, options on neg-

Figure 3.10: Volatility smile for VIXY(+1)

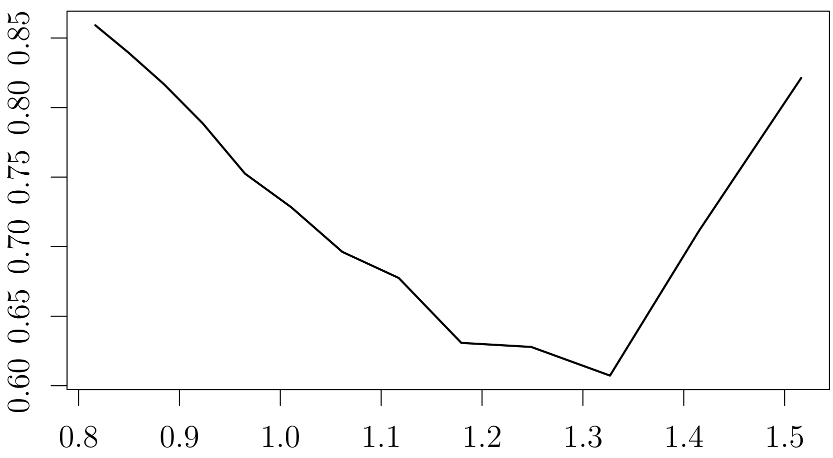

Note: Smile of the options with maturity 0.14, options on volatility LETF VIXY(+1) for 2014/10/01.

Figure 3.11: Volatility smile for UVXY(+2)

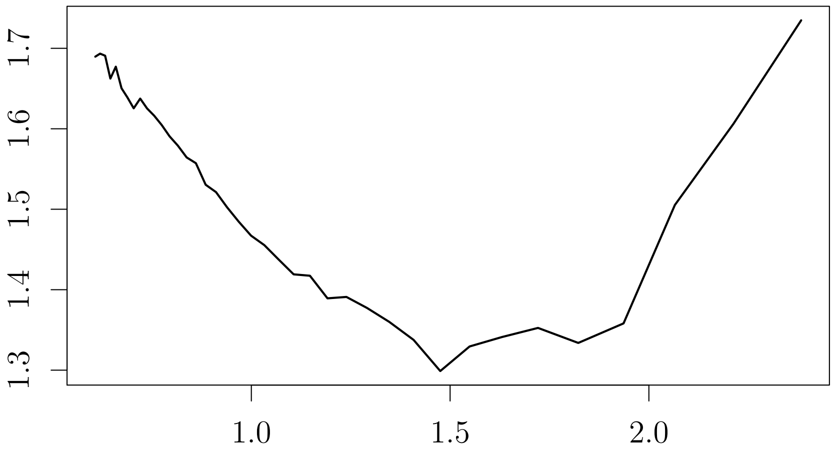

Note: Smile of the options with maturity 0.14, options on volatility LETF UVXY(+2) for 2014/10/01.

ative LETF reveal a smile with a minimum value for a moneyness smaller than one while the smiles from options with leverage ratios 1 and 2 have their minimum for moneynesses larger than one.

3.6 Numerical results

3.6.1 The equity LETF option case

For each equity LETF (and leverage ratio m) the model is calibrated by solving the following optimization problem

$$\min_{v_0,\kappa,\theta,\sigma,\rho} \frac{1}{N} \sum_{i}^{N} \left(\sigma_{imp}^{market}(t_i, K_i, m) - \sigma_{imp}^{model}(t_i, K_i, m) \right)^2, \tag{3.24}$$

where $\sigma_{imp}^{market}(t_i, K_i, m)$ is the Black-Scholes implied volatility for the option with maturity t_i, strike K_i and leverage ratio m. N stands for the number of options available and will vary across the different leverage ratios. Similarly, σ_{imp}^{model} is the Black-Scholes model implied volatility. The sum in Equation (3.24) is restricted to in-the-money options.

The option pricing error for a norm expressed in price is reported and is given by

$$\min_{v_0,\kappa,\theta,\sigma,\rho} \frac{1}{N} \sum_{i}^{N} \left(c^{market}(t_i, K_i, m) - c^{model}(t_i, K_i, m) \right)^2, \tag{3.25}$$

where $c^{market}(t_i, K_i, m)$ is the market price *normalized* by the underlying spot value of a call/put with maturity t_i, strike K_i and leverage ration m.

Firstly, the calibration performance for each equity LETF is analyzed and in Table 3.5 both the estimated parameters as well as the calibration errors in volatility and price are reported. All the LETFs lead to a negative sign for the spot-volatility correlation, which is consistent with the leverage effect, but SH (-1) clearly displays a higher value (or lower value if the absolute value of the correlation coefficient is considered) nearly half of that obtained for the SPY (+1). Regarding the pair κ and θ, UPRO (+3) leads to rather small values (for both parameters) and contrast with the other LETFs. It might be more relevant to consider the ratio $\frac{\kappa}{\sigma^2}$ as it is this quantity that appears in the asymptotic distribution of the volatility. [2] Using the values of the table 14.3, 2.9, 3.1, 0.8, 2.1 and 2.3 are obtained for the different LETFs (the values are reported following the order of the table). These values suggest that SPXU (-3) has the most distinct distribution. The calibration errors expressed using the implied volatility for the norm (i.e. Equation (3.24)) are in line with those obtained in Da Fonseca and Grasselli (2011) for SPY (+1) and SH (-1) but deteriorate as the leverage ratio increases in absolute value terms. This might be due to the larger moneyness range involved in the calibration procedure making the fitting of the smile more difficult.

[2] The volatility process used in the Heston model has an asymptotic distribution that depends on $\frac{\kappa}{\sigma^2}$ and $\frac{\kappa\theta}{\sigma^2}$.

Table 3.5: Calibration results of options on equity LETFs

	v_0	κ	θ	σ	ρ	ErrorVol	Error Price
SPXU	0.0253	2.6308	0.1438	0.4282	-0.664	3.949×10^{-2}	6.093×10^{-4}
SDS	0.0823	8.3064	0.0781	1.6757	-0.535	2.108×10^{-3}	3.891×10^{-5}
SH	0.0708	2.7108	0.0948	0.9343	-0.320	5.835×10^{-4}	5.152×10^{-6}
SPY	0.0854	2.4816	0.1345	1.6613	-0.739	4.654×10^{-4}	2.13×10^{-6}
SSO	0.0698	3.7320	0.0983	1.3296	-0.638	2.505×10^{-3}	3.697×10^{-5}
UPRO	0.0612	0.5308	0.1549	0.4747	-0.649	3.765×10^{-3}	3.946×10^{-5}

Note: Calibrated parameters for each LETF for 2011/10/24. "ErrorVol" reports the error as given by formula Equation (3.24) while "Error Price" gives the value obtained using Equation (3.25). Note that option prices are normalized by the corresponding underlying spot value so the pricing errors can be compared.

In order to assess the ability of information content extracted from options on an LETF to explain option prices written on another LETF, a repricing exercise is performed. More precisely, for a given LEFT option set the ratio of the volatility error value is reported when this set is priced using parameters calibrated on another LETF option set and the volatility error value obtained when the model is calibrated on this set. Also computed are these ratios for the price error norm. The results are reported in Table 3.6 for the first norm and in Table 3.7 for the second norm. The smaller these ratios are, the more the stock distributions implied by the option prices are similar. The volatility smiles can therefore be qualified as consistent.

Table 3.6: Options on equity LETFs: repricing errors - volatility norm

	SPXU	SDS	SH	SPY	SSO	UPRO
SPXU	1.00	2.55	1.24	5.31	2.86	1.65
SDS	20.64	1.00	5.97	29.85	16.08	10.92
SH	5.46	1.86	1.00	9.57	2.86	1.76
SPY	9.20	4.67	6.78	1.00	3.71	5.13
SSO	7.91	0.97	2.60	1.64	1.00	3.13
UPRO	4.01	1.94	1.82	3.25	1.74	1.00

Note: For a given set of calibrated parameters obtained for a given LETF (in the top row), options written on other LETF (given in the left column) are priced and the ratio of error in volatility Equation (3.24) is reported.

Table 3.7: Options on equity LETFs: repricing errors - price norm

	SPXU	SDS	SH	SPY	SSO	UPRO
SPXU	1.00	23.05	10.88	37.69	3885.89	13.15
SDS	9.45	1.00	1.60	314.09	159.44	2.66
SH	10.56	1.31	1.00	30.86	2.87	1.79
SPY	56.87	11.17	18.90	1.00	4.80	10.70
SSO	8.55	0.71	1.83	2.74	1.00	1.26
UPRO	11.62	1.37	2.79	2.21	0.84	1.00

Note: For a given set of calibrated parameters obtained for a given LETF, options written on other LETF are priced and the ratio of error in price Equation (3.25) is reported.

It seems that SDS (-2) is the option set that leads to the largest repricing errors as the values are large. However, when the SDS ($+2$) parameters are used to reprice the other LETF options, whatever LETF is selected, the repricing is quite accurate. The parameters of SPXU (-3) lead to large repricing errors while the options on this LETF can be fairly correctly priced. As a result, it can be concluded that options on LETFs with negative ratios are priced with larger errors. Interestingly, the SPY ($+1$) does not lead to the lowest repricing errors although such result could have been expected.

3.6.2 The volatility LETF option case

The closed-form pricing formulas for LETF options can be obtained by inverting the characteristic function via Fourier Transform. The option pricing formula depends on the parameters of the dynamic system, which is shown in the Appendix. Compared to the dynamic systems under a stochastic volatility framework in the previous two chapters, the jump component also plays a role in the option pricing. The parameters related to the jump risk along with the parameters linked to the stochastic volatility risk are shown in the option pricing formula. In order to analyze the impact of parameters associated with different risks, the sensitivity analysis is carried out here. Specifically, the impact of parameters related to the jump risk and the impact of parameters related to the stochastic volatility risk are analyzed. Graphs showing the impacts of various parameters will be provided.

Figure 3.12: Sensitivity analysis for VIXY(+1)

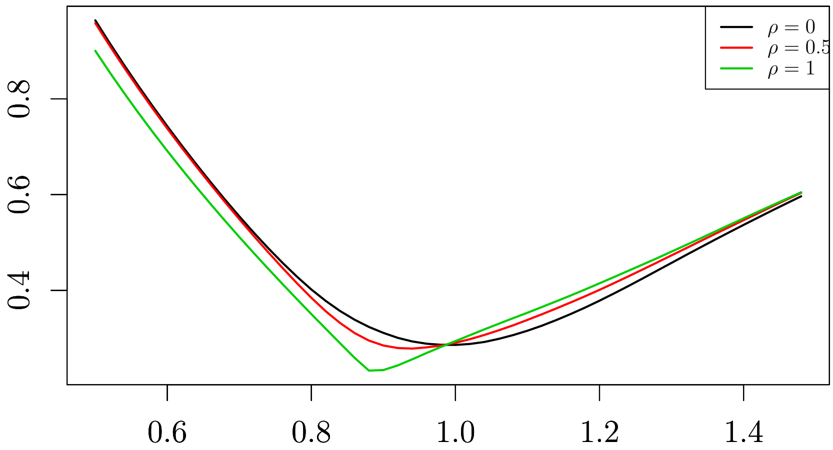

Note: Smile for the maturity 0.2 options on the volatility LETF VIXY(+1).

Figure 3.12 depicts the sensitivity of the volatility smile of VIXY (+1) to the correlation coefficient ρ, contained in Equations (3.10) and (3.11). The volatility curve is symmetric when $\rho = 0$, and the skewness increases when ρ increases. Figure 3.13 compares the price curves of options written on different volatility LETFs, namely, SVXY (-1), VIXY (+1) and UVXY (+2), with the same time to maturity. The leverage ratios 1 and -1 lead to similar curves. In contrast, the leverage ratio +2 leads to higher price levels, which depend on the second moment distribution of the volatility ETF.

Figure 3.13: Sensitivity analysis for options on volatility LETFs

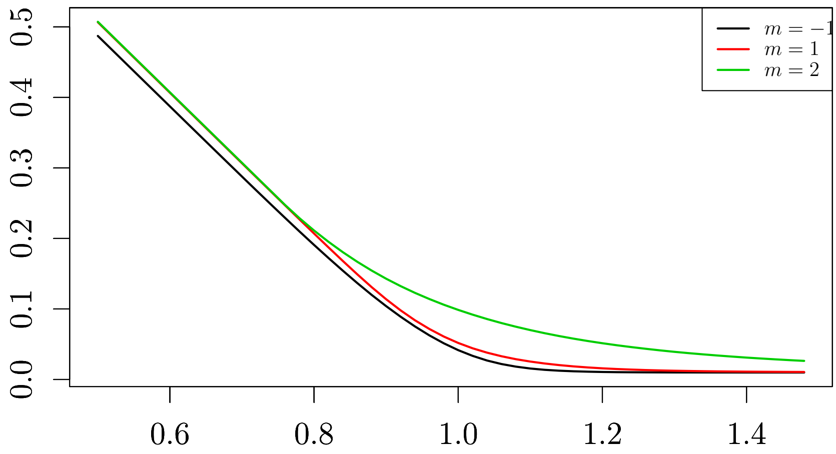

Note: Smile for the maturity 0.2 options on the volatility LETFs SVXY(-1), VIXY(+1) and UVXY(+2).

3.7 Role of jump: analytical extensions of the pricing of options on equity and volatility LETFs

In the previous parts, the thesis focuses on the feature of volatility skew observed in the LETF option market, namely, the negative volatility skew implied by equity LETF option data and the positive volatility skew implied by volatility LETF option data, respectively. However, Bates (1996) found that it is only under implausible parameters that the stochastic volatility model can explain the smile implied by the Deutsche Mark option market. He concludes that by adding jumps to the stochastic volatility model the volatility smile can be better explained. The empirical studies of Bakshi et al. (1997) also demonstrate that the stochastic volatility model can not fully explain the volatility smile. They conjecture that jumps in the volatility may be necessary. Duffie et al. (2000) systematically investigate the implications of stochastic volatility and jumps in the setting of affine jump diffusion. They find that the inclusion of jumps into volatility leads to a more pronounced smirk at both the shortest and longest maturities and reduces the model misspecification. Eraker et al. (2003) investigate the impact of jumps using data of S&P 500 and Nasdaq 100 Index returns. Eraker et al. (2003) confirm strong evidence for jumps in both volatility and returns. Especially in the periods of market stress, the jumps play a greater role than stochastic volatility. They also argue that jumps in volatility are important as they allow the rapid increase in volatility. Broadie et al. (2007) utilize an extensive data on S&P 500 futures option, ranging from January 1987 to March 2003, to examine the jump risk premium, while most previous works employ data of relatively short period. Broadie et al. (2007) employ both time series and cross section of option prices to perform the test. The time series test shows strong evidence for jumps in volatility and the cross section test reveals the important role of jumps in volatility as this improves the model fit to the data.

The specification of jumps is furthermore important. Bates (2000) focuses on the post 1987 S&P 500 futures option market and finds that the time-varying jump risk and stochastic volatility work together to explain the strongly negative skewness. It is worth noticing that the jump intensity is no longer constant as in Bates (1996). Eraker (2004) examines the combined jump diffusion model by utilizing a joint data set of options and stock markets. It also assumes that the jump arrival intensity is state-dependent, while typical jump models usually assume the jump intensity is constant.

Considering the important role of jumps in volatility, jumps are introduced to the dynamics of the underlying in this part. Specifically, a jump term will be added to the volatility process in the Heston model for equity LETFs and to the volatility process in the Logarithmic Model with Stochastic Volatility (LRSV) model for volatility LETFs. As stated in the previous part, the arrival intensity of jumps was assumed to be constant in the early studies, but later on, state-dependent jumps were introduced and it was claimed that the time-varying jump intensity was a desirable model feature (see, for example, the work of Eraker (2004)). The option pricing formula will be derived under both cases, which are the constant intensity and stochastic intensity cases. By incorporating jump risk into the option pricing formula, the role of jump risk in option pricing can be further analyzed. Up to now and to the author's knowledge, this work has not been done.

3.7.1 Heston model extension for equity LETFs

3.7.1 Heston with constant jump intensity

The dynamics of the underlying asset price s_t is specified as follows

$$\begin{aligned} \frac{ds_t}{s_t} &= (r-q)dt + \sqrt{v_t}d\omega_t^1, \\ dv_t &= \kappa(\theta - v_t)dt + \sigma\sqrt{v_t}d\omega_t^2 + JdN_t, \end{aligned}$$

with initial value s_0 known.

In the above system, $\omega_t = (\omega_t^1, \omega_t^2)_{t\geq 0}$ is a Brownian motion with correlation coefficient ρ, r is the risk-free rate, q is the dividend yield, κ is the mean-reverting speed, θ is the long-term mean of variance and σ is the volatility of volatility. N_t is a Poisson Process with constant intensity λ. The magnitude J of jumps is a random variable satisfying the exponential distribution, i.e. $J \sim \exp\left(\frac{1}{J}\right)$.

The characteristic function $\phi\left(t, z_1, z_2\right) = E^Q\left[e^{iz_1 \ln\frac{s_t}{s_0} + iz_2\int_0^t v_u du}\right]$ is

$$\phi\left(t, z_1, z_2\right) = e^{A(t)+B(t)v+iz_1x},$$

with solutions of $A(t)$ and $B(t)$ are in Appendix 3.9.

The characteristic function of $X_t = \ln\frac{l_t}{l_0}$ can be written as

$$\begin{aligned} \Phi_X(z) = E^Q\left[e^{iz\ln\frac{l_t}{l_0}}\right] &= E^Q\left[e^{iz(m\ln\frac{s_t}{s_0} + \frac{m-m^2}{2}\int_0^t v_u du + (1-m)rt)}\right] \\ &= e^{i(1-m)zrt}\phi\left(t, zm, z\left[\frac{m-m^2}{2}\right]\right). \end{aligned}$$

Set $z_1 = zm$ and $z_2 = z\left[\frac{m-m^2}{2}\right]$. The specific expression of $\Phi_X(z)$, which further implies the density function by Fourier transform, can then be obtained.

3.7.1 Heston with stochastic jump intensity

The dynamics of the underlying asset price s_t are specified as follows

$$\begin{aligned}
\frac{ds_t}{s_t} &= (r-q)dt + \sqrt{v_t}d\omega_t^1, \\
dv_t &= \kappa(\theta - v_t)dt + \sigma\sqrt{v_t}d\omega_t^2 + JdN_t, \\
d\lambda_t &= \kappa_\lambda(\theta_\lambda - \lambda_t)dt + \sigma_\lambda\sqrt{\lambda_t}d\omega_t^3,
\end{aligned}$$

with initial value s_0 known.

In the above system, $\omega_t = (\omega_t^1, \omega_t^2, \omega_t^3)_{t\geq 0}$ is a Brownian motion with $corr(d\omega_t^1, d\omega_t^2) = \rho$, $corr(d\omega_t^1, d\omega_t^3) = 0$ and $corr(d\omega_t^2, d\omega_t^3) = 0$, r is the risk-free rate, κ is the mean-reverting speed of the instantaneous volatility v_t, θ is the long-term mean of the instantaneous volatility v_t, v_t is the stochastic volatility of s_t, κ_λ is the mean-reverting speed of the jump intensity λ_t, θ_λ is the long-term mean of the jump intensity λ_t and σ_λ is the volatility of the jump intensity λ_t. N_t is a Poisson Process with stochastic intensity λ_t which follows a mean-reverting process. The magnitude J of jumps is a random variable satisfying the exponential distribution, i.e. $J \sim \exp\left(\frac{1}{J}\right)$.

The characteristic function $\phi(t, z_1, z_2, z_3) = E^Q\left[e^{iz_1x_t + iz_2\lambda_t + iz_3\int_0^t v_u du}\right]$ is

$$\phi(t, z_1, z_2, z_3) = e^{A(t)+B(t)v+C(t)\lambda+iz_1x},$$

with solutions of $A(t)$, $B(t)$ and $C(t)$ which are in Appendix 3.9.

The characteristic function of $X_t = \ln \frac{l_t}{l_0}$ can be written as

$$\begin{aligned}\Phi_X(z) = E^Q\left[e^{iz\ln\frac{l_t}{l_0}}\right] &= E^Q\left[e^{iz(m\ln\frac{s_t}{s_0}+\frac{m-m^2}{2}\int_0^t v_u du+(1-m)rt)}\right]\\ &= e^{i(1-m)zrt}\phi\left(t, zm, 0, z\left[\frac{m-m^2}{2}\right]\right).\end{aligned}$$

Set $z_1 = zm$, $z_2 = 0$ and $z_3 = z\left[\frac{m-m^2}{2}\right]$. The specific expression of $\Phi_X(z)$, which further implies the density function by Fourier transform, can then be obtained.

3.7.2 LRSVJ with constant jump intensity

It is assumed that the price V_t follows the LRSV model, which is discussed in Kaeck and Alexander (2010) and Bao et al. (2012), and is specified as follows

$$\begin{aligned}d\ln V_t &= \kappa(\theta - \ln V_t)dt + \sqrt{v_t}d\omega_t^1,\\ dv_t &= \kappa_v(\theta_v - v_t)dt + \sigma_v\sqrt{v_t}d\omega_t^2 + JdN_t,\end{aligned}$$

with initial value V_0 known.

In the above system, $\omega_t = (\omega_t^1, \omega_t^2)_{t\geq 0}$ is a Brownian motion with correlation coefficient ρ, r is the risk-free rate, κ is the mean-reverting speed of the log-value of V_t, θ is the long-term mean of the log-value of V_t, v_t is the stochastic volatility of V_t, κ_v is the mean-reverting speed of the stochastic volatility v_t, θ_v is the long-term mean of the stochastic volatility v_t and σ_v is the volatility of volatility. N_t is a Poisson Process with constant intensity λ. The magnitude J of jumps is a random variable satisfying the exponential distribution, i.e. $J \sim \exp\left(\frac{1}{J}\right)$.

The characteristic function of $\ln x_t$ can be written as

$$\begin{aligned}\Phi_X(z) = E^Q\left[e^{izx_t}\right] &= E^Q\left[e^{iz(mx_t+\frac{m-m^2}{2}\int_0^t v_u du+(1-m)rt)}\right]\\ &= e^{i(1-m)zrt}\phi\left(t, zm, z\left[\frac{m-m^2}{2}\right]\right).\end{aligned}$$

Set $z_1 = zm$ and $z_2 = z\left[\frac{m-m^2}{2}\right]$. The specific expression of $\Phi_X(z)$, which further implies the density function by Fourier transform, can then be obtained. Corresponding proof is given in Appendix 3.9.

3.7.3 LRSVJ with stochastic jump intensity

The price V_t is assumed to follow the LRSV model, which is discussed in Kaeck and Alexander (2010) and Bao et al. (2012), and is specified as follows

$$\begin{aligned} d\ln V_t &= \kappa(\theta - \ln V_t)dt + \sqrt{v_t}d\omega_t^1, \\ dv_t &= \kappa_v(\theta_v - v_t)dt + \sigma_v\sqrt{v_t}d\omega_t^2 + JdN_t, \\ d\lambda_t &= \kappa_\lambda(\theta_\lambda - \lambda_t)dt + \sigma_\lambda\sqrt{\lambda_t}d\omega_t^3, \end{aligned}$$

with initial value V_0 known.

In the above system, $\omega_t = (\omega_t^1, \omega_t^2, \omega_t^3)_{t\geq 0}$ is a Brownian motion with $corr(d\omega_t^1, d\omega_t^2) = \rho$, $corr(d\omega_t^1, d\omega_t^3) = 0$ and $corr(d\omega_t^2, d\omega_t^3) = 0$, r is the risk-free rate, κ is the mean-reverting speed of the log-value of V_t, θ is the long-term mean of the log-value of V_t, v_t is the stochastic volatility of V_t, κ_v is the mean-reverting speed of the stochastic volatility v_t, θ_v is the long-term mean of the stochastic volatility v_t and σ_v is the volatility of volatility. N_t is a Poisson Process with stochastic intensity λ_t. The magnitude J of jumps is a random variable satisfying the exponential distribution, i.e. $J \sim \exp\left(\frac{1}{J}\right)$.

The characteristic function of $X_t = \ln\frac{l_t}{l_0}$ can be written as

$$\begin{aligned} \Phi_X(z) = E^Q\left[e^{iz\ln\frac{l_t}{l_0}}\right] &= E^Q\left[e^{iz(m\ln\frac{V_t}{V_0} + \frac{m-m^2}{2}\int_0^t v_u du + (1-m)rt)}\right] \\ &= e^{i(1-m)zrt}\phi\left(t, zm, 0, z\left[\frac{m-m^2}{2}\right]\right). \end{aligned}$$

Set $z_1 = zm$, $z_2 = 0$ and $z_3 = z\left[\frac{m-m^2}{2}\right]$. The specific expression of $\Phi_X(z)$, which further implies the density function by Fourier transform, can then be obtained. Corresponding proof is given in Appendix 3.9.

3.8 Conclusion

In this chapter, a comprehensive analysis of options on both equity and volatility LETFs is carried out. More precisely, equity LETFs whose daily returns are multiples of daily S&P 500 returns and volatility LETFs whose daily returns are multiples of daily S&P 500 VIX Short-Term futures returns are considered. Based on specific dynamics and the Fourier Transform algorithm, these options are priced efficiently. Short term asymptotics of implied volatility are also given, as they provide useful tools to simplify the calibration procedure. For a given day, different calibrations are carried out and it is found that calibration errors are larger for options written on equity LETFs with larger leverage ratios (in absolute value term). Using the framework proposed by Bao et al. (2012), this thesis extends it to price options on volatility LETFs; the model being affine, it involves a Fourier transform. Lastly, the role of jumps is also considered and corresponding option pricing formulas are provided as well. The affine framework allows the incorporation of both the constant intensity case and the stochastic intensity case in a very simple way. Further work is needed to assess the importance of jumps from an empirical point of view. This aspect is left for future research.

3.9 Appendix

Proof. of Proposition 1. The pricing PDE for the function

$$f(t,v,y) = E^Q\left[e^{z_1 y_t + z_2\int_0^t v_u du}|y_0 = y, v_0 = v\right] = e^{a(t)+b(t)v+z_1 y}$$

is

$$-\frac{\partial f}{\partial t} + \kappa(\theta - v)\frac{\partial f}{\partial v} + \left(r - q - \frac{1}{2}v\right)\frac{\partial f}{\partial y} + \frac{1}{2}\sigma^2 v\frac{\partial^2 f}{\partial v^2} + \frac{1}{2}v\frac{\partial^2 f}{\partial y^2} + \rho\sigma v\frac{\partial^2 f}{\partial y\partial v} + z_2 v f = 0$$

which infers the following ODEs:

$$\frac{da}{dt} = \kappa\theta b(t) + z_1(r-q), \tag{3.26}$$

$$\frac{db}{dt} = \frac{1}{2}\left(z_1^2 - z_1\right) + z_2 + \left(\rho\sigma z_1 - \kappa\right)b(t) + \frac{1}{2}\sigma^2 b^2(t), \tag{3.27}$$

with initial conditions $a(0) = 0$ and $b(0) = 0$.

To look for the closed form solution of Equation (3.27), there should exist a function $g(t)$ such that $b(t) = -\frac{g'(t)}{\frac{1}{2}\sigma^2 g(t)}$, where $g(t)$ satisfies the ODE

$$g''(t) - \left(\rho\sigma z_1 - \kappa\right)g'(t) + \left(\frac{1}{4}\sigma^2(z_1^2 - z_1) + \frac{1}{2}\sigma^2 z_2\right)g(t) = 0.$$

Therefore, $g(t) = C_1 e^{-\lambda_+ t} + C_2 e^{-\lambda_- t}$, with $\frac{C_1}{C_2} = -\frac{\lambda_-}{\lambda_+}$ and $\lambda_\pm = \frac{(\kappa - z_1\rho\sigma)\pm\sqrt{(\kappa - z_1\rho\sigma)^2 - \sigma^2(z_1^2 - z_1 + 2z_2)}}{2}$.
And we have

$$b(t) = \frac{(z_1^2 - z_1 + 2z_2)}{2}\frac{1 - e^{-\sqrt{\Delta}t}}{\lambda_+ - \lambda_- e^{-\sqrt{\Delta}t}}.$$

Also, Equation (3.26) implies that

$$a(t) = -\frac{2\kappa\theta}{\sigma^2}\ln\left[\frac{g(t)}{g(0)}\right] + (r-q)z_1 t,$$

which can be further simplified to be

$$a(t) = \frac{2\kappa\theta}{\sigma^2}\left(t\lambda_- - \ln\left(\frac{\lambda_+ - \lambda_- e^{-\sqrt{\Delta}t}}{\lambda_+ - \lambda_-}\right)\right) + (r-q)z_1 t.$$

In all, the closed-form solutions for $a(t)$ and $b(t)$ are

$$\begin{aligned} a(t) &= \frac{2\kappa\theta}{\sigma^2}\left(t\lambda_- - \ln\left(\frac{\lambda_+ - \lambda_- e^{-\sqrt{\Delta}t}}{\lambda_+ - \lambda_-}\right)\right) + (r-q)z_1 t, \\ b(t) &= \frac{(z_1^2 - z_1 + 2z_2)}{2}\frac{1 - e^{-\sqrt{\Delta}t}}{\lambda_+ - \lambda_- e^{-\sqrt{\Delta}t}}, \end{aligned}$$

and

$$\begin{aligned} \lambda_\pm &= \frac{(\kappa - z_1\rho\sigma) \pm \sqrt{\Delta}}{2}, \\ \Delta &= (\kappa - z_1\rho\sigma)^2 - \sigma^2(z_1^2 - z_1 + 2z_2). \end{aligned}$$

■

Proof. of Proposition 3. The pricing PDE for the function

$$f(t,v,y) = E^Q\left[e^{z_1 y_t + z_2\int_0^t v_u du}|y_0 = y, v_0 = v\right] = e^{A(t)+B(t)v+z_1 y}$$

is

$$-\frac{\partial f}{\partial t} + \kappa_v(\theta_v - v)\frac{\partial f}{\partial v} + \kappa(\theta - y)\frac{\partial f}{\partial y} + \frac{1}{2}\sigma_v^2 v\frac{\partial^2 f}{\partial v^2} + \frac{1}{2}v\frac{\partial^2 f}{\partial y^2} + \rho\sigma_v v\frac{\partial^2 f}{\partial y\partial v} + z_2 v f = 0$$

which infers the following ODEs:

$$\begin{aligned} \frac{\partial A}{\partial t} &= \kappa_v\theta_v B(t) + \kappa\theta C(t) \\ \frac{\partial B}{\partial t} &= z_2 + \frac{1}{2}C^2(t) + (\rho\sigma_v C(t) - \kappa_v)B(t) + \frac{1}{2}\sigma_v^2 B^2(t) \\ \frac{\partial C}{\partial t} &= -\kappa C(t) \end{aligned}$$

with initial conditions $A(0) = 0$, $B(0) = 0$ and $C(0) = z_1$.

Therefore, we have $C(t) = z_1\exp(-\kappa t)$. The function $B(t)$ in the above ODE is a Ricati equation with time-dependent coefficients, which can be solved by applying numerical methods such as Runge-Kutta. The function $A(t)$ can also be solved by utilizing the Runge-Kutta method.

■

Proof. of Constraint Condition on z. In Equation (3.16), the constraint condition on z is $\Im(z) < -1$. The proof is as follows

$$
\begin{aligned}
c(t, l_0, v_0) &= e^{-rt} \int_{-\infty}^{\infty} (l_0 e^x - K)_+ f(x) dx \\
&= \frac{e^{-rt}}{2\pi} \int_{-\infty}^{\infty} (l_0 e^x - K)_+ \int_{-\infty}^{\infty} \varphi(t, z) e^{-izx} dz dx \\
&= \frac{e^{-rt}}{2\pi} \int_{-\infty}^{\infty} \varphi(t, z) \int_{k_0}^{\infty} \left(l_0 e^{(1-iz)x} - K e^{-izx} \right) dx dz
\end{aligned}
$$

Consider the inner integral, which is

$$
\begin{aligned}
\int_{k_0}^{\infty} \left(l_0 e^{(1-iz)x} - K e^{-izx} \right) dx &= \int_{k_0}^{\infty} l_0 e^{(1-iz)x} dx - \int_{k_0}^{\infty} K e^{-izx} dx \\
&= l_0 \frac{e^{(1-iz)x}}{1-iz} \Big|_{k_0}^{\infty} - K \frac{e^{-izx}}{-iz} \Big|_{k_0}^{\infty}.
\end{aligned}
$$

As the inner integral can be valued under the following two constraints

$$
\begin{aligned}
e^{(1-iz)\infty} &= 0, \\
e^{-iz\infty} &= 0,
\end{aligned}
$$

which is equivalent to the constraint

$$
\Im(z) < -1.
$$

If $\Im(z) < -1$, we have

$$
\int_{k_0}^{\infty} \left(l_0 e^{(1-iz)x} - K e^{-izx} \right) dx = \frac{K e^{-izk_0}}{iz(iz-1)},
$$

with $k_0 = \ln \left(\frac{K}{l_0} \right)$.

■

Proof. Heston model with constant jump intensity In the case of the Heston model with constant jump intensity, the pricing PDE for the function

$$
f(t, v, x) = E^Q \left[e^{iz_1 \ln \frac{s_t}{s_0} + iz_2 \int_0^t v_u du} | x_0 = x, v_0 = v \right] = e^{A(t) + B(t) v + iz_1 x}
$$

is

$$-\frac{\partial f}{\partial t}+\kappa(\theta-v)\frac{\partial f}{\partial v}+\left(r-q-\frac{1}{2}v\right)\frac{\partial f}{\partial x}+\frac{1}{2}\sigma^2 v\frac{\partial^2 f}{\partial v^2}+\frac{1}{2}v\frac{\partial^2 f}{\partial x^2}+\rho\sigma v\frac{\partial^2 f}{\partial x\partial v}$$
$$+iz_2 vf+\lambda\int_0^\infty\left[f(t,v+J,x)-f(t,v,x)\right]\bar{\omega}(J)dJ=0,$$

which infers the following ODEs:

$$\begin{aligned}\frac{\partial A}{\partial t}&=\kappa\theta B(t)+iz_1(r-q)+\lambda\frac{\eta B(t)}{1-\eta B(t)},\\ \frac{\partial B}{\partial t}&=-\frac{1}{2}\left(z_1^2+iz_1\right)+iz_2+\left(i\rho\sigma z_1-\kappa\right)B(t)+\frac{1}{2}\sigma^2B^2(t),\end{aligned}$$

with initial conditions $A(0)=0$, $B(0)=0$ and $i=\sqrt{-1}$.

The above ODEs generate the closed-form solutions for $A(t)$ and $B(t)$, which are

$$A(t)=-\frac{2\kappa\theta}{\sigma^2}\left\{r_1t+\ln\left[\frac{r_1e^{-\sqrt{\Delta}t}-r_2}{\sqrt{\Delta}}\right]\right\}+\frac{\lambda\eta}{\sqrt{\Delta}}\left\{a\ln\left[\frac{\sqrt{\Delta}}{e^{-\sqrt{\Delta}t}(\eta\omega+r_1)-(\eta\omega+r_2)}\right]-b\sqrt{\Delta}t\right\}$$
$$+(r-q)z_1ti,$$

$$B(t)=-\frac{2}{\sigma^2}\frac{r_1r_2\left(1-e^{-\sqrt{\Delta}t}\right)}{\left(r_2-r_1e^{-\sqrt{\Delta}t}\right)},$$

with

$$\begin{aligned}r_1&=\frac{(\rho\sigma z_1i-\kappa)+\sqrt{\Delta}}{2},\\ r_2&=\frac{(\rho\sigma z_1i-\kappa)-\sqrt{\Delta}}{2},\\ \Delta&=\left(\rho\sigma z_1i-\kappa\right)^2-\sigma^2(-z_1^2-z_1i+2z_2i),\\ \omega&=-\frac{z_1^2+z_1}{2},\\ a&=\frac{\omega\sqrt{\Delta}}{(\omega\eta+r_1)(\omega\eta+r_2)},\\ b&=\frac{\omega}{\omega\eta+r_2},\\ i&=\sqrt{-1}.\end{aligned}$$

■

Proof. Heston model with stochastic jump intensity In the case of the Heston model with stochastic jump intensity, the pricing PDE for the function

$$f(t,v,x)=E^Q\left[e^{iz_1x_t+iz_2\lambda_t+iz_3\int_0^t v_u du}|x_0=x,v_0=v\right]=e^{A(t)+B(t)v+C(t)\lambda+iz_1x}$$

is

$$-\frac{\partial f}{\partial t}+\kappa(\theta-v)\frac{\partial f}{\partial v}+\kappa_\lambda(\theta_\lambda-\lambda)\frac{\partial f}{\partial \lambda}+\left(r-q-\frac{1}{2}v\right)\frac{\partial f}{\partial x}+\frac{1}{2}\sigma^2 v\frac{\partial^2 f}{\partial v^2}+\frac{1}{2}\sigma_\lambda^2\lambda\frac{\partial^2 f}{\partial \lambda^2}$$
$$+\frac{1}{2}v\frac{\partial^2 f}{\partial x^2}+\rho\sigma v\frac{\partial^2 f}{\partial x\partial v}+iz_3 vf+\lambda\int_0^\infty\left[f(t,v+J,x)-f(t,v,x)\right]\bar{\omega}(J)dJ=0,$$

which infers the following ODEs

$$\begin{aligned}
\frac{\partial A}{\partial t}&=\kappa\theta B(t)+\kappa_\lambda\theta_\lambda C(t)+iz_1(r-q),\\
\frac{\partial B}{\partial t}&=-\frac{1}{2}\left(z_1^2+iz_1\right)+iz_3+\left(i\rho\sigma z_1-\kappa\right)B(t)+\frac{1}{2}\sigma^2B^2(t),\\
\frac{\partial C}{\partial t}&=\frac{\eta B(t)}{1-\eta B(t)}-\kappa_\lambda C(t)+\frac{1}{2}\sigma_\lambda^2C^2(t),
\end{aligned}$$

with initial conditions $A(0)=0$, $B(0)=0$, $C(0)=0$ and $i=\sqrt{-1}$.

The above ODEs generate the closed-form solutions for $A(t)$, $B(t)$ and $C(t)$, which are

$$\begin{aligned}
A(t)&=-\frac{2\kappa\theta}{\sigma^2}\left\{r_1t+\ln\left[\frac{r_1e^{-\sqrt{\Delta}t}-r_2}{\sqrt{\Delta}}\right]\right\}-\frac{2\kappa_\lambda\theta_\lambda}{\sigma_\lambda^2}\left\{\lambda_1t+\ln\left[\frac{\lambda_1e^{-\sqrt{\Delta}t}-\lambda_2}{\sqrt{\Delta}}\right]\right\}+(r-q)z_1ti,\\
B(t)&=-\frac{2}{\sigma^2}\frac{r_1r_2\left(1-e^{-\sqrt{\Delta}t}\right)}{\left(r_2-r_1e^{-\sqrt{\Delta}t}\right)},\\
C(t)&=-\frac{2}{\sigma_\lambda^2}\frac{\lambda_1\lambda_2\left(1-e^{-\sqrt{\Delta_\lambda}t}\right)}{\left(\lambda_2-\lambda_1e^{-\sqrt{\Delta_\lambda}t}\right)},
\end{aligned}$$

with

$$\begin{aligned}
r_1&=\frac{(\rho\sigma z_1i-\kappa)+\sqrt{\Delta}}{2},\\
r_2&=\frac{(\rho\sigma z_1i-\kappa)-\sqrt{\Delta}}{2},\\
\Delta&=(\rho\sigma z_1i-\kappa)^2-\sigma^2(-z_1^2-z_1i+2z_3i),\\
R_\lambda(t)&=-\kappa_\lambda-\frac{\Delta\sigma^2e^{-\sqrt{\Delta}t}}{\left(1-e^{-\sqrt{\Delta}t}\right)\left[2\eta r_1r_2\left(1-e^{-\sqrt{\Delta}t}\right)+\sigma^2\left(r_2-r_1e^{-\sqrt{\Delta}t}\right)\right]},\\
S_\lambda(t)&=-\frac{\sigma_\lambda^2\eta r_1r_2\left(1-e^{-\sqrt{\Delta}t}\right)}{2\eta r_1r_2\left(1-e^{-\sqrt{\Delta}t}\right)+\sigma^2\left(r_2-r_1e^{-\sqrt{\Delta}t}\right)},\\
\Delta_\lambda&=R_\lambda^2(t)-4S_\lambda(t),\\
\lambda_1&=\frac{R_\lambda(t)+\sqrt{\Delta_\lambda}}{2},\\
\lambda_2&=\frac{R_\lambda(t)-\sqrt{\Delta_\lambda}}{2}.
\end{aligned}$$

■

Proof. LRSVJ with constant jump intensity In the case of the LRSV with jumps model, the pricing PDE for the function

$$f(t,v,y) = E^Q\left[e^{iz_1 \ln\frac{V_t}{V_0} + iz_2\int_0^t v_u du} | y_0 = y, v_0 = v\right] = e^{A(t)+B(t)v+C(t)y}$$

is

$$\begin{aligned} -\frac{\partial f}{\partial t} + \kappa_v(\theta_v - v)\frac{\partial f}{\partial v} + \kappa(\theta - x)\frac{\partial f}{\partial x} + \frac{1}{2}\sigma_v^2 v\frac{\partial^2 f}{\partial v^2} + \frac{1}{2}v\frac{\partial^2 f}{\partial x^2} + \rho\sigma_v v\frac{\partial^2 f}{\partial x\partial v} + iz_2 vf \\ +\lambda\int_0^\infty \left[f(t,v+J,x) - f(t,v,x)\right]\bar{\omega}(J)dJ = 0, \end{aligned} \tag{3.28}$$

which infers the following ODEs

$$\begin{aligned} \frac{\partial A}{\partial t} &= \kappa_v\theta_v B(t) + \kappa\theta C(t) + \lambda\frac{\eta B(t)}{1-\eta B(t)}, \\ \frac{\partial B}{\partial t} &= iz_2 + \frac{1}{2}C^2(t) + \left(\rho\sigma_v C(t) - \kappa_v\right)B(t) + \frac{1}{2}\sigma_v^2 B^2(t), \\ \frac{\partial C}{\partial t} &= -\kappa C(t), \end{aligned}$$

with initial conditions $A(0) = 0$, $B(0) = 0$, $C(0) = iz_1$ and $i = \sqrt{-1}$.

Therefore, we have $C(t) = iz_1 \exp(-\kappa t)$. The function $B(t)$ in the above ODE is a Riccati equation with time-dependent coefficients, which can be solved by applying numerical methods such as Runge-Kutta. The function $A(t)$ can also be solved by utilizing the Runge-Kutta method.

■

Proof. LRSVJ with stochastic jump intensity In the case of the LRSV with jumps model, the pricing PDE for the function

$$f(t,v,\lambda,x) = E^Q\left[e^{iz_1 \ln\frac{V_t}{V_0} + iz_2\int_0^t v_u du} | x_0 = x, v_0 = v, \lambda_0 = \lambda\right] = e^{A(t)+B(t)v+C(t)\lambda+D(t)x}$$

is

$$\begin{aligned} -\frac{\partial f}{\partial t} + \kappa_v(\theta_v - v)\frac{\partial f}{\partial v} + \kappa_\lambda(\theta_\lambda - \lambda)\frac{\partial f}{\partial \lambda} + \kappa(\theta - x)\frac{\partial f}{\partial x} + \frac{1}{2}\sigma_v^2 v\frac{\partial^2 f}{\partial v^2} + \frac{1}{2}\sigma_\lambda^2\lambda\frac{\partial^2 f}{\partial \lambda^2} + \frac{1}{2}v\frac{\partial^2 f}{\partial x^2} \\ +\rho\sigma_v v\frac{\partial^2 f}{\partial x\partial v} + iz_2 vf + \lambda\int_0^\infty \left[f(t,v+J,x) - f(t,v,x)\right]\bar{\omega}(J)dJ = 0, \end{aligned} \tag{3.29}$$

which infers the following ODEs

$$
\begin{aligned}
\frac{\partial A}{\partial t} &= \kappa_v \theta_v B(t) + \kappa_\lambda \theta_\lambda C(t) + \kappa \theta D(t), \\
\frac{\partial B}{\partial t} &= i z_3 + \frac{1}{2} D^2(t) + \left(\rho \sigma_v D(t) - \kappa_v\right) B(t) + \frac{1}{2} \sigma_v^2 B^2(t), \\
\frac{\partial C}{\partial t} &= \frac{1}{2} \sigma_v^2 C^2(t) - \kappa_\lambda C(t) + \frac{\eta B(t)}{1 - \eta B(t)}, \\
\frac{\partial D}{\partial t} &= -\kappa D(t),
\end{aligned}
$$

with initial conditions $A(0) = 0$, $B(0) = 0$, $C(0) = i z_2,$, $D(0) = i z_1$ and $i = \sqrt{-1}$.

Therefore, we have $C(t) = i z_1 \exp(-\kappa t)$. The function $B(t)$ in the above ODE is a Ricati equation with time-dependent coefficients, which can be solved by applying numerical methods such as Runge-Kutta. The function $A(t)$ and $D(t)$ can also be solved by utilizing the Runge-Kutta method.

■

Chapter 4

Variance and Skew Risk Premiums for the Volatility Market: The VIX Evidence

4.1 Introduction

The rapid growth of volatility products, among which the VIX index is by far the most well known, has turned volatility into an asset class, see Whaley (1993) and Zhang et al. (2010). The availability of VIX options suggests applying option-implied moment estimation methodologies, which were extensively used on equity (index) options, to that market as they allow the extraction of information on the VIX distribution without specifying any parametric model for it. They are often qualified as model-free approaches. These methodologies are favoured over more traditional historical estimation strategies as options embed a more forward looking point of view of asset moments' distribution. Also, options contain risk-neutral information and, when combined with historical information, enable the determination of risk premiums that are the key variables for risk management.

These model-free methodologies have been extensively applied to equity index options and/or individual stock options, and to foreign exchange options, and are based on the analytical results developed in Derman et al. (1997) and Carr and Madan (1998). The literature is so vast that this thesis is restricted to quoting the important works of Bakshi et al. (2003) and Neuberger (2012) as entry points in this field. Among many possible applications the following are mentioned: the use of higher risk-neutral moments for asset pricing models in Bakshi et al. (2003), the estimation of an investor's risk aversion from volatility spread in Duan and Zhang (2014) or volatility forecasting using implied moments in Neumann and Skiadopoulos (2013) and Byun and Kim (2013), and more recently the analysis of variance and skew swaps for the S&P 500 option market in Kozhan et al. (2013). However, the use of these results for the VIX option market remains largely unexplored.

Following Kozhan et al. (2013), VIX options are used to compute variance swap and skew swap excess returns and analyze their relationships to VIX index and S&P 500 index excess returns. All the variables involved are obtained from options in a model-free way and correspond to tradable strategies some of which, such as the variance swap, are actively used on the market today. A by-product of the results is to draw some conclusions on variance and skew risk premiums for the VIX market that will certainly hold for other less developed volatility markets. The results also underline certain differences between the equity (index) option market and the volatility (index) option market that may not be a surprise as equity and volatility dynamics are profoundly different.

This chapter contributes to the literature by analyzing variance and skew risk premiums for the volatility market and finds that both variables are negative. For this market, it is shown that variance swap excess return can be partially explained by volatility index excess return and equity index excess return but also by skew swap excess return. However, considering all these explanatory variables together does not fully capture the return of a variance swap trading strategy, e.g. the Capital Asset Pricing Model (CAPM) does not hold. To explain the skew swap excess return the most important variable is the variance swap excess return from which we deduce that higher order moments of the volatility distribution can hardly be hedged using equity index trading strategies. Overall, the results are found to depict the volatility index market as being structurally different from the equity index market.

The chapter is organized is as follows. The key ingredients to obtain the variables from option prices are presented in Section 4.2. A description of the empirical data used in the thesis analysis is provided in Section 4.3. Regression tests and analysis are performed in Section 4.4, and Section 4.5 concludes.

4.2 Pricing formulas

The main purpose of this chapter is to analyze the variance and skew risk premiums for the volatility market and these keys variables will be computed using VIX call and put options. To this end, $C_{t,T}(K)$ and $P_{t,T}(K)$ will denote the European call and put option prices at time t with maturity T and strike K on the VIX whose value at time t is VIX_t. It is often more convenient to use the forward value of the VIX, and $F_{t,T}$ is written for the forward value at time t with maturity T that is related to the spot value through the standard equality $F_{t,t} = \text{VIX}_t$. Use is also made of $r_{t,T} = \ln F_{T,T} - \ln F_{t,T}$, the log return of a position on the forward contract. The availability of these derivative products allows the computing of the variance and skew risk premiums in a model-free way as shown in the literature, with the important contribution provided by Kozhan et al. (2013) that will be closely followed (see also Neuberger (2012)).

Extracting distribution information from option prices, like higher moments, has a long history, for example, Carr and Madan (1998). See among many others the works of Bakshi et al. (2003) for individual options; Bakshi and Madan (2006) and Carr and Wu (2009) for a variance risk premium analysis of equity index options (options on S&P 500, S&P 100 and other major indices as well as equity); Fleming (1998), Neumann and Skiadopoulos (2013), Byun and Kim (2013) and Konstantinidi and Skiadopoulos (2016) for forecasting aspects (using S&P 500 options); Ammann and Buesser (2013) for variance risk premium properties for the foreign exchange market;

investors' risk aversion analysis as in Kostakis et al. (2011) and Duan and Zhang (2014) (using S&P 500 options); and variance risk premiums for the commodity markets in Prokopczuk and Wese Simen (2014).

The work of Huang and Shaliastovich (2014) exploits VIX options to extract volatility higher moments (in their case the second moment, the volatility of the VIX or the volatility of volatility) and performs a joint analysis with the second moment extracted from S&P 500 options (i.e. the square of the VIX) along with high frequency variables such as realized volatility and bi-power variation (these two latter variables allow the authors to isolate the role of jumps). As this thesis follows Kozhan et al. (2013), it differs from Huang and Shaliastovich (2014) by also focusing on the skewness of the VIX distribution and this aspect is important as it controls the shape of the VIX option smile and is also related to the "inverse" leverage effect, or positive skew, for the volatility market.[1] What is more, it is really at the skewness level that the volatility index option market departs from the equity index option market.

The variance risk premium A variance swap contract, receiver of the floating leg and payer of the fixed leg, is a contract between two counterparties that involves receiving at maturity T of the contract the realized variance of a given asset while at initiation t of the contract there is a payment of a premium (i.e. the fixed leg). The premium, also called variance swap rate, is given by

$$Var_{t,T} = \frac{2}{B_{t,T}} \left(\int_0^{F_{t,T}} \frac{P_{t,T}(K)}{K^2} dK + \int_{F_{t,T}}^{+\infty} \frac{C_{t,T}(K)}{K^2} dK \right) \tag{4.1}$$

with $B_{t,T}$ being the zero-coupon at time t with maturity T. It is shown in the literature that a variance swap contract enables the hedging of changes in the variance of the underlying asset and in the present case this will be the VIX. Equation (4.1) involves a continuum of options and as in the market only a finite number of options

[1] The literature of parametric approaches to VIX option pricing is substantial, such as the works of Grünbichler and Longstaff (1996), Detemple and Osakwe (2000), Sepp (2008), Lian and Zhu (2013) and Park (2016). For variance, skew and kurtosis swaps within the affine framework see Zhao et al. (2013).

is available, this quantity is approximated by the following sum

$$Var_{t,T} = 2 \sum_{K_i \leq F_{t,T}} \frac{P_{t,T}(K_i)}{B_{t,T} K_i^2} \Delta I(K_i) + 2 \sum_{F_{t,T} \leq K_i} \frac{C_{t,T}(K_i)}{B_{t,T} K_i^2} \Delta I(K_i), \tag{4.2}$$

with the weight function $\Delta I(K_i)$ defined as

$$\Delta I(K_i) = \begin{cases} \frac{K_{i+1} - K_{i-1}}{2}, 0 \leq i \leq N (\text{with } K_{-1} = 2K_0 - K_1, K_{N+1} = 2K_N - K_{N-1}) \\ 0, \quad \text{otherwise.} \end{cases}$$

The floating leg of the swap is the realized variance of the underlying asset and is given by

$$rVar_{t,T} = \sum_{i=t}^{T-1} \left[2 \left(\exp\left(r_{i,i+1} \right) - 1 - r_{i,i+1} \right) \right], \tag{4.3}$$

with $r_{i,i+1} = \ln F_{i+1,T} - \ln F_{i,T}$ the daily log-price increment for the forward of maturity T and by combining Equations (4.1) and (4.3) the value of a realization of the variance swap, $rVar_{t,T} - Var_{t,T}$, is deduced from which the variance risk premium is obtained after averaging under the historical probability measure. Also of interest is the excess return of an investment made on the variance swap, which is denoted by

$$xVar_{t,T} = \frac{rVar_{t,T}}{Var_{t,T}} - 1. \tag{4.4}$$

As the options have monthly maturities there will be monthly observations for the variance risk premium and variance swap excess return. As a result, in the previous equations t will run through the first days following the option maturity dates while T will be the first maturity date available posterior to a given t. Note that $rVar_{t,T}$ is known at time T while $Var_{t,T}$ is known at time t. So actually, for one-month options, $rVar_{t,T}$ is determined one month later than $Var_{t,T}$.

The skew risk premium A skew swap, receiver of the floating leg and payer of the fixed leg, is a contract between two counterparties that involves receiving, at maturity T of the contract the realized skewness of a given asset while at initiation t of the contract there is a payment of a premium (i.e. the fixed leg). The premium, also called skew swap rate, is given by

$$Skew_{t,T} = \frac{6}{B_{t,T}} \left(-\int_0^{F_{t,T}} \frac{F_{t,T} - K}{K^2 F_{t,T}} P_{t,T}(K) dK + \int_{F_{t,T}}^{+\infty} \frac{K - F_{t,T}}{K^2 F_{t,T}} C_{t,T}(K) dK \right) \tag{4.5}$$

and as explained in Kozhan et al. (2013) it depends on the skewness of the underlying asset distribution (i.e. the skewness of the log of VIX distribution) and is implied from the options. By defining

$$V^E_{t,T} = \frac{2}{B_{t,T}} \left(\int_0^{F_{t,T}} \frac{P_{t,T}(K)}{K F_{t,T}} dK + \int_{F_{t,T}}^{+\infty} \frac{C_{t,T}(K)}{K F_{t,T}} dK \right) \tag{4.6}$$

then $Skew_{t,T} = 3(V^E_{t,T} - Var_{t,T})$. As $Var_{t,T}$ can be approximated by Equation (4.2), to determine $Skew_{t,T}$ from option market prices Equation (4.6) just needs to be discretized and this is done as

$$V^E_{t,T} = 2 \sum_{K_i \leq F_{t,T}} \frac{P_{t,T}(K_i)}{B_{t,T} K_i F_{t,T}} \Delta I(K_i) + 2 \sum_{F_{t,T} \leq K_i} \frac{C_{t,T}(K_i)}{B_{t,T} K_i F_{t,T}} \Delta I(K_i), \tag{4.7}$$

with $\Delta I(K_i)$ previously defined.

The floating leg of the skew swap is given by

$$rSkew_{t,T} = \sum_{i=t}^{T-1} \left[3 \Delta V^E_{i,T} \left(\exp\left(r_{i,i+1}\right) - 1 \right) + 6 \left(2 - 2 \exp\left(r_{i,i+1}\right) + r_{i,i+1} + r_{i,i+1} \exp\left(r_{i,i+1}\right) \right) \right], \tag{4.8}$$

with $r_{i,i+1} = \ln F_{i+1,T} - \ln F_{i,T}$ the daily log-price increment for the forward of maturity T and $\Delta V^E_{i,T} = V^E_{i+1,T} - V^E_{i,T}$ the daily change of $V^E_{t,T}$. Combining Equations (4.2), (4.7) and (4.8) the value of a realization of the skew swap, $Skew_{t,T} - rSkew_{t,T}$, is deduced from which the skew risk premium is obtained after averaging under the historical probability measure. As for the variance risk premium, of interest is the excess return of an investment made on the skew swap, which is denoted by

$$xSkew_{t,T} = \frac{rSkew_{t,T}}{Skew_{t,T}} - 1. \tag{4.9}$$

Similarly to variance swap variables there will be monthly observations for the skew risk premium and skew swap excess return. As a result, in the previous equations t will run through the first days following the option maturity dates while T will be the first maturity date available posterior to a given t. This thesis drops the dependency with respect to T in the different variables related to premiums, either variance or skew, to lighten the notations although the reader should keep in mind that they are of monthly frequency.

Remark 4 *In Kozhan et al. (2013), the authors define the skew as* $Skew_{t,T}/(Var_{t,T})^{\frac{3}{2}}$ *and the realized skew as* $rSkew_{t,T}/(Var_{t,T})^{\frac{3}{2}}$*, thereby following the usual mathematical definition while this thesis does not normalize by the term* $(Var_{t,T})^{\frac{3}{2}}$*. It would be more accurate to term Equations* (4.5) *and* (4.8) *as risk-neutral and realized third moments but nevertheless the word skew will be used. Following Kozhan et al. (2013), most, if not all, of the regressions will involve the skew swap excess return given by Equation* (4.9) *and whether the normalization by* $(Var_{t,T})^{\frac{3}{2}}$ *is performed or not is irrelevant for that quantity with the consequence that the results of this thesis can be compared to those of Kozhan et al. (2013). Lastly, in Kozhan et al. (2013) Table 3 in their paper mentions the "normalized" implied skew and realized skew while the corresponding section (3.1 Time variation in risk premiums) refers only to third implied and realized moments (see Equations (31) and (32) in their paper).*

4.3 Data and descriptive statistics

Figure 4.1: VIX futures open interest

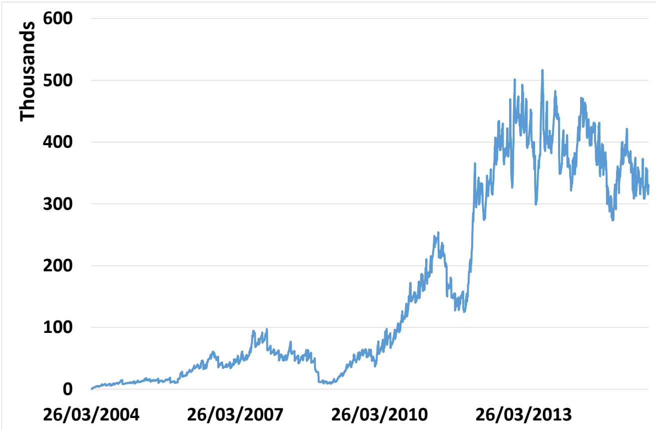

Note: Figure 4.1 VIX Futures open interest from March 2004 October 2015. The trading activity on these products took off in 2010 as VIX futures are the natural tools to hedge options written on the VIX.

To compute the variance and skew risk premiums European options are used, both calls and puts, written on the VIX that are traded on the Chicago Board Options Exchange (CBOE) and mature every month. The data are provided by Thomson Reuters Ticker History (TRTH) from SIRCA[2] and contain option information such as ticker, option type, maturity date, strike and bid-ask option quotes. The sample period starts from January 4, 2010 and ends on September 10, 2015 and the frequency is daily. VIX options started to be traded in 2006 while for futures contracts on the VIX it was in March 2004 but as can be seen from Figure 4.1 the trading activity on VIX futures contracts, that constitute the natural hedging tool for VIX options, only took off in 2010. Along with the fact that the author wanted to avoid the Global Financial Crisis, this justifies starting the sample in 2010. The VIX futures contracts are obtained from Datastream and cover the same period and these are used as forward values for the VIX. For each option the corresponding futures

[2]http://www.sirca.org.au/

contract value is used. Whenever a risk free rate is needed Libor rates provided by Bloomberg are used for this thesis.

In sharp contrast to the options on the S&P 500, options on the VIX display a positive skew that is also related to the positive relationship between the VIX and its volatility, see Figure 4.2. Figure 4.2 also reports the smile for S&P 500 options with the usual negative slope related to the leverage effect. Thanks to the availability of the VVIX (VIX of VIX options) this fact can be intuited from the evolutions of the VIX and the VVIX shown in Figure 4.3. It mirrors the well known leverage effect of S&P 500 options that is negative and will explain some of the differences between variance and skew premiums for S&P 500 and VIX options.

Figure 4.4 shows the evolution of risk-neutral variance (Var) and realized variance ($rVar$), while Figure 4.5 depicts the comovement between risk-neutral skew ($Skew$) and realized skew ($rSkew$). Both figures suggest positive correlations between the risk-neutral and realized variance (skew). In general, the curve of Var ($Skew$) is above that of $rVar$ ($rSkew$), except for some spikes where the curve of Var ($Skew$) is below that of $rVar$ ($rSkew$). As a result, the sample averages of the Var and the $Skew$ are higher than those of $rVar$ and $rSkew$, respectively, leading to negative risk premiums. Lastly, variance of risk-neutral variables are lower than their realized counterparts.

The variance and skew risk premiums, namely, the excess return from the variance swap ($xVar$) and the excess return from the skew swap ($xSkew$), are computed on a monthly basis using the pricing formulas given in the previous section. The comovement of variance and skew risk premiums shown in Figure 4.6 demonstrates their positive correlation. Magnitudes of both $xVar$ and $xSkew$ increase dramatically when the market is volatile, as there are spikes for both $xVar$ and $xSkew$ during the 2010-2012 period. Moreover, the larger spikes given by $xSkew$ suggest that skew risk premium is more sensitive to market downturns. In other words, it is likely that $xSkew$ captures more important uncertainty information in the market. More in-depth analysis will be given later.

Figure 4.2: Smile of VIX and S&P 500 options

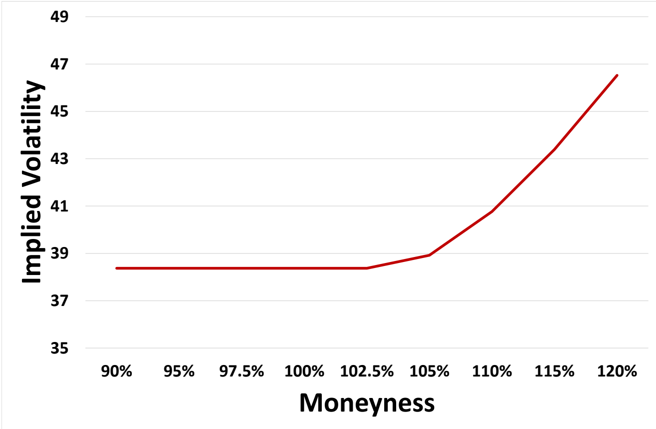

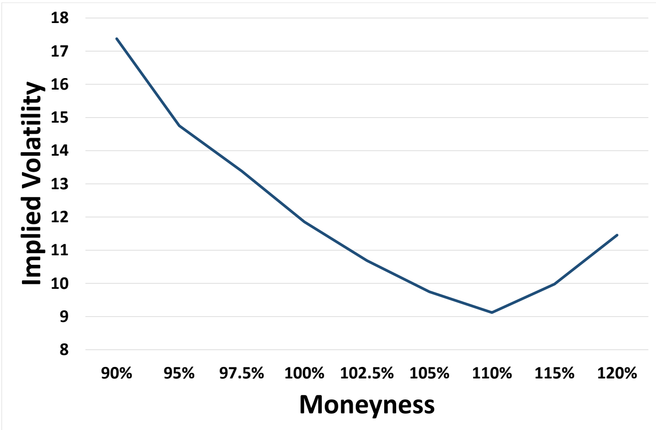

Note: Implied volatility for VIX options (upper figure) and S&P 500 options (lower figure) on June 2, 2014 with 3-month time to maturity. The positive skew is one of the main features of the VIX smile and contrasts with the downward sloping curve observed for S&P 500 options.

Figure 4.3: Evolutions of VIX and VVIX

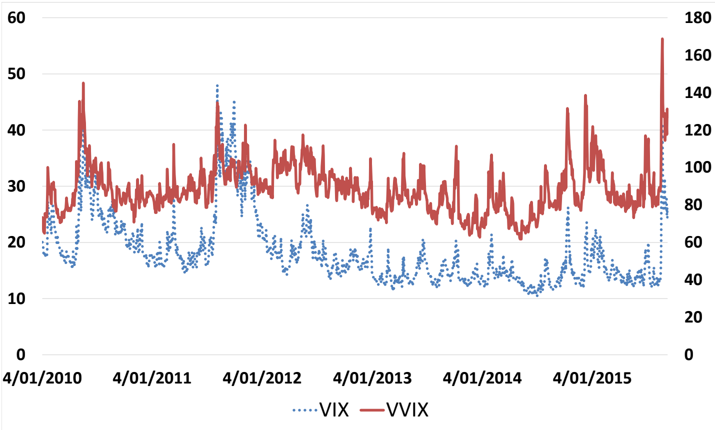

Note: Evolutions of VIX and VVIX (VIX of VIX options) from January 4, 2010 to September 10, 2015 (round dot for the VIX and solid line for the VVIX). The positive correlation between these two indices is apparent.

Figure 4.4: Risk-neutral and realized variances

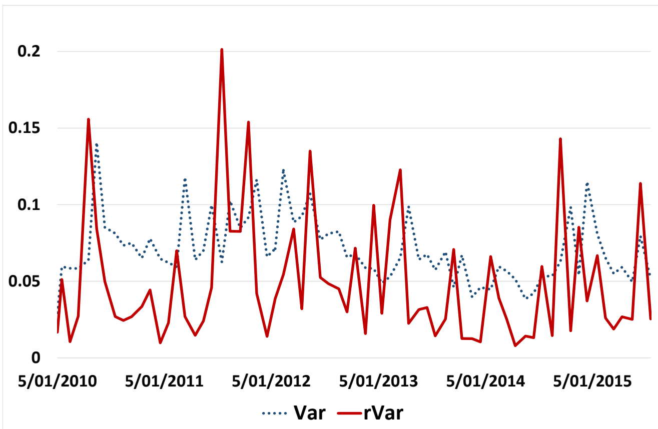

Note: Evolutions of risk-neutral and realized variances from January 4, 2010 to September 10, 2015 (round dot for the risk-neutral variance and solid line for the realized variance). In general, risk-neutral variance is greater than realized variance, while the volatility of the former is smaller than the latter.

Figure 4.5: Risk-neutral and realized skews

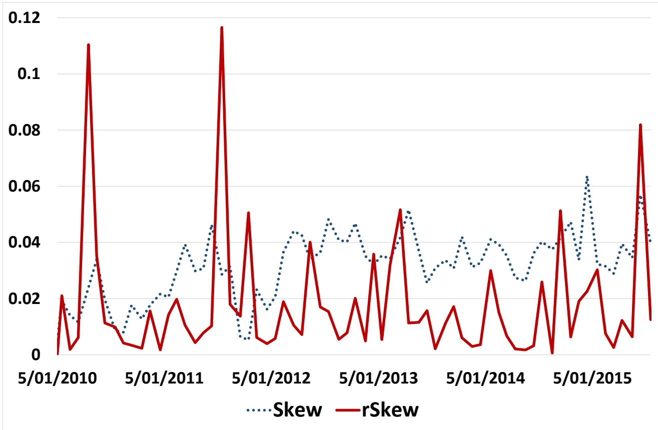

Note: Evolutions of risk-neutral and realized skews from January 4, 2010 to September 10, 2015 (round dot for the risk-neutral skew and solid line for the realized skew). In general, risk-neutral variance is greater than realized variance, while the volatility of the former is smaller than the latter.

Figure 4.6: Evolutions of VIX variance and skew risk premiums

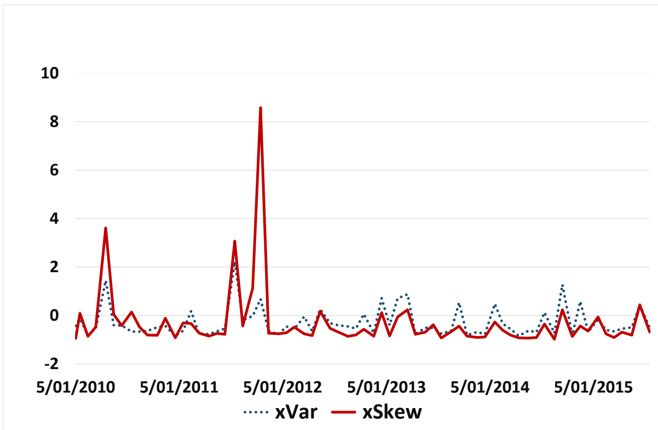

Note: Evolutions of VIX variance and skew risk premiums from January 4, 2010 to September 10, 2015 (round dot for the variance swap excess return and solid line for the skew swap excess return). The positive correlation between these two indices is apparent. Moreover, skew risk premium is more sensitive to market crashes as the magnitude of spikes is greater when a crisis occurs.

Following the methodology presented in the previous section, the variables are computed on a monthly basis. Taking into account the data sample, monthly observations ranging from January 2010 (involving options with maturity February 2010) to July 2015 (involving options with maturity August 2015) will be produced. Table 4.1 reports the descriptive statistics of the variables, namely, Var, $rVar$, $Skew$, $rSkew$, $xVar$ and $xSkew$. The sample average values of the risk-neutral variance and realized variance are 0.071 and 0.049, respectively. Holding options provides insurance against bad states of the economy, which suggests that option-implied risk-neutral volatility is usually slightly higher than the actual historical realized volatility. Therefore, a negative variance swap excess return with value of -0.283 will be generated, implying that an investor is willing to lose 28.3% of the premium in order to hedge variance risk. It is interesting to note that the value is close to the one obtained in Kozhan et al. (2013) for the variance swap excess return extracted from S&P 500 options. For the skewness, the average risk-neutral skew is 0.031 while the realized skew is only 0.018, leading to an excess return for the skew swap of -0.293, or -29.3%, a value close to the variance swap excess return value. An investor entering in a skew swap paying a fixed leg (i.e. the premium) and receiving a floating leg will lose on average 29.3% of the premium to hedge skew risk.[3] The excess return for the skew swap and variance swap are close and this contrasts with the results for the S&P 500 for which excess return for the skew swap is roughly twice that for the variance swap. For the standard deviations, the salient fact is the value for the skew swap excess return that is twice the value for the variance swap contract and this result is in line with the values for S&P 500 options of Kozhan et al. (2013).

[3]Similar results are obtained using a parametric approach in Zhao et al. (2013)

Table 4.1: Descriptive statistics

	Mean	Std. dev.	Q1	Median	Q3
Var	0.071	0.022	0.057	0.065	0.081
$rVar$	0.049	0.041	0.023	0.032	0.068
$xVar$	-0.283	0.616	-0.668	-0.511	-0.118
$Skew$	0.031	0.012	0.024	0.033	0.040
$rSkew$	0.018	0.022	0.005	0.011	0.019
$xSkew$	-0.293	1.341	-0.835	-0.686	-0.329

Note: Descriptive statistics such as mean, standard deviation, the 25th percentile, median, and 75th percentile, for the variables: the risk-neutral variable Var given by Equation (4.2), the realized variance $rVar$ given by Equation (4.3), the variance swap excess return $xVar$ given by Equation (4.4), the risk-neutral skew $Skew$ given by Equation (4.5), the realized skew given by Equation (4.8) and the skew swap excess return $xSkew$ given by Equation (4.9). Sample with monthly frequency ranging from January 2010 to July 2015.

The correlations between the variables are reported in Table 4.2. Consistent with the positive slope observed on the VIX option volatility smile, the correlation between the risk-neutral variance and skew is positive at 0.202; an increase of the VIX level is associated with an increase of its volatility leading to a right tail volatility distribution thicker than the left tail distribution, thus a larger (positive) value for the skewness. This result is in line with the implementation of parametric models such as Sepp (2008) or Lian and Zhu (2013), although the approach used by Kozhan et al. (2013) is model-free. Thus, the results of this thesis can be used to assess the relevance of the few existing parametric models implemented for the VIX option market.

Regarding realized variables, a much stronger dependency, at 0.888, occurs between the realized variance and skew. The relationship between the variables $xVar$, Var and $rVar$ is negative but has a weak correlation of -0.098 which is obtained between the risk-neutral variance (Var) and the variance swap excess return ($xVar$) while there is a strong and positive correlation of 0.933 between the realized variance ($rVar$) and variance swap excess return ($xVar$). Similar results are obtained for skew related variables; the correlation between the risk-neutral skew and skew swap excess return is negative and equal to -0.287 and smaller (in absolute value) than the correlation between this same excess return and the realized skew that is equal to 0.661, suggesting that high demand for hedging variance risk and skew risk will take place at the same time in the market.

Overall, the information content of the shape of the VIX option volatility smile, and more precisely the positive slope, applies to the realized distributions as well as to the swap trading strategies. Although there are some similarities with the results found for S&P 500 options by Kozhan et al. (2013), some specifics to the volatility derivative option market appear that will have important consequences as will be seen when applying the regression analysis.

Table 4.2: Correlations

	Var	$rVar$	$xVar$	$Skew$	$rSkew$	$xSkew$
Var	1.000	0.209	-0.098	0.202	0.115	0.137
$rVar$		1.000	0.933	0.058	0.888	0.702
$xVar$			1.000	0.046	0.868	0.607
$Skew$				1.000	0.133	-0.287
$rSkew$					1.000	0.661
$xSkew$						1.000

Note: Correlation between the variables: the risk-neutral variable Var given by Equation (4.2), the realized variance $rVar$ given by Equation (4.3), the variance swap excess return $xVar$ given by Equation (4.4), the risk-neutral skew $Skew$ given by Equation (4.5), the realized skew $rSkew$ given by Equation (4.8) and the skew swap excess return $xSkew$ given by Equation (4.9). Sample with monthly frequency ranging from January 2010 to July 2015.

4.4 Empirical results

In order to deepen the understanding of the relations between the variables, a thorough empirical analysis will be carried out in this section. The first aspect focused on is whether the risk-neutral variance and skew, which are forward looking measures, contain any predictive information regarding their realized counterpart. The second aspect worth analyzing is whether the excess return from investing in a variance (skew) swap can be explained by the Capital Asset Pricing Model (CAPM). It is known from Ang et al. (2006) that market-wide volatility risk can explain the cross-section of stock returns. Yang et al. (2013) further prove that higher-order moment risk, such as market-wide skew, is also a pricing factor for cross-sectional stock returns. More recently, Kozhan et al. (2013) show that excess return from variance or skew swap from equity index options can be partially explained by market index excess returns. They further enhance their analysis by considering cross-moment effects by quantifying the impact, along with index market return, of variance swap excess return on skew swap excess return and vice-versa. The objective of this thesis is to perform similar analysis for the volatility market that during the past years has grown so much that it has become an asset class in itself and deserves a specific analysis.

Risk-neutral and realized variance (skew) It is of interest to assess whether risk-neutral variables, either variance or skew, can explain their corresponding realized counterpart as this would give some insights into the market price of risks. Therefore, the univariate regression of realized variance (skew) on risk-neutral variance (skew) is performed given by the set of equations

$$rVar_t = a_0 + a_1 Var_t + \epsilon_t^a, \tag{4.10}$$

$$rSkew_t = b_0 + b_1 Skew_t + \epsilon_t^b, \tag{4.11}$$

where $Skew_t$ instead of $Skew_{t,T}$, and $rSkew_t$ instead of $rSkew_{t,T}$ are used to simplify the notations. The results are reported in Table 4.3.

Table 4.3: Realized moments versus implied moments

	Const.	Var	$Skew$	Adj. R^2(%)
$rVar$	0.022	0.392		2.91
	(1.63)	(2.24)		
$rSkew$	0.010		0.243	0.29
	(1.37)		(1.25)	

Note: Regressions of $rVar$, the realized variance, given by Equation (4.3) on Var, the risk-neutral variable, given by Equation (4.2) and $rSkew$, the realized skew, given by Equation (4.8) on $Skew$, the risk-neutral skew, given by Equation (4.5). The t-statistics are computed according to Newey and West (1987). Sample with monthly frequency ranging from January 2010 to July 2015.

For Equation (4.10) the coefficient is 0.392, thus consistent with the correlation value reported in Table 4.2, and significant. Note, however, that the R^2 is relatively low at 2.91%. [4] Regarding the skew variables, the risk-neutral skew provides no information on the realized skew as the coefficient is not significant and the R^2 is close to 0%. These two results suggest that the driving factors for the risk-neutral and realized variance (skew) are different.

Factor models for variance swap excess return: This part focuses on understanding the determinants of variance swap excess return, and to what extent they are related to market returns and other risk factors. First, regressions are considered

$$xVar_t = a_0 + a_1 xm_t^{\text{VIX}} + \epsilon_t^a, \tag{4.12}$$

$$xVar_t = b_0 + b_1 xm_t^{\text{SP}} + \epsilon_t^b, \tag{4.13}$$

with the results reported in Table 4.4 columns (1) and (2), respectively. These equations measure how variance swap excess return from the volatility market is spanned by volatility index excess return, given by xm^{VIX}, and equity index excess return, given by xm^{SP}. Both of these returns can be achieved by trading on futures contracts available for these two indices (for VIX futures contracts see Zhang and Zhu (2006) and Zhu and Zhang (2007)). Equation (4.12) leads to a positive and significant coefficient for xm^{VIX} with a R^2 of 41.9%. The positive sign is consistent with the positive skew of the volatility smile observed on the VIX option market (and reported in Figure 4.2). Indeed, an increase of the volatility leads to an increase of the volatility of volatility, thus a positive relationship exists between xm^{VIX} and $xVar$. Note also that the constant term is significant and negative at -0.18 and larger than the mean value of -0.283 reported in Table 4.1. As xm^{VIX} is the excess return that can be achieved by trading on the volatility market and as the VIX is closely related to the S&P 500, one of the largest indices, thus it can be considered as the market volatility excess return. Equation (4.13) regresses variance swap excess return on S&P 500 excess return, which leads to a negative and significant parameter of -0.9261 with an R^2 of 24%. Here, also, the sign is consistent with the well known leverage effect as a negative value for xm^{SP} (i.e. bear market condition) will lead to

[4] In fact it is an adjusted R-square but the term "adjusted" will be omitted hereafter.

an increase of the VIX (i.e. xm^{VIX}) and the positive skew of the VIX option volatility smile, illustrated in the previous regression, implies an increase of VIX's volatility, i.e., an increase of $xVar$. Hence, the consistency of these regression results in the shapes of both the S&P 500 smile and VIX smile. The fact that the R^2 of Equation (4.12) is larger than the R^2 of Equation (4.13) is reasonable as $xVar$ is related to the volatility of the VIX, namely the volatility of volatility, while the VIX is related to the volatility of the S&P 500. Lastly, as xm^{SP} can be identified with the (equity) market excess return and as the constant term in Equation (4.13) is significant, this suggests that the classical CAPM does not hold for the variance swap contract written on the volatility.

Table 4.4: Factor models for variance swap excess return

	$xVar$						
	(1)	(2)	(3)	(4)	(5)	(6)	(7)
Const.	-0.186	-0.188	-0.182	-0.201	-0.151	-0.130	-0.137
	(-3.31)	(-2.36)	(-3.21)	(-2.57)	(-2.89)	(-2.03)	(-2.61)
xm^{VIX}	2.010		1.906		1.539		1.148
	(6.10)		(5.44)		(5.26)		(4.18)
xm^{SP}		-9.621	-0.874			-8.096	-3.093
		(-3.89)	(-0.43)			(-4.46)	(-1.92)
$xSkew$				0.279	0.197	0.250	0.207
				(2.47)	(2.65)	(3.41)	(2.97)
Adj. R^2(%)	41.89	24.18	41.09	35.9	57.44	52.99	57.99

Note: Regressions of $xVar$, the variance swap excess return given by Equation (4.4), on explanatory variables based on $(xm^{\text{VIX}}, xm^{\text{SP}}, xSkew)$. xm^{VIX} is the excess return of the VIX index, xm^{SP} is the excess return of the S&P 500 and $xSkew$, given by Equation (4.9), is the skew swap excess return. The t-statistics are computed according to Newey and West (1987). Sample with monthly frequency ranging from January 2010 to July 2015.

Using xm^{VIX} and xm^{SP} as explanatory variables for $xVar$, leads to estimating the following factor model

$$xVar_t = a_0 + a_1 xm_t^{\text{VIX}} + a_2 xm_t^{\text{SP}} + \epsilon_t, \tag{4.14}$$

with the results given in Table 4.4 column (3). The coefficient on the second variable turns out to be not significant, although it has the correct sign, suggesting that regarding variance swap excess return, the information content of S&P 500 excess return is already spanned by the VIX excess return. The constant term is significant and negative much in line with the values obtained either for Equation (4.12) or Equation (4.13).

The $xVar$ variable depends on the second moment of the VIX distribution (both risk-neutral and historical) and so far the determinants considered have been the first moment of the VIX distribution, through the VIX excess return, and the first moment of the S&P 500 distribution also through the same variable. The following regression

$$xVar_t = a_0 + a_1 xSkew_t + \epsilon_t, \tag{4.15}$$

with results reported in column (4) of Table 4.4, assesses the impact of the third moment distribution, through the skew swap excess return, on the second moment distribution given by $xVar$. The coefficient of $xSkew$ is positive and significant while the R^2 is high at 35.9%. The finding is in line with the high correlation between $xVar$ and $xSkew$ reported in Table 4.2. It is interesting to note that the positive sign is also consistent with the positive slope of the VIX option smile. Indeed, as already explained an increase of the VIX implies an increase of the VIX's volatility, thus a thicker right tail distribution leading to a greater skew value. Note also that the constant term is negative and significant at -0.201, suggesting that skew swap excess return cannot fully explain variance swap excess return and, thus, the existence of another source of risk for variance risk premium.

Combining the previous regressions, the following equations are considered

$$xVar_t = a_0 + a_1 xm_t^{\text{VIX}} + a_2 xSkew_t + \epsilon_t^a, \tag{4.16}$$

$$xVar_t = b_0 + b_1 xm_t^{\text{SP}} + b_2 xSkew_t + \epsilon_t^b, \tag{4.17}$$

as this allows us to understand whether skew swap excess return carries complementary information to the VIX and S&P 500 excess returns considered separately. The results are reported in columns (5) and (6) of Table 4.4 for Equations (4.16) and (4.17), respectively. The first regression leads to significant coefficients for both

xm^{VIX} and $xSkew$ implying complementary information between these two variables. Note also the sign values, which are consistent with intuition. Lastly, the R^2 culminates at 57.44% and the constant term is still significant. If the pair $(xm^{\text{SP}}, xSkew)$ of explanatory variables is considered instead, very similar conclusions are obtained. Namely, coefficients are both significant with correct signs and the R^2 at 52.99% is slightly lower than the previous case but remains high while the constant term is negative and significant.

Using all the variables as explanatory variables the following regression

$$xVar_t = a_0 + a_1 xm_t^{\text{SP}} + a_2 xm_t^{\text{VIX}} + a_3 xSkew_t + \epsilon_t \tag{4.18}$$

is performed with results given in column (7) of Table 4.4. In line with the regression Equations (4.14) an(4.16), the S&P 500 excess return is not significant, while the others display coefficient signs consistent with the VIX smile. The R^2 is nearly equal to the one obtained when regressing only on the pair $(xm^{\text{VIX}}, xSkew)$ and the constant term is significant and negative, suggesting that the CAPM does not hold as the S&P 500 excess return is often used as a proxy for the market excess return.

Factor models for skew swap excess return In this section the determinants of skew swap excess return are analyzed by performing several regressions, starting by considering the two regressions

$$xSkew_t = a_0 + a_1 xm_t^{\text{VIX}} + \epsilon_t^a, \tag{4.19}$$

$$xSkew_t = b_0 + b_1 xm_t^{\text{SP}} + \epsilon_t^b, \tag{4.20}$$

with the results reported in Table 4.5 column (1) for Equation (4.19) and column (2) for Equation (4.20). The first regression leads to a positive and significant regression coefficient for the variable xm^{VIX} thereby suggesting that an increase of volatility excess return induces an increase of skew swap excess return. The more the market is volatile, the more skewed the volatility distribution and the more attractive the skew swap for an investor. Again, this result is consistent with the positive slope of the VIX option smile as explained in the previous regressions. It can also be intuited from Table 4.2 as an increase of VIX level leads to a higher level of VIX's volatility, either risk-neutral or realized, which is positively related to VIX skewness distribution, either risk-neutral or realized, so a positive relationship between xm^{VIX} and $xSkew$ is natural. The R^2 is 11.49%, lower than the 41.89% found when VIX excess return is used to explain variance swap excess return. Therefore, the VIX excess return has more explanatory power for second moment related variables than third moment related variables, a result that seems very reasonable but nevertheless appealing to find. In contrast to the results obtained for variance swap excess return regressions, the constant term is not significant and will not be for any regression having the skew swap excess return as the dependent variable. From Equation (4.20) we deduce that S&P 500 excess return has no explanatory power for skew swap excess return (or third moment related variables) as the coefficient is not significant, although its sign is consistent with the shapes of the smiles (i.e. VIX and S&P 500 option smiles). The very weak relationship between these two variables is also confirmed by the R^2 of 0.66% that is close to zero.

Table 4.5: Factor models for skew swap excess return

	$xSkew$						
	(1)	(2)	(3)	(4)	(5)	(6)	(7)
Const.	-0.177	-0.233	-0.221	0.081	0.087	0.060	0.042
	(-0.87)	(-1.25)	(-1.31)	(0.32)	(0.33)	(0.25)	(0.18)
xm^{VIX}	2.395		3.668		-0.457		0.920
	(2.84)		(2.16)		(-0.52)		(1.40)
xm^{SP}		-6.093	10.743			8.870	12.004
		(-0.89)	(0.96)			(0.97)	(1.19)
$xVar$				1.322	1.419	1.555	1.442
				(3.60)	(2.78)	(2.68)	(2.73)
Adj. R^2(%)	11.49	0.66	13.25	35.9	35.18	38.4	38.13

Note: Regressions of $xSkew$, the skew swap excess return given by Equation (4.9), on explanatory variables based on $(xm^{\mathrm{VIX}}, xm^{\mathrm{SP}}, xVar)$. xm^{VIX} is the excess return of the VIX index, xm^{SP} is the excess return of the S&P 500 and $xVar$ the variance swap excess return given by Equation (4.4). The t-statistics are computed according to Newey and West (1987). Sample with monthly frequency ranging from January 2010 to July 2015.

Combining xm^{VIX} and xm^{SP} as explanatory variables for $xSkew$ leads to the regression

$$xSkew_t = a_0 + a_1 xm_t^{\text{VIX}} + a_2 xm_t^{\text{SP}} + \epsilon_t^a, \tag{4.21}$$

with the estimates given in column (3) of Table 4.5. The results are consistent with those of Equations (4.19) and (4.20) as only the coefficient of xm^{VIX} is significant and positive, as expected. The R^2 is 13.25%, marginally higher than its counterpart in regression Equation (4.19) (i.e. 11.49%).

Let us now focus on the explanatory power of the variance swap excess return $xVar$ for the skew swap excess return $xSkew$ by performing the set of regressions

$$xSkew_t = a_0 + a_1 xVar_t + \epsilon_t^a, \tag{4.22}$$

$$xSkew_t = b_0 + b_1 xm_t^{\text{VIX}} + b_1 xVar_t + \epsilon_t^b, \tag{4.23}$$

$$xSkew_t = c_0 + c_1 xm_t^{\text{SP}} + c_2 xVar_t + \epsilon_t^c, \tag{4.24}$$

with results reported in columns (4), (5) and (6) of Table 4.5. For Equation (4.22), it is already known that the regression coefficient a_1 will be significant and positive, consistent with financial intuition, while the R^2 is equal to 35.9% from the regression Equation (4.15). But in contrast with these latter regression results, the constant term will not be significant (as already mentioned). Equation (4.23) and its estimated coefficients clearly show that VIX excess return does not provide any more information than $xVar$ when it comes to explaining skew swap excess return as the xm^{VIX} coefficient is not significant and the R^2 is around 35%, thus identical to the one obtained when regressing on $xVar$ alone. Very similar conclusions can be achieved if the pair $(xm^{\text{SP}}, xVar)$ of explanatory variables is considered (although the R^2 mildly increases from 35.9%, when $xVar$ is considered alone, to 38.3% for Equation (4.24)).

Lastly, combining all the variables, the following factor model is estimated

$$xSkew_t = a_0 + a_1 xm_t^{\text{VIX}} + a_2 xm_t^{\text{SP}} + a_2 xVar_t + \epsilon_t^a, \tag{4.25}$$

with the results given in column (7) of Table 4.5. The estimates are very much in line with those of the previous regressions. More precisely, only the coefficient of variance swap excess return ($xVar$) is found to be significant and with correct sign; the R^2 at 38% is close to its value when regressed on the pair $(xm^{\text{SP}}, xVar)$ of Equation (4.24); the constant term is not significant.

Considering jointly Tables 4.4 and 4.5, it can be concluded that to explain variance swap excess return, or variables related to second moment of the volatility, third moment of the volatility, given by skew swap excess return, and variables related to first moments, either volatility or stock, provide complementary information. However, to explain volatility higher moments (such as skewness), lower order moment variables (first moments of volatility or stock) perform very poorly, with the S&P 500 excess return being irrelevant. Though this latter finding appears to be reasonable it provides some confidence in the consistency of the results. Putting these results into a hedging portfolio point of view suggests that higher moment related variables (of the volatility) can only be hedged using contracts related to higher moments if a static hedge is performed and to some extent a separation between the volatility and equity markets.[5] Needless to say, a dynamic hedging strategy would allow that problem to be solved.

Fama-French factor models Following Kozhan et al. (2013) two linear models using Fama-French factors are built and take xm^{SP} as a reasonable proxy for the equity market excess return. Thus, the two variables SMB (the size factor) and HML (the book-to-market factor) are considered along with the variance excess returns $xVar$ and skew excess returns $xSkew$. We estimate the models

$$xVar_t = a_0 + a_1 xm_t^{\text{VIX}} + a_2 xSkew_t + a_3 SMB_t + a_4 HML_t + \epsilon_t^a, \tag{4.26}$$

$$xVar_t = b_0 + b_1 xm_t^{\text{VIX}} + b_2 xm_t^{\text{SP}} + b_3 xSkew_t + b_4 SMB_t + b_5 HML_t + \epsilon_t^b, \tag{4.27}$$

$$xSkew_t = c_0 + c_1 xm_t^{\text{VIX}} + c_2 xVar_t + c_3 SMB_t + c_4 HML_t + \epsilon_t^c, \tag{4.28}$$

$$xSkew_t = e_0 + e_1 xm_t^{\text{VIX}} + e_2 xm_t^{\text{SP}} + e_3 xVar_t + e_4 SMB_t + e_5 HML_t + \epsilon_t^e, \tag{4.29}$$

[5] Indeed, by construction the linear regression suggests a static hedging strategy.

and the coefficient values, reported in Table 4.6, allow us to draw conclusions very similar to those obtained by Kozhan et al. (2013). If $xVar$ or $xSkew$ is considered as a dependent variable, the Fama-French factors are not significant. This slightly contrasts with Carr and Wu (2009) where it is shown that for both S&P 500 (SPX) and S&P 100 (OEX) the size factor is significant. To some extent there is an inconsistency between Kozhan et al. (2013) and Carr and Wu (2009) as they find contradicting conclusions for the size factor for the S&P 500 that may be explained by their use of different samples.

Table 4.6: Fama-French risk factors for variance and skew swap excess returns

	Const.	xm^{VIX}	xm^{SP}	$xVar$	$xSkew$	SMB	HML	Adj. R^2(%)
$xVar$	-0.147	1.525			0.203	-0.018	0.003	56.53
	(-2.70)	(5.56)			(2.74)	(-0.78)	(0.12)	
$xVar$	-0.134	1.154	-2.948		0.212	-0.016	0.002	56.95
	(-2.51)	(4.38)	(-1.83)		(3.06)	(-0.70)	(0.065)	
$xSkew$	0.070	-0.435		1.406		0.110	-0.011	36.53
	(0.29)	(-0.53)		(2.96)		(1.62)	(-0.21)	
$xSkew$	0.032	0.802	10.785	1.428		0.096	-0.005	38.74
	(0.14)	(1.29)	(1.05)	(2.64)		(1.54)	(-0.098)	

Note: Regressions of the skew swap excess return $xVar$, given by Equation (4.4), and the skew swap excess return $xSkew$, given by Equation (4.9), on explanatory variables based on $(xm^{\text{VIX}}, xm^{\text{SP}}, SMB, HML)$. xm^{VIX} is the excess return of the VIX index, xm^{SP} is the excess return of the S&P 500 and the two Fama-French factors SMB (the size factor) and HML (the book-to-market factor). The t-statistics are computed according to Newey and West (1987). Sample with monthly frequency ranging from January 2010 to July 2015.

The impacts of SMB and HML are insignificant here and this disappointing performance of the two Fama-French factors (i.e. SMB and HML) might be explained by the fact that they are built using two equity portfolios. As mentioned earlier, volatility products can be treated as an asset class itself, with specific properties different from the equity market. Although these two markets are related, the well-known leverage effect being a good example, specific or bespoke factors are needed for this market. A similar problem appeared for the currency market and it is precisely the contribution of Lustig et al. (2011) who propose a common risk factor for that market that they name HML_{FX}. Its relevance was illustrated in Jurek and Xu (2014) on a problem related to carry trade. The results of this work suggest that similar factors, specific to the volatility market, should be built, but this objective is beyond the scope of the present thesis.

Differences between volatility index and equity index markets It is of interest to compare the results obtained here for the volatility index market, through the use of VIX options, and those obtained for the equity index market, through the use of S&P 500 options, analyzed in Kozhan et al. (2013) as these are two different asset classes (i.e. volatility versus equity). It would allow us to assess whether there are structural differences between these two markets. Note that Table 4.2, reporting variables' correlation, already displays important differences to those observed for the S&P 500. Also, the close relationship between the VIX and the S&P 500 suggests considering them jointly. As the most important variables are the skew swap excess return, denoted $xSkew$ in this work while denoted xs in Kozhan et al. (2013), and the variance swap excess return, denoted $xVar$ in this work while denoted xv in Kozhan et al. (2013), the comparison will be restricted to these variables as well as to the regressions involving them.

The first important difference is the correlation between $xSkew$ and $xVar$ that is equal to 0.897 in Kozhan et al. (2013), a value much higher than the 0.607 obtained here, that leads these authors to question whether there are two separate risk premiums. In Kozhan et al. (2013), when regressing the variance swap excess return on equity index excess return, the constant term is significant and a similar conclusion is achieved for the skew swap excess return, suggesting that the CAPM does not hold (see Table 4 of Kozhan et al. (2013)). For the VIX, this conclusion mainly holds for $xVar$, see Table 4.4 column (2) along with Equation (4.13), but for the skew, Table 4.5 column (2) along with Equation (4.20) show that the constant term is not significant.[6]

Regarding the S&P 500 option market, regression of $xVar$ on the equity index excess return xm^{SP} and the skew swap excess return ($xSkew$) leads to an insignificant constant term and similar conclusion can be drawn after swapping $xVar$ and $xSkew$

[6]Note that in this latter case the R^2 is close to zero, so to some extent the conclusion also holds for the skew but the argument is different.

(see Table 5 of Kozhan et al. (2013)). Thus, these authors rightly conclude that $xVar$ is spanned by the pair $(xm^{\text{SP}}, xSkew)$ and $xSkew$ by $(xm^{\text{SP}}, xVar)$. For the VIX market the situation is slightly different as the constant term remains significant only when $xVar$ is regressed on the other two variables, see Table 4.4 column (6) where the t-statistic is found to be -2.03, suggesting that an additional factor is needed to fully explain the variance swap excess return beyond the information provided by xm^{SP} and $xSkew$.

Related to the high correlation level between $xVar$ and $xSkew$ in Kozhan et al. (2013) (i.e. 0.897), whenever one of the variables is used as the explanatory variable while the other is used as a dependent one, the R^2 is extremely high leaving little room for other factors (still these authors found xm^{SP} to be significant). In the VIX case, although there is a decent correlation between $xVar$ and $xSkew$, additional variables such as equity index excess return xm^{SP} or volatility excess return xm^{VIX} do improve the R^2 when $xVar$ is the dependent variable.

Lastly, the coefficient signs remain consistent with intuition for all factor models, and in particular adding a new explanatory variable to a given regression does not change the coefficient signs. From a hedging point of view, it means that one does not have to reverse a position on a given instrument, an aspect that is extremely appealing in practice. This sharply contrasts with Kozhan et al. (2013) as they find a negative coefficient sign for xm^{SP} (equity index excess return) when the skew swap excess return $xSkew$ is regressed on this variable alone (see Table 4 in that paper) while the sign turns out to be positive when the variance swap excess return is added as an explanatory variable. This is a direct consequence of the strong correlation between $xSkew$ and $xVar$ extracted from S&P 500 options. Also, for skew swap excess return the equity index excess return is irrelevant for the volatility option market while it is relevant for the S&P 500 option market. This suggests that, for variables related to volatility higher moments, variables related to equity (index) moments convey little information, and as a result there is an idiosyncratic volatility factor.

These are the salient differences between the equity index option market and the volatility index option market underlining the very specific characteristics of the volatility market with the related consequences in terms of hedging strategies.

4.5 Conclusion

In this chapter, an analysis is provided of variance and skew risk premiums for the volatility market using VIX options and the methodology proposed by Kozhan et al. (2013). It is found that variance swap excess return can be partially explained by equity index and volatility index excess returns along with skew swap excess return. In contrast, to explain skew swap excess return only the variance swap contract is relevant, investing in the equity index (i.e. S&P 500 in that case) is of no use and the volatility index provides no additional information beyond the variance swap contract. Quite remarkably, all the results are consistent with the shape of the smiles observed on the S&P 500 and VIX option markets. Certain results are in sharp contrast to those obtained for the S&P 500 option market, as they underline certain specifics of the volatility market.

This work suggests several extensions. First, applying the methodology to other volatility option markets, such as crude oil for example, should confirm the results obtained here. Second, the availability of exotic volatility options, such as options on leveraged volatility exchange traded funds as presented in Bao et al. (2012), is an alternative to extract implied-moments for the volatility distribution and assessing whether all these products convey consistent information is an important question. These open problems are left for future research.

Chapter 5

Higher Moment Risk Premiums for the Crude Oil Market: A Downside and Upside Conditional Decomposition

5.1 Introduction

Energy commodities have become a major part of financial markets as a result of the rapid growth in trading volume and the variety of derivative products, among which the crude oil futures and options have taken up a significant proportion. Specifically, the trading volume of crude oil futures and options accounted for over 50% of the total trading volume of energy contracts on the New York Mercantile Exchange (NYMEX) in 2015. As for the equity (index) option market, the commodity option market enables the study of variance risk premium, i.e., the premium asked by market participants to invest/trade volatility risk. For the literature on variance risk premium, without being exhaustive, reference is made to Bakshi et al. (2003), Carr and Wu (2009), Trolle and Schwartz (2010) and Prokopczuk and Wese Simen

(2014).

The fact that financial markets react differently to positive and negative shocks has been widely acknowledged in previous literature. Consequently, semivariance measures, considered in Barndorff-Nielsen et al. (2008) or Patton and Sheppard (2015), were found to carry more information than unconditional measures of the equity market. For the specific case of the crude oil market and the relevance of semivariance measures see Chevallier and Sévi (2012) or Sévi (2014). Following that line of research, it is therefore natural to assess whether tail risk premium or conditional variance risk premium carries more information than standard (i.e. unconditional) variance risk premium. In Bollerslev et al. (2015), Lettau et al. (2014) and Kilic and Shaliastovich (2015), it is confirmed that conditional variance risk premium has higher forecasting power for equity index excess returns.

Beyond the variance risk premium, skew risk premium has recently attracted a strong interest among academics. In Kozhan et al. (2013), see also the important and related work of Neuberger (2012), the authors found that skew risk premium naturally completes the variance risk premium for the equity index option market. The specifics of the volatility index option market (i.e. VIX options) are analyzed here with respect to variance and skew risk premiums and show the consistency of the results with the shapes of the volatility smile observed in the equity and volatility index option markets.

Based on these works, this chapter contributes to the literature by performing a conditional decomposition of variance and skew risk premiums extracted from options written on the USO (an exchange traded fund tracking the daily price changes of the WTI light sweet crude oil). The time variation property of these risk premiums is assessed and the relations between these decomposed higher moment risk premiums and the USO excess returns are analyzed. Lastly, how these decomposed higher moment risk premiums enable a much better prediction of USO excess returns are shown.

The chapter is organized as follows. Section 2 presents a formal definition of the key variables used in this work. Section 3 provides a description of the data used in the empirical analysis. The empirical implementation and the results are discussed in Section 4 and Section 5 concludes.

5.2 Pricing formulas

In this part, the variance swap contract and related variables such as variance risk premium, are first presented then the conditional decompositions as well as excess returns of investments made on such contracts. This will allow specification of the notations used throughout this work. The skew swap and related variables that are important for this work are pursued and constitute a contribution to the literature.

5.2.1 Variance risk premiums

The valuation of a variance swap contract of maturity T requires the computation of the fixed leg that is paid at time t, the initiation date of the contract. Let S_t be the underlying asset price at time t, then the log return from t to T is $r_{t,T} = \ln S_T - \ln S_t$. In this work the asset S_t will be the USO, an exchange traded fund tracking the daily price changes of the WTI light sweet crude oil. Firstly, the USO excess return from t to T is defined as

$$xm_{t,T}^{USO} = r_{t,T} - r_{t,T}^{f}, \tag{5.1}$$

where $r_{t,T}^{f} = r^{f}(T-t)$ with r^{f} the risk-free rate.

Following the literature, to value the fixed leg of the swap, Kozhan et al. (2013) proposes the following formula

$$iv_{t,T} = E_t^{Q}[g^{v}(r_{t,T})], \tag{5.2}$$

where $E_t^{Q}[.]$ denotes the risk-neutral expectation conditional on time t and $g^{v}(r) = 2\,(e^{r} - 1 - r)$. A Taylor expansion of this function around zero shows that it is equal to r^2, thus its choice for this product.

It was shown in the literature that any twice-continuously differentiable payoff function can be spanned by a continuum of out-of-the-money (OTM) European calls and puts. Specifically, Kozhan et al. (2013) show that based on the payoff function g^v the risk-neutral variance $iv_{t,T}$ can be expressed as follows

$$\begin{aligned} iv_{t,T} &= 2\int_{S_t}^{+\infty} \frac{C_{t,T}(K)}{B_{t,T}K^2}dK + 2\int_0^{S_t} \frac{P_{t,T}(K)}{B_{t,T}K^2}dK \\ &= iv_{t,T}^u + iv_{t,T}^d, \end{aligned} \tag{5.3}$$

where $C_{t,T}(K)$ and $P_{t,T}(K)$ denote the prices at time t of calls and puts with expiry date T and strike price K, and $B_{t,T}$ is the zero-coupon bond at time t with maturity T. In fact, $iv_{t,T}^u$ and $iv_{t,T}^d$ can be spanned by a continuum of OTM calls and puts, respectively, which correspond to the first and second integrals in Equation (5.3). A detailed proof is presented in Appendix A. The decomposition is quite intuitive, the upside risk-neutral variance $iv_{t,T}^u$ is constructed upon a set of call options that will pay only when the underlying asset return from t to T, i.e. $r_{t,T} = \ln S_T - \ln S_t$, is positive. In fact, it captures the second moment of the upper tail distribution. Likewise, the downside risk-neutral variance $iv_{t,T}^d$ is constructed upon a set of put options that will pay only when the underlying asset return from t to T is negative and, in that case, it captures the second moment of the lower tail distribution. As we have

$$g^v(r_{t,T}) = g^v(r_{t,T})\mathbf{1}_{\{r_{t,T}>0\}} + g^v(r_{t,T})\mathbf{1}_{\{r_{t,T}\leq 0\}}, \tag{5.4}$$

it is natural to also name $iv_{t,T}^u$ and $iv_{t,T}^d$ the upside and downside risk-neutral variances and state

$$\begin{aligned} iv_{t,T}^u &= E_t^Q[g^v(r_{t,T})\mathbf{1}_{\{r_{t,T}>0\}}], \\ iv_{t,T}^d &= E_t^Q[g^v(r_{t,T})\mathbf{1}_{\{r_{t,T}\leq 0\}}]. \end{aligned} \tag{5.5}$$

As there are only a finite number of options available in the market, iv_t^u and iv_t^d can be approximated in practice by the following sums:

$$
\begin{aligned}
iv^u_{t,T} &= 2 \sum_{S_t \leq K_i} \frac{C_{t,T}(K_i)}{B_{t,T} K_i^2} \Delta I(K_i), \\
iv^d_{t,T} &= 2 \sum_{K_i \leq S_t} \frac{P_{t,T}(K_i)}{B_{t,T} K_i^2} \Delta I(K_i),
\end{aligned}
\tag{5.6}
$$

with the weight function $\Delta I(K_i)$ defined as

$$
\Delta I(K_i) = \begin{cases} \frac{K_{i+1} - K_{i-1}}{2}, 0 \leq i \leq N \quad (\text{with } K_{-1} = 2K_0 - K_1, K_{N+1} = 2K_N - K_{N-1}) \\ 0, \quad \text{otherwise.} \end{cases}
$$

By definition of the variance swap contract, the floating leg is given by

$$
rv_{t,T} = g^v(r_{t,T}) = \sum_{i=t}^{T-1} g^v(r_{i,i+1}), \tag{5.7}
$$

where $r_{i,i+1}$ is the daily log return of the underlying asset (so we split the interval $[t \;\; T]$, which will be one-month long in this work, into daily sub-intervals), and $E^P_t[.]$ denotes the historical expectation conditional on time t. Following Kilic and Shaliastovich (2015), the realized variance $rv_{t,T}$ is decomposed into two parts that are related to the two opposite sides of the asset return distribution. More precisely, the following will be written

$$
\begin{aligned}
rv_{t,T} &= \sum_{i=t}^{T-1} g^v(r_{i,i+1}) \mathbf{1}_{\{r_{i,i+1} > 0\}} + \sum_{i=t}^{T-1} g^v(r_{i,i+1}) \mathbf{1}_{\{r_{i,i+1} \leq 0\}} \\
&= rv^u_{t,T} + rv^d_{t,T},
\end{aligned}
\tag{5.8}
$$

where $rv^u_{t,T}$ and $rv^d_{t,T}$ denote the upside and downside realized variances, respectively.

These variables are defined; the payoff of a variance swap (payer of the fixed leg and receiver of the floating leg) is given by $rv_{t,T} - iv_{t,T}$ and after averaging under the historical probability measure, the variance risk premium is obtained. As explained in Kozhan et al. (2013), it is convenient to define the excess return of an investment in the variance swap and this is given by

$$vp_{t,T} = \frac{rv_{t,T}}{iv_{t,T}} - 1. \tag{5.9}$$

The decomposition performed on the variance swap allows the definition of the upside and downside variance swaps as $rv^u_{t,T} - iv^u_{t,T}$ and $rv^d_{t,T} - iv^d_{t,T}$, respectively, as well as the corresponding risk premiums. Here also, it is convenient to define excess returns associated with these swaps and this leads to

$$vp^u_{t,T} = \frac{rv^u_{t,T}}{iv^u_{t,T}} - 1, \quad vp^d_{t,T} = \frac{rv^d_{t,T}}{iv^d_{t,T}} - 1. \tag{5.10}$$

Remark 5 *The decomposition of the variance risk premium into two components follows Kilic and Shaliastovich (2015) where the authors qualified them as "good" (for the upside) and "bad" (for the downside) risk premiums, a naming justified by the fact that they analyze an equity index (the S&P 500) for which a positive (negative) return is often favourably (unfavourably) considered. In the case of crude oil, such naming is inappropriate as too high an oil price leads to a decrease of consumption and a weakening of the economy.*

Remark 6 *In Kilic and Shaliastovich (2015), the decomposition of Equation* (5.8) *is computed using high frequency data and as explained by these authors it is known that, according to Barndorff-Nielsen et al. (2008), under the hypothesis that* $(r_t)_{t\geq 0}$ *satisfies the dynamic* $r_t = \int_0^t \mu_s ds + \int_0^t \sigma_s dw_s + J_t$ *with* $(w_t)_{t\geq 0}$ *a Brownian motion and* J_t *a pure jump process, then the following convergences in probability hold*

$$rv^u_{t,T} \to \frac{1}{2}\int_t^T \sigma_s^2 ds + \sum_{t\leq s\leq T} (\Delta r_s)^2 \mathbf{1}_{\{\Delta r_s \geq 0\}},$$
$$rv^d_{t,T} \to \frac{1}{2}\int_t^T \sigma_s^2 ds + \sum_{t\leq s\leq T} (\Delta r_s)^2 \mathbf{1}_{\{\Delta r_s \leq 0\}},$$

with $\Delta r_s = r_s - r_{s-}$.

For the risk-neutral part of the variance swap, the decomposition in Equation (5.3) *is performed. Note that while the upside risk-neutral variance depends on positive evolutions of the underlying asset over the interval* $[t\ T]$*, the upside realized variance does not and similar remark applies to the downside decomposition. As a result, it does not lead exactly to risk premiums as, by definition, a risk premium requires the same quantity to be computed under the risk-neutral and historical probabilities. Still, these authors will be followed and the average value of* $rv^u_{t,T} - iv^u_{t,T}$ *and* $rv^d_{t,T} - iv^d_{t,T}$ *qualified as risk premiums.*

5.2.2 Skew risk premiums

For the skew swap Kozhan et al. (2013) are closely followed and that work is referred to for further details. These authors propose computing the fixed leg of the swap at time t with maturity T as

$$is_{t,T} = E^Q_t[g^s(r_{t,T})], \tag{5.11}$$

where $g^s(r) = 6\,(2 + r - 2e^r + re^r)$. A Taylor expansion of g^s shows that it behaves like r^3 and this justifies its use to compute the skewness. [1]The expectation in Equation (5.12) can be expressed as a function of a continuum of OTM options as it can be written as

$$is_{t,T} = 3(v^E_{t,T} - iv_{t,T}), \tag{5.12}$$

where the quantity $v^E_{t,T}$ is defined as

$$\begin{aligned} v^E_{t,T} &= \frac{2}{B_{t,T}} \int_{S_t}^{+\infty} \frac{C_{t,T}(K)}{KF_{t,T}} dK + \frac{2}{B_{t,T}} \int_0^{S_t} \frac{P_{t,T}(K)}{KF_{t,T}} dK \\ &= v^{u,E}_{t,T} + v^{d,E}_{t,T}. \end{aligned}$$

Thanks to the decomposition of $iv_{t,T}$ into upside and downside parts and similar

[1]Kozhan et al. (2013) are referred to for an explanation of why the function g^s is used instead of r^3 as well as g^v given in the variance swap section instead of r^2.

decomposition that can also be performed on $v^E_{t,T}$, still denoted by $v^{u,E}_{t,T}$ and by $v^{d,E}_{t,T}$, it is concluded that $is_{t,T}$ can be decomposed as

$$\begin{aligned} is_{t,T} &= 3(v^{u,E}_{t,T} - iv^u_{t,T}) - 3(v^{d,E}_{t,T} - iv^d_{t,T}) \\ &= is^u_{t,T} - is^d_{t,T}. \end{aligned} \tag{5.13}$$

As $is^u_{t,T}$ only involves OTM calls, it depends on the third moment of the underlying asset return conditional on this return to be positive and, as such, it depends on the asset's right or upper tail distribution. A similar remark applies to $is^d_{t,T}$; this time OTM puts are involved and with the difference that it is conditional on the asset return to be negative, so it depends on the asset's left or lower tail distribution. As a result, the following can be written

$$g^s(r_{t,T}) = g^s(r_{t,T})\mathbf{1}_{\{r_{t,T}>0\}} - g^s(|r_{t,T}|)\mathbf{1}_{\{r_{t,T}\leq 0\}}, \tag{5.14}$$

from which is deduced

$$is^u_{t,T} = E^Q_t\left[g^s(r_{t,T})\mathbf{1}_{\{r_{t,T}>0\}}\right], \quad is^d_{t,T} = E^Q_t\left[g^s(|r_{t,T}|)\mathbf{1}_{\{r_{t,T}\leq 0\}}\right]. \tag{5.15}$$

In practice, there are only a finite number of options available in the market, so $v^{u,E}_{t,T}$ and $v^{d,E}_{t,T}$ can be approximated by the following sums:

$$\begin{aligned} v^{u,E}_{t,T} &= 2\sum_{S_t \leq K_i} \frac{C_{t,T}(K_i)}{B_{t,T}K_iF_{t,T}}\Delta I(K_i), \\ v^{d,E}_{t,T} &= 2\sum_{K_i \leq S_t} \frac{P_{t,T}(K_i)}{B_{t,T}K_iF_{t,T}}\Delta I(K_i), \end{aligned} \tag{5.16}$$

with weight function $\Delta I(K_i)$ as previously defined.

Regarding the floating leg of the skew swap, it is in fact the expectation of the payoff function $g^s(r)$ under the physical measure P, and it is given by

$$rs_{t,T} = g^s(r_{t,T}) = \sum_{i=t}^{T-1} g^s(r_{i,i+1}) \tag{5.17}$$

with, as in the previous case, $r_{i,i+1}$ the daily log return of the underlying asset (so we split the interval $[t\ T]$, which will be one-month long in this work, into daily sub-intervals).

The decomposition of Equation (5.14) leads to defining the upside and downside realized skew, namely, $rs^u_{t,T}$ and $rs^d_{t,T}$, and these variables are

$$\begin{aligned} rs^u_{t,T} &= \sum_{i=t}^{T-1} g^s(r_{i,i+1})\mathbf{1}_{\{r_{i,i+1}>0\}}, \\ rs^d_{t,T} &= \sum_{i=t}^{T-1} g^s(|r_{i,i+1}|)\mathbf{1}_{\{r_{i,i+1}\leq 0\}}. \end{aligned} \tag{5.18}$$

The skew swap contract value, payer of the fixed leg and receiver of the floating leg, can be written as $rs_{t,T} - is_{t,T}$ and after averaging under the historical probability measure the skew risk premium is obtained. As for the variance swap, it is convenient to define the excess return of an investment on a skew swap contract as

$$sp_{t,T} = \frac{rs_{t,T}}{is_{t,T}} - 1. \tag{5.19}$$

Lastly, the decompositions performed on the risk-neutral and realized skews lead to defining the upside and downside skew swaps and after averaging under the historical probability measure to obtain the upside and downside skew risk premiums. Again, it is convenient to compute the excess returns associated with these upside and downside skew swaps; they are given by

$$\begin{aligned} sp^u_{t,T} &= \frac{rs^u_{t,T}}{is^u_{t,T}} - 1, \\ sp^d_{t,T} &= \frac{rs^d_{t,T}}{is^d_{t,T}} - 1. \end{aligned} \tag{5.20}$$

To implement these variables, options on crude oil are used where only monthly maturities are available. As a consequence, the risk-neutral expectations can only be evaluated 12 times a year and t will run through the first days following the option maturity dates. Therefore, all the variables are on a monthly basis. Also, to simplify notations the dependency with respect to T is dropped, and iv_t is used instead of $iv_{t,T}$ in the following parts and the same rule applies to all the other variables.

5.3 Data and descriptive statistics

The empirical analysis spans the period from January 2010 to June 2016 and the sample frequency is daily. To compute the variance and skew risk premiums as well as their decompositions, both European call and put options written on the USO from Thomson Reuters Ticker History (TRTH) of SIRCA are obtained.[2] Option information such as Ticker, date, last price, close bid, close ask, expiration date, strike price and option type is extracted and consistently with the pricing formulas presented in the previous section only OTM options are used. As previously mentioned, the empirical study is carried out at monthly frequency, so only one-month maturity options will be used here, and the computation will run through the first days following the option maturity dates.

[2] http://www.sirca.org.au/

Figure 5.1: Evolution of USO price

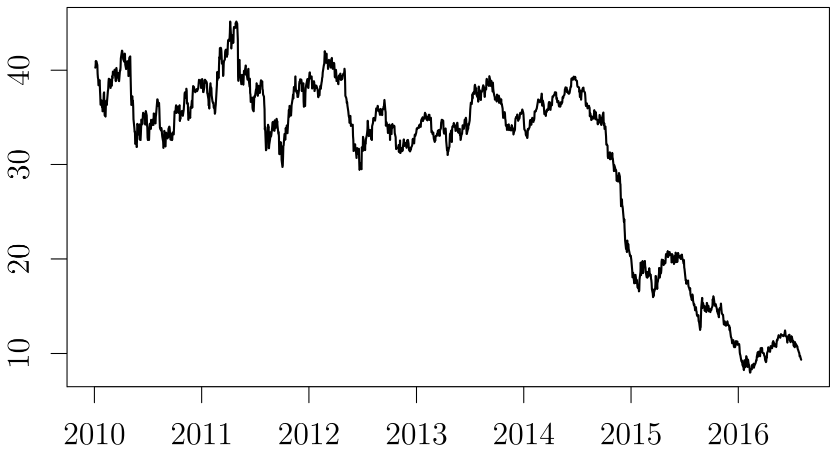

Note: The curve shows the time series of USO price from January 2010 to July 2016. The market went through turmoil in 2015 and 2016.

Also, because the moneyness range of options varies greatly across time, especially for the puts, it is restricted from 0.5 to 2.0 to avoid illiquidity issues caused by deep OTM options. Libor rates are used to proxy the risk-free rates, all of them provided by Bloomberg.

Figure 5.1 contains the evolution of the USO for the period considered while Figure 5.2 illustrates the distribution of its daily log returns as well as the normal distribution having the same mean and standard deviation as the data sample. Compared to the normally distributed curve, the USO density curve exhibits a slightly negative skewness, fatter tails, and a higher peak, it highlights the importance of higher moment risks such as skewness and kurtosis.

Figure 5.3 exhibits the time series of total, upside and downside risk-neutral variances, namely, iv, iv^u and iv^d, from January 2010 to June 2016. The comovement of the three variables demonstrates their positive correlations. In general, the curve of iv^d is above that of iv^u, so the average value of iv^d is expected to be larger, which implies that the variance of the left tail is larger than the variance of the right tail. It can also be seen that compared to iv^d, the curve of iv^u exhibits more spikes.

Figure 5.4 shows the time series of total, upside and downside realized variances, namely, rv, rv^u and rv^d, over the same period. All the three variables are positively correlated as the curves move together, and the moving trend is similar to that of their risk-neutral counterparts. The magnitude of rv^d is slightly larger than that of rv^u but their difference is smaller compared to iv^u and iv^d. Moreover, there are more spikes on the downside realized variance curve compared to the upside realized variance curve.

Figure 5.2: Density curve of USO returns

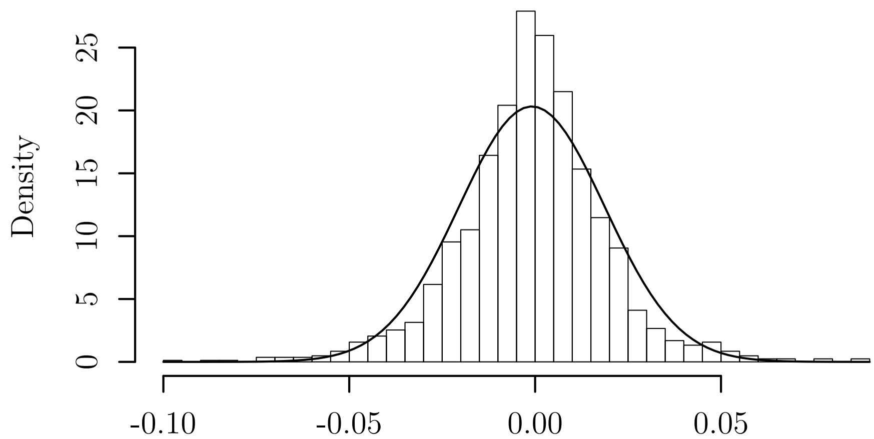

Note: The histogram shows the empirical density of the daily log returns of USO from January 2010 to July 2016. The curve stands for the normal distribution with the same mean and standard deviation of the sample data.

Figure 5.5 displays the time series of total, upside and downside variance risk premiums, namely, vp, vp^u and vp^d. Generally, vp, vp^u and vp^d show similar evolution patterns over time, which suggests positive correlations among the variables. On average, vp, vp^u and vp^d are negative, indicating that positive premiums are paid to hedge against the total, upside and downside volatility of the underlying asset. Moreover, the curve of vp^d shows more larger spikes than that of vp^u. There are

Figure 5.3: Decomposition of risk-neutral variance

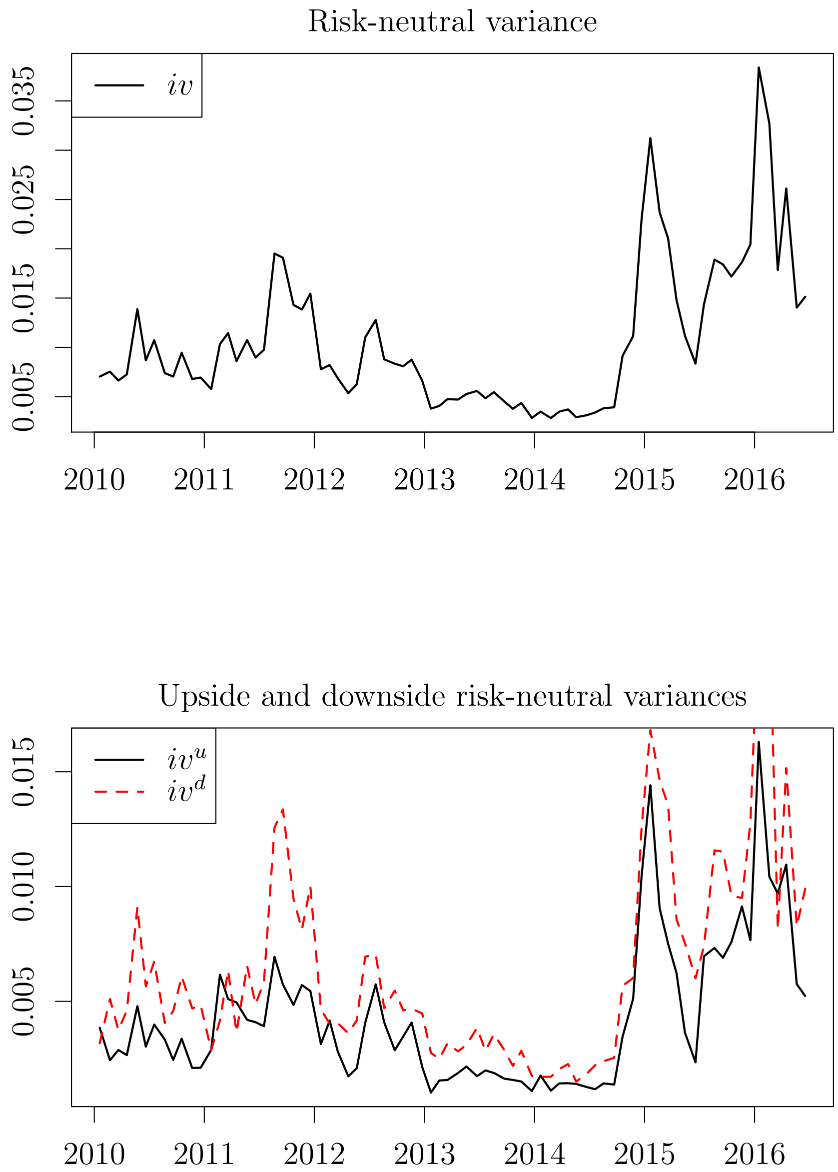

Note: The upper figure shows the evolution of risk-neutral variance (iv, given by Equation (5.3)) from January 2010 to June 2016, based on monthly observations. The lower figure shows the evolutions of upside risk-neutral variance (iv^u, given by Equation (5.6), black solid line) and downside risk-neutral variance (iv^d, given by Equation (5.6), red dashed line) for the same period, also based on monthly observations. In general, the downside risk-neutral variance is greater and more volatile than the upside risk-neutral variance, and the two sum up to the total risk-neutral variance.

Figure 5.4: Decomposition of realized variance

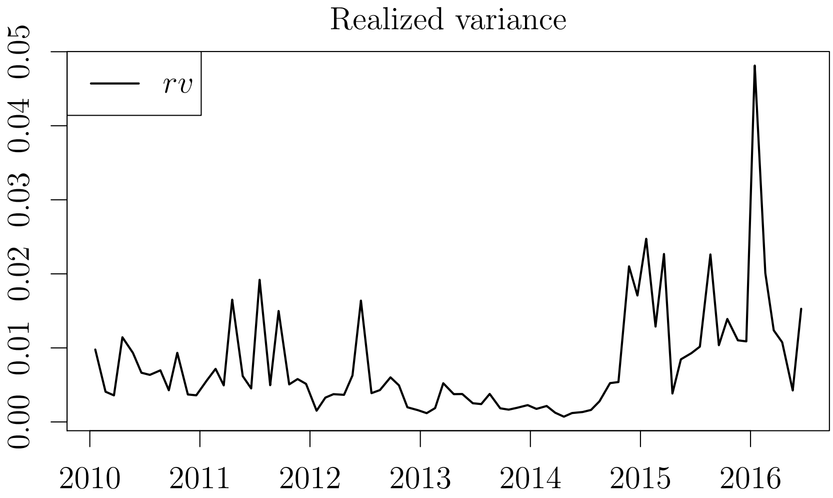

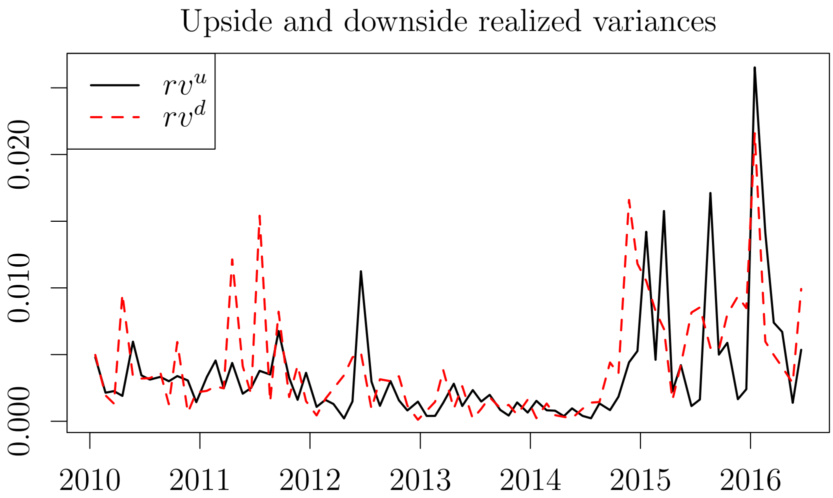

Note: The upper figure shows the evolution of realized variance (rv, given by Equation (5.7)) from January 2010 to June 2016, based on monthly observations. The lower figure shows the evolutions of upside realized variance (rv^u, given by Equation (5.8), black solid line) and downside realized variance (rv^d, given by Equation (5.8), red dashed line) for the same period, also based on monthly observations. In general, the volatility of the downside realized variance is greater than the upside realized variance, and the two sum up to the total realized variance.

mainly two concentrated periods of spikes revealed by the curves of vp^u and vp^d, namely, the period from 2010 to 2012 and the period from 2014 to 2016 during which the crude oil price dropped dramatically. The curves of vp^u and vp^d exhibit spikes at different times, indicating that the decomposed variance premiums are driven by different underlying state variables.

Figure 5.6 shows the time series of total, upside and downside risk-neutral skews, namely, is, is^u and is^d. The comovement of is^u and is^d suggests a positive correlation between these variables. Comparing the upper and lower figures, and consistently with the decomposition of is, is^u captures the positive spikes of is and is^d captures the negative spikes of is. Also of interest is to note that is can remain unchanged from one observation date to the next while is^u and is^d vary substantially. As a result, the disaggregation of is into is^u and is^d can provide additional information. A similar remark applies to iv, although here iv^u and iv^d add up to give iv. Both the average value and volatility of is^d are greater than those of is^u, as the curve of is^d is above that of is^u for the most part and it displays more larger spikes as well.

Figure 5.7 shows the time series of total, upside and downside realized skews, namely, rs, rs^u and rs^d. It depicts a similar moving trend to their risk-neutral counterparts. A positive correlation between rs^u and rs^d can be observed as they comove together. As for the risk-neutral variances, rs^u captures the positive spikes of rs while rs^d captures the negative spikes of rs, as shown in Figure 5.7. Lastly, rs^d reveals higher values on average compared to rs^u.

Figure 5.8 exhibits the time series of total, upside and downside skew risk premiums, namely, sp, sp^u and sp^d. The three variables display distinct extreme values from those of the series in Figures 5.6 and 5.7 as spikes in risk premiums, decomposed or not, are due to strong differences between realized and risk-neutral variables. This suggests that the risk premium components contain different information. Also, during the two crisis periods, namely, years 2010 to 2012 and 2014 to 2016, many spikes are present in sp^u and sp^d curves while for the sp curve there is

Figure 5.5: Decomposition of variance risk premium

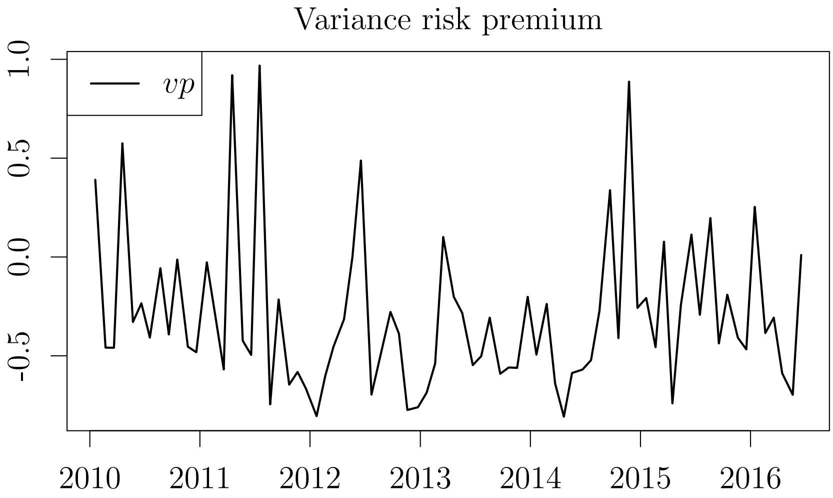

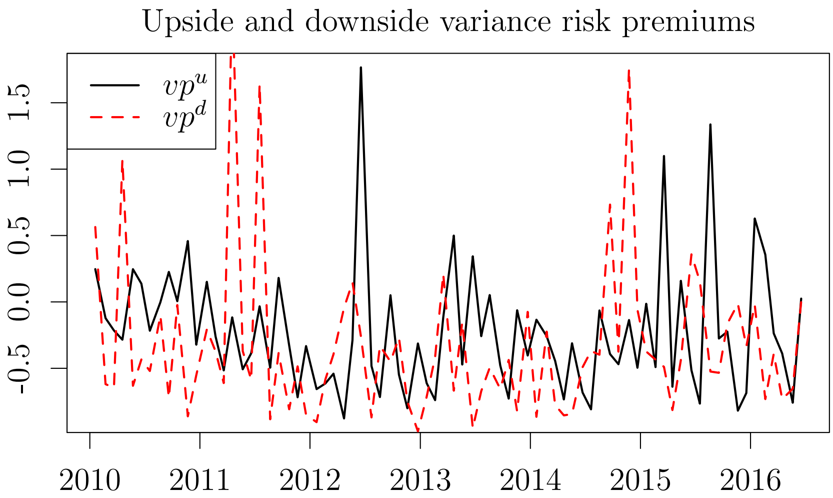

Note: The upper figure shows the evolution of variance risk premium (vp, given by Equation (5.9)) from January 2010 to June 2016, based on monthly observations. The lower figure shows the evolutions of upside variance risk premium (vp^u, given by Equation (5.10), black solid line) and downside variance risk premium (vp^d, given by Equation (5.10), red dashed line) for the same period, also based on monthly observations. In general, the volatility of the downside variance risk premium is greater.

Figure 5.6: Decomposition of risk-neutral skew

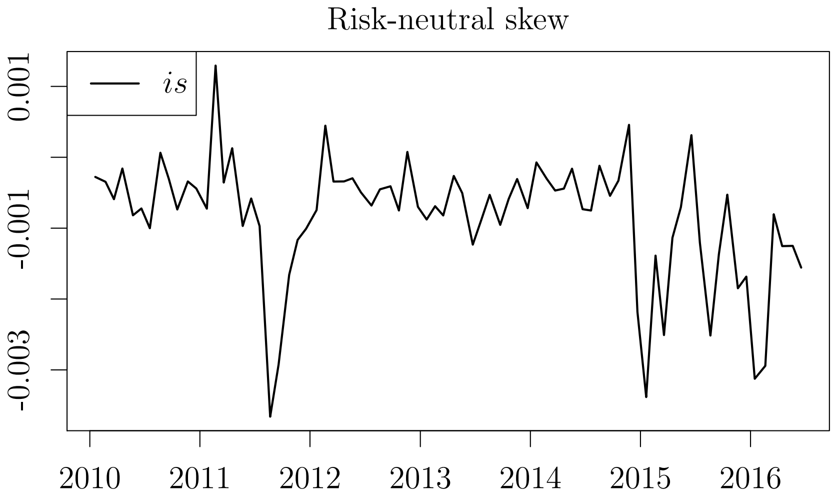

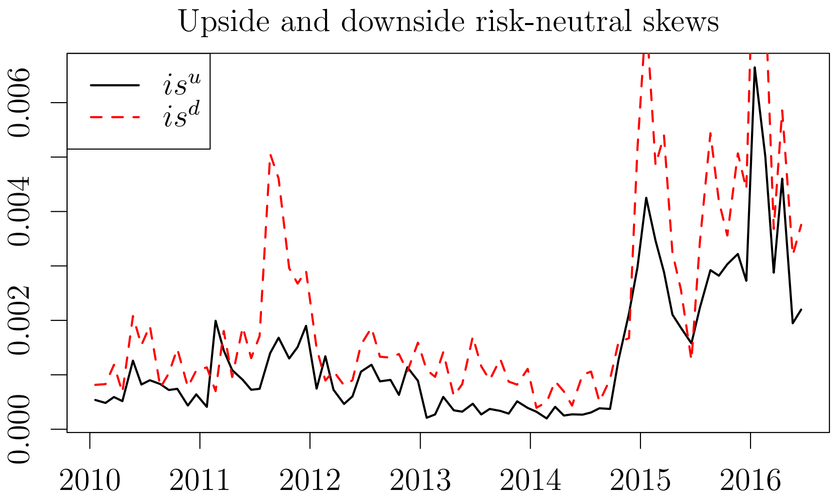

Note: The upper figure shows the evolution of risk-neutral skew (is, given by Equation (5.12)) from January 2010 to June 2016, based on monthly observations. The lower figure shows the evolutions of upside risk-neutral skew (is^u, given by Equation (5.13), black solid line) and downside risk-neutral skew (is^d, given by Equation (5.13), red dashed line) for the same period, also based on monthly observations. In general, the volatility of the downside risk-neutral skew is greater than the upside risk-neutral skew, and the two sum up to the total risk-neutral skew.

Figure 5.7: Decomposition of realized skew

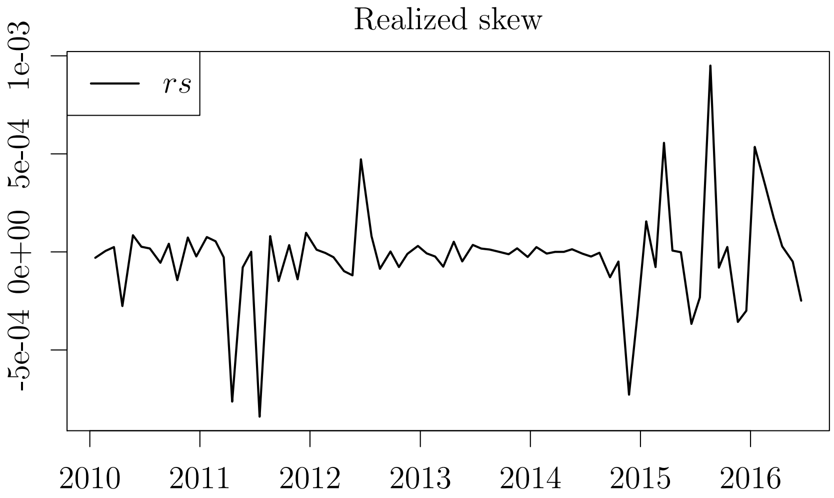

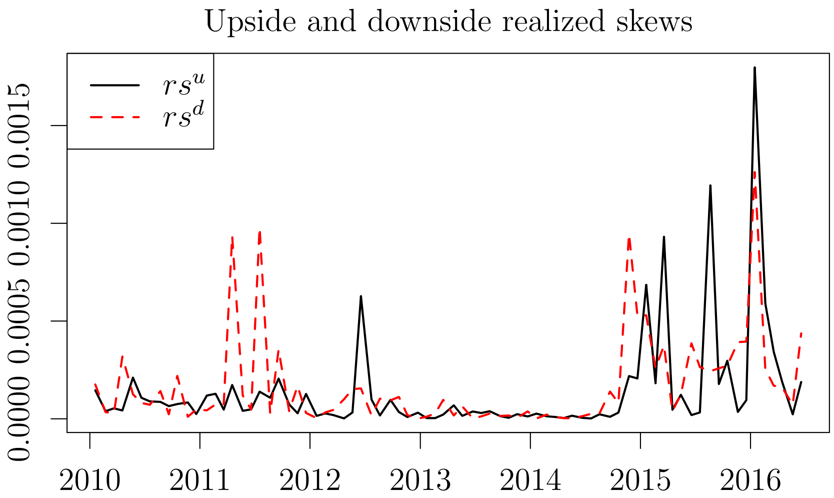

Note: The upper figure shows the evolution of realized skew (rs, given by Equation (5.17)) from January 2010 to June 2016, based on monthly observations. The lower figure shows the evolutions of upside realized skew (rs^u, given by Equation (5.18), black solid line) and downside realized skew (rs^d, given by Equation (5.18), red dashed line) for the same period, also based on monthly observations. In general, the volatility of the downside realized skew is greater than the upside realized skew, and the two sum up to the total realized skew.

Figure 5.8: Decomposition of skew risk premium

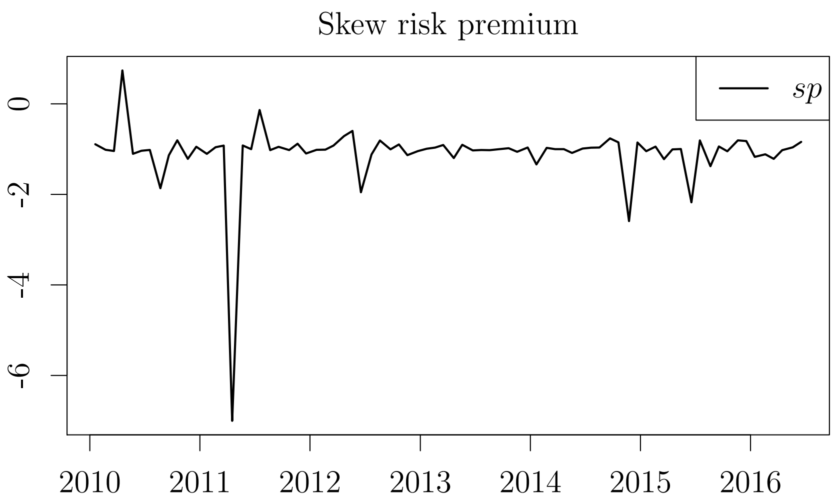

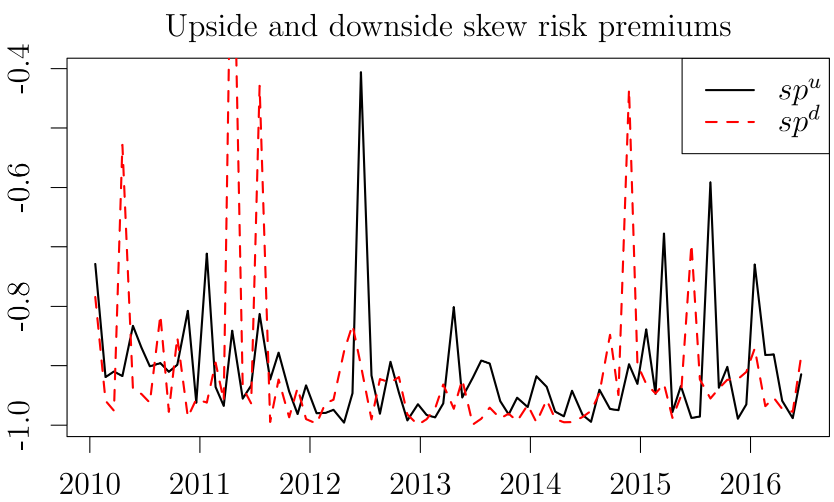

Note: The upper figure shows the evolution of skew risk premium (sp, given by Equation (5.19)) from January 2010 to June 2016, based on monthly observations. The lower figure shows the evolutions of upside skew risk premium (sp^u, given by Equation (5.20), black solid line) and downside skew risk premium (sp^d, given by Equation (5.20), red dashed line) for the same period, also based on monthly observations. In general, the volatility of the downside skew risk premium is greater than the upside skew risk premium.

only one extreme value around 2011. The finding suggests that the sp curve, which aggregates sp^u and sp^d, is less informative than its constituents considered separately. Lastly, the curve of sp^d exhibits larger spikes than that of sp^u.

Table 5.1 reports descriptive statistics such as mean and standard deviation for the realized and risk-neutral variance and skewness. Regarding the variance, either realized or risk-neutral, the downside component is larger than the upside component. A similar remark applies to the skewness, as it results in negative skews (realized and risk-neutral). For both the variance and the skew, the realized values are smaller than the risk-neutral values, which implies that investors are willing to pay in order to hedge variance and skew risks. Lastly, the asymmetry between downside and upside risk-neutral variables (variance and skew) explains the downward slope of the volatility smile observed in the USO option market and is similar to what is known for the equity index options (S&P 500).

Table 5.1: Descriptive statistics of variances and skews

	Mean	Std. dev.		Mean	Std. dev.
rv	7.64e-03	7.48e-03	rs	-2.526e-05	2.422e-04
rv^u	3.54e-03	4.32e-03	rs^u	1.417e-04	2.779e-04
rv^d	4.10e-03	4.09e-03	rs^d	1.670e-04	2.426e-04
iv	10.65e-03	7.36e-03	is	-8.446e-04	8.754e-04
iv^u	4.27e-03	3.10e-03	is^u	1.335e-03	1.257e-03
iv^d	6.38e-03	4.45e-03	is^d	2.179e-03	1.919e-03

Note: Descriptive statistics such as mean, standard deviation for the variables: the realized skew (rs, given by Equation (5.17)), the upside realized skew (rs^u, given by Equation (5.18)) and the downside realized skew (rs^d, given by Equation (5.18)), the risk-neutral skew (is, given by Equation (5.12)), the upside risk-neutral skew (is^u, given by Equation (5.15)) and the downside risk-neutral skew (is^d, given by Equation (5.15)). Sample with monthly frequency ranging from January 2010 to June 2016.

Table 5.2 reports descriptive statistics for the key variables vp, vp^u, vp^d, sp, sp^u and sp^d for the period under study. On average, the variance risk premiums are negative, with the downside variance risk premium as the lowest. Note that in Kilic and Shaliastovich (2015), who investigates the upside and downside variance risk premiums for the S&P 500 market, iv^u is positive while iv^d is negative[3], highlighting

[3]Kilic and Shaliastovich (2015) defines moment risk premium as the difference between risk-neutral and realized moments, it will result in risk a premium of opposite sign than ours.

a difference between equity index and commodity markets. In other words, in the equity market, a downward market movement is bad news but an upward market movement is good news. In sharp contrast, in the commodity market, both upward and downward market shifts are bad news. Regarding the skew risk premiums, all of them are negative. Moreover, it is noted that upside and downside skew risk premiums are quite close. For the standard deviations, both downside variance and skew risk premiums are higher than their upside counterparts and the difference is even larger for the skew. This suggests that the downside skew risk premium is the most sensitive variable to left tail market crashes.

Table 5.2: Descriptive statistics of risk premiums

	Mean	Std. dev.	Q1	Median	Q3
vp	-0.304	0.395	-0.565	-0.408	-0.207
vp^u	-0.239	0.474	-0.531	-0.315	-0.020
vp^d	-0.323	0.605	-0.676	-0.435	-0.178
sp	-1.096	0.808	-1.071	-1.000	-0.919
sp^u	-0.915	0.094	-0.975	-0.938	-0.899
sp^d	-0.912	0.153	-0.981	-0.956	-0.921

Note: Descriptive statistics such as mean, standard deviation, the 25th percentile, median, and 75th percentile for the variables: the variance risk premium (vp, given by Equation (5.9)), the upside variance risk premium (vp^u, given by Equation (5.10)), the downside variance risk premium (vp^d, given by Equation (5.10)), the skew risk premium (sp, given by Equation (5.19)), the upside skew risk premium (sp^u, given by Equation (5.20)) and the downside skew risk premium (sp^d, given by Equation (5.20)). Sample with monthly frequency ranging from January 2010 to June 2016.

Table 5.3: Correlations

	vp	vp^u	vp^d	sp	sp^u	sp^d
vp	1.000	0.487	0.885	-0.339	0.536	0.807
vp^u		1.000	0.051	-0.154	0.899	0.088
vp^d			1.000	-0.418	0.153	0.923
sp				1.000	-0.195	-0.601
sp^u					1.000	0.172
sp^d						1.000

Note: Correlation between the variables: the variance risk premium (vp, given by Equation (5.9)), the upside variance risk premium (vp^u, given by Equation (5.10)) and the downside variance risk premium (vp^d, given by Equation (5.10)), the skew risk premium (sp, given by Equation (5.19)), the upside skew risk premium (sp^u, given by Equation (5.20)) and the downside skew risk premium (sp^d, given by Equation (5.20)). Sample with monthly frequency ranging from January 2010 to June 2016.

Table 5.3 provides a correlation matrix for total, upside and downside variance (skew) risk premiums. Both vp^u and vp^d have strong correlations with vp, as high as 0.487 and 0.885, respectively. As expected, vp^u and vp^d are weakly correlated, only 0.051. In contrast, sp^d has a much higher correlation with sp as -0.601 is found for the former while for the latter it is -0.195. Note that in both cases, downside decompositions carry more information (i.e. higher correlations) with respect to aggregated or unconditional risk premiums than upside decompositions.

5.4 Empirical analysis

In order to deepen our understanding of the information content of the variables constructed in the previous part, namely, the upside and downside variance and skew risk premiums, a thorough empirical analysis of these variables is performed. The first part aims to test time-varying properties of the total and decomposed risk premiums. Time variation of variance and skew risk premiums for the U.S. equity index market (i.e. S&P 500 index options) has been documented in the literature such as Kozhan et al. (2013) while similar conclusion was obtained for the volatility index market (i.e. VIX index options). The second part proposes several factor models for the total as well as decomposed risk premiums using the USO excess return as the explanatory variable. The third part is about predictability of USO excess returns by these variables and to show that upside and downside risk premiums jointly have higher forecasting power than the (unconditional) variance and skew risk premiums. As shown by Bollerslev et al. (2009), the variance risk premium contains significant predictive information for equity index excess returns within a forecast horizon of six months. The more recent work of Kilic and Shaliastovich (2015) decomposed the variance premium into "good" and "bad" variance premiums and further demonstrated that the two components jointly have a stronger predictive power for equity index excess returns over a longer horizon (they study the same data as Bollerslev et al. (2009)). The objective of this thesis is to analyze the predictability of USO excess returns by the upside and downside variance and skew risk premiums over forecast horizons spanning from one week to nine months. The results extend existing results in the literature in both directions. First, along with variance risk premiums (unconditional and conditional) the thesis also considers skew risk premiums (unconditional and conditional), thus it extends the study of Chevallier and Sévi (2013) that analyzes the predictability of crude oil futures returns using the (unconditional) variance risk premium.[4] Second, it underlines the specifics, compared with the equity index option market and volatility index option market, of the crude oil option market.

5.4.1 Time variation of risk premiums

Time variation of variance risk premiums: Following Kozhan et al. (2013), the time variation of the total variance risk premiums are tested by performing the univariate regression of realized variance on risk-neutral variance, as well as the univariate regressions of upside and downside realized variances on upside and downside risk-neutral variances

$$rv_t = \alpha_0 + \alpha_1 iv_t + \epsilon_t^{\alpha}, \tag{5.21}$$

$$rv_t^u = \beta_0 + \beta_1 iv_t^u + \epsilon_t^{\beta}, \tag{5.22}$$

$$rv_t^d = \gamma_0 + \gamma_1 iv_t^d + \epsilon_t^{\gamma}, \tag{5.23}$$

and the results are reported in Table 5.4.

Under the null hypothesis that the variance risk premium is constant over time, the slope should be one and the intercept should be zero. Regarding Equation (5.21), the slope of total risk-neutral variance (iv) is 0.798, thus significantly smaller than 1 (and different from 0), which indicates that vp is time varying. A similar conclusion applies to iv^d as the slope coefficient is 0.528 and highly significant. It contrasts with iv^u as the estimated coefficient in that case is 1.042 and highly significant from

[4]The point of view of Chevallier and Sévi (2013) is somewhat different than ours as they consider along the variance risk premium other explanatory variables such as Han Index, Killian Index and the De RoonS Index, among others.

which it is deduced that the upside variance risk premium is not time varying if Kozhan et al's (2013) interpretation is followed. The empirical results, at least for iv and iv^d, are consistent with Figure 5.5, which shows the time-varying evolutions of total and downside variance risk premiums. Regarding the R^2, the values are as high as 61.29%, 55.28% and 32.08% and all the intercepts are not significantly different from zero.

Table 5.4: Time variation of upside and downside variance premiums

	Const.	iv	iv^u	iv^d	Adj. R^2(%)
rv	-0.0008	0.798***			61.29
	(-0.91)	(8.82)			
rv^u	-0.0009		1.042***		55.28
	(-1.46)		(6.49)		
rv^d	0.0008			0.528***	32.08
	(1.31)			(6.34)	

Note: Regressions of the realized variance (rv, given by Equation (5.7)) on the risk-neutral variance (iv, given by Equation (5.3)), the upside realized variance (rv^u, given by Equation (5.8)) on the upside risk-neutral variance (iv^u, given by Equation (5.3)) and the downside realized variance (rv^d, given by Equation (5.8)) on the downside risk-neutral variance (iv^d, given by Equation (5.3)). The t-statistics are computed according to Newey and West (1987). $*$, $**$ and $***$ denote the significance level of 5%, 1% and 0.1% respectively. Sample with monthly frequency ranging from January 2010 to June 2016.

Time variation of skew risk premiums: To test the dynamics of skew risk premiums, either total, upside or downside skew risk premiums, the following univariate regressions are run

$$rs_t = \alpha_0 + \alpha_1 is_t + \epsilon_t^{\alpha}, \tag{5.24}$$

$$rs_t^u = \beta_0 + \beta_1 is_t^u + \epsilon_t^{\beta}, \tag{5.25}$$

$$rs_t^d = \gamma_0 + \gamma_1 is_t^d + \epsilon_t^{\gamma}, \tag{5.26}$$

and the results reported in Table 5.5.

Regarding Equation (5.24) about the total skew risk premium, the slope is significantly different from zero at 5%, while both slopes of upside and downside skew risk premiums are highly significantly different from one. This indicates that all the skew risk premiums are time varying. Moreover, the R^2 for Equation (5.24) is as low as 10.15%, while for Equations (5.25) and (5.26) they increase to 49.75% and 26.11%, respectively. It is demonstrated that after decomposition, the upside and downside risk-neutral skew provides more information on its realized counterparts.

Table 5.5: Time variation of upside and downside skew premiums

	Const.	is	is^u	is^d	Adj. R^2(%)
rs	-0.0001**	-0.093*			10.15
	(-2.96)	(-2.50)			
rs^u	-0.00006*		0.157***		49.75
	(-2.04)		(5.81)		
rs^d	0.00002			0.066***	26.11
	(0.63)			(4.73)	

Note: Regressions of the realized skew (rs, given by Equation (5.17)) on the risk-neutral variance (is, given by Equation (5.12)), the upside realized variance (rs^u, given by Equation (5.18)) on the upside risk-neutral variance (is^u, given by Equation (5.15)) and the downside realized variance (rs^d, given by Equation (5.18)) on the downside risk-neutral variance (is^d, given by Equation (5.15)). The t-statistics are computed according to Newey and West (1987). $*$, $**$ and $***$ denote the significance level of 5%, 1% and 0.1% respectively. Sample with monthly frequency ranging from January 2010 to June 2016.

5.4.2 Factor models for risk premiums

In this part, to better understand the source of risk premiums, what extent they are related to USO excess returns is analyzed. As previously stated, the ratio expressions given by Equations (5.9), (5.10), (5.19) and (5.20) are adopted, so that the risk premiums can be interpreted as the excess returns of investments made on the corresponding moment swap contracts. For example, vp^d is actually the excess return from an investment made on the downside variance swap contract, for which the value of the floating leg is rv^d and the value of the fixed leg is iv^d. Therefore, the synthetic downside variance swap vp^d enables the buyer of the contract to hedge against an increase of the downside variance. Moreover, for simplicity, the underlying of vp^d is named the downside USO, as it is related to negative USO returns. Similarly, the underlying of vp^u is the upside USO, it is related to positive USO returns. The same interpretation also applies to sp^u and sp^d.

Factor models for total variance and skew risk premiums: Regarding the total variance and skew risk premiums, the following regressions are considered

$$vp_t = \alpha_0 + \alpha_1 xm_t^{USO} + \epsilon_t^{\alpha}, \tag{5.27}$$

$$sp_t = \beta_0 + \beta_1 xm_t^{USO} + \epsilon_t^{\beta}, \tag{5.28}$$

where xm^{USO} denotes the USO monthly excess return starting on day t as defined in Equation (5.1). The results for Equations (5.27) and (5.28) are reported in Table 5.6.

Table 5.6: Market excess returns and risk premiums

	Const.	xm^{USO}	Adj. R^2(%)
vp	-0.314***	-1.450*	10.46
	(-8.01)	(-2.15)	
sp	-1.098***	-0.225	-1.24
	(-15.84)	(-0.22)	
vp^u	-0.198***	2.554***	22.82
	(-3.79)	(4.56)	
sp^u	-0.908***	0.377**	11.66
	(-84.20)	(2.95)	
vp^d	-0.366***	-4.045***	38.16
	(-7.66)	(-4.57)	
sp^d	-0.920***	-0.726**	19.22
	(-66.13)	-3.23	

Note: The table shows to what extent the risk premiums, namely, the variance premium (vp, given by Equation (5.9)), the skew premium (sp, given by Equation (5.19)), the upside variance premium (vp^u, given by Equation (5.10)), the upside skew premium (sp^u, given by Equation (5.20)), the downside variance premium (vp^d, given by Equation (5.10)) and the downside skew premium (sp^d, given by Equation (5.20)), can be explained by the USO excess return (xm^{USO}, given by Equation (5.1)). The t-statistics are computed according to Newey and West (1987). $*$, $**$ and $***$ denote the significance level of 5%, 1% and 0.1% respectively. The monthly observations range from January 2010 to June 2016.

The first regression leads to a highly significant and negative coefficient for xm^{USO} and R^2 of 10.44%, and the coefficient's sign is consistent with the leverage effect implied by the negative slope of the volatility smile observed on USO options. If the market goes down, i.e., a negative value for xm^{USO}, it will lead to an increase of market volatility and thus an increase of vp. Furthermore, as the market volatility increases, the left tail of USO distribution grows larger and will result in a volatility smile with a steeper slope. The coefficient of xm^{USO} in the second regression is not significantly different from zero, so the relationship between xm^{USO} and sp cannot be confirmed here. Note that xm^{USO} explains more vp than sp.

Factor models for upside variance and skew risk premiums: It is considered whether the upside variance and skew risk premiums, which can be interpreted as the excess return of investments made on those swap contracts, can be explained by market excess returns. The following regressions are run

$$vp_t^u = \alpha_0 + \alpha_1 xm_t^{USO} + \epsilon_t^{\alpha}, \tag{5.29}$$

$$sp_t^u = \beta_0 + \beta_1 xm_t^{USO} + \epsilon_t^{\beta}, \tag{5.30}$$

with the estimation results reported in Table 5.6. Regarding the regression for the upside variance risk premium, the slope estimate is positive and highly significant and indicates that a positive relationship exists between the USO excess return and upside variance risk premium. Similarly, Equation (5.30) also leads to a positive and significant coefficient for xm^{USO}, thus a positive relationship also exists between the USO excess return and upside skew risk premium. Also, the R^2 for Equation (5.29) is 22.82% while it is 11.66% for Equation (5.30), indicating that xm^{USO} explains more the variable vp^u than sp^u. Moreover, before decomposition, xm^{USO} contributes only to 10.44% of vp (the regression Equation (5.27)), while after decomposition, xm^{USO} contributes to 22.82% of vp^u. A similar remark applies to sp and sp^u, as xm^{USO} is not correlated to the former while it explains a considerable part of the latter.

Factor models for downside variance and skew risk premiums: Univariate regressions of downside variance and skew risk premiums on the USO excess return are performed

$$vp_t^d = \alpha_0 + \alpha_1 xm_t^{USO} + \epsilon_t^{\alpha}, \tag{5.31}$$

$$sp_t^d = \beta_0 + \beta_1 xm_t^{USO} + \epsilon_t^{\beta}, \tag{5.32}$$

and the results are reported in Table 5.6. The coefficients for vp^d and sp^d are both negative and significant, the R^2 are equal to 38.16% and 19.22% for Equations (5.31) and (5.32), respectively. Similarly to the previous case, xm^{USO} explains more of vp^d than sp^d. In conclusion, the higher the risk premium moment order, the less xm^{USO} can explain. Interestingly, xm^{USO} explains more vp^d than vp or vp^u. Likewise, among sp, sp^u and sp^d, xm^{USO} explains more of sp^d.

5.4.3 Predictability

Predictability by upside and downside variance risk premiums: In this part, the focus is on the role of upside and downside variance risk premiums in predicting USO excess returns. The following regressions are considered

$$xm_{t,h}^{USO} = \alpha_{0,h} + \alpha_{1,h} vp_t + \epsilon_t^{\alpha}, \tag{5.33}$$

$$xm_{t,h}^{USO} = \beta_{0,h} + \beta_{1,h} vp_t^u + \epsilon_t^{\beta}, \tag{5.34}$$

$$xm_{t,h}^{USO} = \gamma_{0,h} + \gamma_{1,h} vp_t^d + \epsilon_t^{\gamma}, \tag{5.35}$$

$$xm_{t,h}^{USO} = \delta_{0,h} + \delta_{1,h} vp_t^u + \delta_{2,h} vp_t^d + \epsilon_t^{\delta}, \tag{5.36}$$

where h denotes the horizon of prediction and $xm_{t,h}^{USO}$ denotes the future USO excess return over the horizon h that is computed as

$$xm_{t,h}^{USO} = \frac{1}{h}\sum_{i=0}^{h} r_{t+i,T+i} - r_{t+h,T+h}^f, \tag{5.37}$$

with $r_{t,T}$ and $r_{t,T}^f$ representing the monthly USO return, as previously defined, and the monthly risk-free rate starting at day t and ending at time T, respectively. The results for Equations (5.33) - (5.36) are presented in Table 5.7.

Equation (5.33) analyzes the predictability of USO excess returns by the variance risk premium over various time horizons ranging from one week to nine months. The regression results show that vp remains a significant predictor variable only over a short horizon of two weeks, with a low R^2 of 6.70%.[5] In contrast, Bollerslev et al. (2009) demonstrate that variance risk premium serves as a significant predictor for equity index returns over a forecasting horizon of six months, which is much longer than the two-week horizon in the crude oil market, and illustrates a first difference between the equity index market and the crude oil market. Also, the coefficient of vp in Equation (5.33) is negative, which indicates that investors are willing to pay a premium to hedge against the volatility of the underlying asset (i.e. the USO) regardless of the moving direction.

Table 5.7: Market return prediction using upside and downside variance premiums

		xm^{USO}						
		1w	2w	1m	2m	3m	6m	9m
1	Const.	-0.035*	-0.030	-0.022	-0.017	-0.015	-0.013	-0.013
		(-2.49)	(-1.91)	(-1.29)	(-0.89)	(-0.71)	(-0.59)	(-0.83)
	vp	-0.074***	-0.057*	-0.032	-0.013	-0.008	0.002	0.005
		(-3.33)	(-2.44)	(-1.34)	(-0.75)	(-0.42)	(0.18)	(0.49)
	Adj. R^2(%)	9.84	6.70	1.64	-0.65	-1.05	-1.38	-1.07
2	Const.	0.006	0.002	0.0007	-0.003	-0.006	-0.010	-0.012
		(0.57)	(0.21)	(0.06)	(-0.23)	(-0.40)	(-0.55)	(-0.87)
	vp^u	0.083***	0.068***	0.060***	0.043***	0.029**	0.014	0.010
		(5.21)	(5.30)	(4.84)	(4.08)	(2.81)	(1.77)	(1.24)
	Adj. R^2(%)	19.91	15.93	14.27	9.29	5.28	2.29	1.35
3	Const.	-0.041**	-0.035**	-0.029*	-0.022	-0.018	-0.015	-0.014
		(-3.29)	(-2.85)	(-2.23)	(-1.61)	(-1.16)	(-0.67)	(-0.92)
	vp^d	-0.089***	-0.070***	-0.049***	-0.028***	-0.018*	-0.004	0.0002
		(-4.84)	(-4.33)	(-3.57)	(-3.88)	(-2.06)	(-0.75)	(0.030)
	Adj. R^2(%)	35.56	26.73	14.53	5.46	2.48	-0.94	-1.47
4	Const.	-0.023	-0.020	-0.015	-0.012	-0.012	-0.011	-0.012
		(-1.90)	(-1.77)	(-1.38)	(-1.11)	(-0.87)	(-0.66)	(-0.96)
	vp^u	0.088***	0.071***	0.063***	0.045***	0.030**	0.015	0.010
		(6.78)	(6.06)	(5.21)	(4.00)	(2.73)	(1.82)	(1.30)
	vp^d	-0.092***	-0.072***	-0.051***	-0.029***	-0.019*	-0.005	-0.0001
		(-5.41)	(-4.77)	(-3.97)	(-4.24)	(-2.21)	(-0.95)	(-0.03)
	Adj. R^2(%)	58.67	45.16	30.56	15.62	8.18	1.47	-0.12

Note: The table shows the predictability of future USO excess returns (xm^{USO}) which is defined as Equation (5.37), by using the variance premium (vp, given by Equation (5.9)) alone, and using the upside variance premium (vp^u, given by Equation (5.10)) and downside variance premium (vp^d, given by Equation (5.10)) jointly. The forecasting horizon h can be 1 week (1w), 2 weeks (2w), 1 month (1m), 2 months (2m), 3 months (3m), 6 months (6m) and 9 months (9m). The t-statistics are computed according to Newey and West (1987). $*$, $**$ and $***$ to denote the significance level of 5%, 1% and 0.1% respectively. The monthly observations range from January 2010 to June 2016.

[5] In fact it is an adjusted R-square but the term "adjusted" is omitted hereafter.

For comparison, Equation (5.34) investigates the predictability of USO excess returns by the upside variance risk premium over various forecasting horizons. Compared to vp, the predictive information of vp^u remains significant over the much longer horizon of three months. For the three-month ahead USO excess return regression, vp^u is only moderately significant and leads to a low R^2 of 5.28%. Considering the forecasting horizon of two months, the coefficient of vp^u is highly significant with an R^2 of 15.93% and suggests that vp^u contains more predictive information than vp.

Equation (5.35) investigates the predictive information of vp^d for the USO excess return xm^{USO}. For the two-week forecasting horizon, vp^d is highly significant with an R^2 of 26.73%, thus vp^d is the most informative variable among vp, vp^u and vp^d. Moreover, the longest forecastable horizon for vp^d is three months, even though vp^d is lowly significant in that case (i.e. the t-statistic is at a significance level of 5%).

The results of univariate regressions from the previous parts show that among the total and decomposed variance risk premiums, the latter, and especially vp^d, work better as predictor variables, in terms of forecasting horizons and level of significance, and generally vp^d contributes a little more to explain the future USO excess returns than vp^u. The joint predictive information of vp^u and vp^d for USO excess returns in Equation (5.36) is further analyzed. Compared to the univariate regressions, the R^2 increases for all forecasting horizons, which underlines the complementary contributions of vp^u and vp^d. Naturally, the R^2 decreases from 58.67% to 8.18% when the forecasting horizon increases from one week to three months, where for the three-month horizon vp^u is only moderately significant while vp^d is lowly significant. For the two-week ahead USO excess return, vp^u and vp^d jointly contribute to explain 45.16% of xm^{USO}, with both coefficients highly significant. In summary, it is statistically important to include upside and downside variance premiums to better predict future USO returns.

Predictability by upside and downside skew risk premiums: In this part, similar analysis is carried out for the predictability of USO excess returns by upside and downside skew risk premiums and a comparison is performed when the total skew risk premium is used. The following regressions are run

$$xm_{t,h}^{USO} = \alpha_{0,h} + \alpha_{1,h} sp_t + \epsilon_t^{\alpha}, \tag{5.38}$$

$$xm_{t,h}^{USO} = \beta_{0,h} + \beta_{1,h} sp_t^u + \epsilon_t^{\beta}, \tag{5.39}$$

$$xm_{t,h}^{USO} = \gamma_{0,h} + \gamma_{1,h} sp_t^d + \epsilon_t^{\gamma}, \tag{5.40}$$

$$xm_{t,h}^{USO} = \delta_{0,h} + \delta_{1,h} sp_t^u + \delta_{2,h} sp_t^d + \epsilon_t^{\delta}, \tag{5.41}$$

and the results are reported in Table 5.8.

Table 5.8: Market return prediction using upside and downside skew premiums

		xm^{USO}						
		1w	2w	1m	2m	3m	6m	9m
1	Const.	-0.010	-0.009	-0.007	-0.010	-0.007	-0.011	-0.013
		(-0.56)	(-0.57)	(-0.48)	(-0.67)	(-0.40)	(-0.45)	(-0.85)
	sp	0.002	0.003	0.005	0.002	0.005	0.002	0.001
		(0.15)	(0.22)	(0.54)	(0.42)	(1.55)	(0.79)	(0.39)
	Adj. R^2(%)	-1.28	-1.24	-1.02	-1.25	-0.82	-1.22	-1.43
2	Const.	0.281***	0.257***	0.251***	0.192***	0.127*	0.053	0.043
		(4.27)	(4.75)	(4.71)	(3.98)	(2.42)	(1.47)	(1.23)
	sp^u	0.321***	0.296***	0.290***	0.224***	0.153*	0.072	0.063
		(4.13)	(4.59)	(4.56)	(3.87)	(2.46)	(1.38)	(1.24)
	Adj. R^2(%)	11.54	12.09	13.45	10.35	6.06	2.50	3.07
3	Const.	-0.265**	-0.222**	-0.164**	-0.091***	-0.060*	-0.015	-0.007
		(-2.94)	(-2.79)	(-2.61)	(-3.33)	(-2.34)	(-0.74)	(-0.48)
	sp^d	-0.277**	-0.229**	-0.165**	-0.086***	-0.051*	-0.002	0.008
		(-2.97)	(-2.81)	(-2.63)	(-3.46)	(-2.40)	(-0.10)	(0.48)
	Adj. R^2(%)	20.95	17.46	9.91	2.67	0.61	-1.40	-1.29
4	Const.	0.063	0.074	0.114	0.115*	0.079	0.046	0.044
		(0.65)	(0.86)	(1.49)	(2.16)	(1.53)	(1.14)	(1.22)
	sp^u	0.403***	0.365***	0.341***	0.253***	0.171*	0.075	0.062
		(5.14)	(5.12)	(4.79)	(3.98)	(2.52)	(1.50)	(1.43)
	sp^d	-0.321***	-0.269**	-0.203**	-0.114***	-0.070**	-0.010	0.002
		(-3.32)	(-3.21)	(-3.19)	(-4.16)	(-3.08)	(-0.66)	0.11
	Adj. R^2(%)	39.83	36.41	28.91	16.03	8.32	1.27	1.63

Note: The table shows the predictability of future USO excess returns (xm^{USO}) which is defined as Equation (5.37), by using the variance premium (sp, given by Equation (5.19)) alone, and using the upside variance premium (sp^u, given by Equation (5.20)) and downside variance premium (sp^d, given by Equation (5.20)) jointly. The forecasting horizon h can be 1 week (1w), 2 weeks (2w), 1 month (1m), 2 months (2m), 3 months (3m), 6 months (6m) and 9 months (9m). The t-statistics are computed according to Newey and West (1987). $*$, $**$ and $***$ denote the significance level of 5%, 1% and 0.1% respectively. The monthly observations range from January 2010 to June 2016.

Equation (5.38) focuses on the predictability of USO excess returns by the total skew risk premium (sp) over horizons ranging from one week to nine months. The results show that sp does not contain any predictive information about xm^{USO}, as the coefficients are insignificant and the R^2 are low for all horizons. In contrast, as previously shown, the total variance risk premium (vp) contains significant predictive information regarding xm^{USO} for a forecasting horizon of up to two weeks.

Equation (5.39) investigates the predictive information for xm^{USO} contained in the upside skew risk premium (sp^u) over the same forecasting horizons. The coefficient of sp^u remains significant up to an horizon of three months, even though the significance level at three months is only at 5%. Unlike sp, sp^u contains predictive information for xm^{USO} as suggested by both the significant coefficients and the R^2. Moreover, sp^u is positively correlated with future USO excess returns as the coefficients of sp^u remain positive for all horizons. Note that the intercept term is also significant for up to three months.

For comparison, Equation (5.40) analyzes the predictive information for xm^{USO} contained in the downside skew risk premium (sp^d). Similarly to the case of sp^u, both the intercept and slope of sp^d remain significant for up to three months but note that the R^2 only remain decent, that is to say above 10%, for horizons up to one month. Here also, the constant terms remain significant and of constant sign for forecasting horizons less than or equal to three months. The negative sign of sp^d shows that sp^d is negatively correlated to xm^{USO}.

Equation (5.41) further analyzes the joint predictive information of sp^u and sp^d for xm^{USO}. Firstly, both sp^u and sp^d remain significant up to three months, with a high degree of significance for shorter horizons. Compared to the univariate regressions on sp^u and sp^d, for all the horizons, the R^2 is much higher and larger than the sum of the R^2 of the univariate regressions. This suggests that these variables not only do not have redundant information but, indeed, have complementary information. The constant terms that were significant in the univariate regressions are no longer significant (except for the two-month regression). Lastly, the coefficient signs are consistent with those of the univariate regressions. Again, decomposed skew risk premiums have a much stronger predictive power for USO excess returns than the (undecomposed) skew risk premium.

Predictability by combining upside and downside risk premiums: The previous two parts demonstrate the advantage of decomposing variance and skew risk premiums. In this part, the impact of this decomposition is further explored by considering the predictability of USO excess returns by combining upside variance and skew risk premiums as explanatory variables on the one hand and downside variance and skew risk premiums as explanatory variables on the other. Lastly, also considered are the combination of upside and downside variance and skew risk premiums. For simplicity, the total higher moment risk premiums are used to refer to the total variance risk premium and the total skew risk premium. Similarly, the upside (downside) higher moment risk premiums are used to refer to the upside (downside) variance risk premium and the upside (downside) skew risk premium. The following regressions are run

$$xm_{t,h}^{USO} = \alpha_{0,h} + \alpha_{1,h} vp_t + \alpha_{1,h} sp_t + \epsilon_t^{\alpha}, \tag{5.42}$$

$$xm_{t,h}^{USO} = \beta_{0,h} + \beta_{1,h} vp_t^u + \beta_{2,h} sp_t^u + \epsilon_t^{\beta}, \tag{5.43}$$

$$xm_{t,h}^{USO} = \gamma_{0,h} + \gamma_{1,h} vp_t^d + \gamma_{2,h} sp_t^d + \epsilon_t^{\gamma}, \tag{5.44}$$

$$xm_{t,h}^{USO} = \delta_{0,h} + \delta_{1,h} vp_t^u + \delta_{1,h} vp_t^d + \delta_{1,h} sp_t^u + \delta_{1,h} sp_t^d + \epsilon_t^{\delta}, \tag{5.45}$$

and the results reported in Table 5.9.

Equation (5.42) shows that total higher moment risk premiums can forecast USO excess returns only for a horizon of two weeks as beyond that horizon the R^2 is close to zero and only the variance variable is significant. In sharp contrast, upside high moment risk premiums, given by Equation (5.43), and downside high moment risk premiums, given by Equation (5.44), lead to a forecast of USO excess returns for up to two months, thus confirming the interest of decomposition for forecasting. For the upside higher moment risk premiums the variance seems to contain all the information as it is the only significant variable and, as a result, the R^2 obtained for these regressions are close to those obtained when only the upside variance variable is used. For the do-

Table 5.9: Market return prediction using upside and downside variance and skew premiums

		xm^{USO}						
		1w	2w	1m	2m	3m	6m	9m
1	Const.	-0.050**	-0.040*	-0.023	-0.017	-0.009	-0.010	-0.010
		(-2.84)	(-2.08)	(-1.19)	(-0.79)	(-0.37)	(-0.39)	(-0.78)
	vp	-0.082***	-0.062**	-0.032	-0.013	-0.005	0.003	0.006
		(-3.73)	(-2.63)	(-1.37)	(-0.73)	(-0.24)	(0.35)	(0.53)
	sp	-0.012	-0.008	-0.0004	0.00005	0.004	0.003	0.002
		(-1.17)	(-0.82)	(-0.05)	(0.01)	(0.87)	(0.85)	(0.70)
	Adj. R^2(%)	9.64	5.98	0.32	2.01	-2.10	-2.55	-2.37
2	Const.	-0.226	-0.026	0.100	0.144	0.099	0.032	0.074
		(-1.60)	(-0.19)	(0.70)	(0.97)	(0.64)	(0.26)	(0.82)
	vp^u	0.132***	0.074*	0.039	0.012	0.007	0.005	-0.008
		(3.70)	(2.18)	(1.12)	(0.35)	(0.20)	(0.19)	(-0.40)
	sp^u	-0.267	-0.033	0.114	0.169	0.121	0.048	0.098
		(-1.64)	(0.84)	(0.68)	(0.94)	(0.63)	(0.30)	(0.84)
	Adj. R^2(%)	20.54	14.84	13.57	9.31	4.85	1.20	1.96
3	Const.	0.251**	0.129	0.061	0.077	0.066	0.062	0.029
		(2.88)	(1.45)	(0.68)	(0.78)	(0.58)	(0.70)	(0.63)
	vp^d	-0.169***	-0.115***	-0.073*	-0.055	-0.041	-0.025	-0.012
		(-6.06)	(-4.12)	(-2.42)	(-1.64)	(-1.03)	(-0.83)	(-0.76)
	sp^d	0.349***	0.196	0.107	0.118	0.101	0.091	0.052
		(3.30)	(1.79)	(0.94)	(0.92)	(0.68)	(0.75)	(0.96)
	Adj. R^2(%)	40.03	27.83	14.09	5.31	2.28	-0.21	-1.87
4	Const.	0.270	0.306	0.307	0.324	0.239	0.120	0.119
		(1.65)	(1.76)	(1.67)	(1.51)	(0.89)	(0.70)	(1.42)
	vp^u	0.070*	0.025	0.004	-0.012	-0.010	-0.0003	-0.010
		(2.43)	(0.83)	(0.13)	(-0.32)	(-0.25)	(-0.01)	(-0.59)
	vp^d	-0.155***	-0.108***	-0.070*	-0.055	-0.041	-0.024	-0.013
		(-5.30)	(-3.62)	(-2.25)	(-1.72)	(-0.99)	(-0.94)	(-0.84)
	sp^u	0.077	0.245	0.317	0.304	0.213	0.075	0.107
		(0.57)	(1.59)	(1.76)	(1.58)	(1.03)	(0.56)	(1.23)
	sp^d	0.270*	0.137	0.057	0.087	0.081	0.080	0.046
		(2.18)	(1.11)	(0.49)	(0.75)	(0.56)	(0.80)	(0.91)
	Adj. R^2(%)	60.85	46.26	32.07	17.60	8.74	0.91	-0.02

Note: The table compares the predictability of future USO excess returns (xm^{USO}) which is defined as Equation (5.37), by dividing the risk premiums into two groups: the upside variance and skew premiums and the downside variance and skew premiums. The forecasting horizon h can be 1 week (1w), 2 weeks (2w), 1 month (1m), 2 months (2m), 3 months (3m), 6 months (6m) and 9 months (9m). The t-statistics are computed according to Newey and West (1987). $*$, $**$ and $***$ denote the significance level of 5%, 1% and 0.1% respectively. The monthly observations range from January 2010 to June 2016.

wnside higher moment risk premiums and for short horizons, both the variance and skew are significant, and in that case the R^2 is higher than those obtained when regressing on the downside variance alone (i.e. Equation (5.35)) or the downside skew alone (i.e. Equation (5.40)), whereas for longer horizons the variance is the only significant variable with the natural consequence that the R^2 in those cases are close to those obtained when regressing on the variance alone. Lastly, in Equation (5.45), all the variables are considered, which leads to regressions with very large R^2 for up to two months and among all the variables vp^d seems to be the most important. The coefficients' signs are consistent with those obtained in the previous regressions. Note also that there is a complementary effect between upside and downside variables as the R^2 in a given regression involving these variables largely dominates those obtained when only upside or downside variables are used and further confirms, if need be, the interest of the decomposition proposed in this work.

5.5 Conclusion

In this chapter, we provide a comprehensive analysis of the total and decomposed variance and skew risk premiums for the USO, an exchange traded fund tracking the daily price changes of the WTI light sweet crude oil. So far, most of the literature mainly discusses the use of decomposed variance risk premiums for the S&P 500 option market. This chapter contributes to the literature by extending the analysis of decomposed variance risk premiums to the crude oil market, but also extends the discussion to skew risk premiums. To build these variables two key works are relied upon: the decomposition proposed by Kilic and Shaliastovich (2015) for the variance risk premium, and the computation methodology for variance and skew risk premiums developed by Kozhan et al. (2013).

Three main findings are found: firstly, all the risk premiums, no matter whether they are decomposed or not, are time varying; secondly, if one factor model is applied to the total, upside and downside variance and skew risk premiums with the USO excess returns as explanatory variable, it is found that this better explains the decomposed higher moment risk premiums (both variance and skew) than their total counterparts; thirdly, by analyzing the predictability of crude oil market excess returns by decomposed variance and skew risk premiums, it is found that the decomposed high moment risk premiums contain much more predictive information than their undecomposed counterparts. The downside higher moment risk premiums, the variance and to a lesser extent the skewness, are especially informative about future evolutions of the crude oil market excess return.

It would be interesting to fully explore how the decomposed risk premiums combine with observable economic variables commonly used in the literature, see for example Chevallier and Sévi (2013), for analyzing the crude oil market. Also, other commodity markets such as gas and gold option markets could be considered along with commodity volatility option markets. These open questions are left for further research.

5.6 Appendix

Proof. of decomposition of risk-neutral variance and skew. Following Bakshi et al. (2003), any twice-continuously differentiable function $H(S)$ where S is spot price of the underlying can be spanned by a position in bonds, stocks and out-of-money options

$$H(S) = H(\bar{S}) + (S - \bar{S})H_S(\bar{S}) + \int_{\bar{S}}^{\infty} H_{SS}(K)(S-K)^+ dK + \int_0^{\bar{S}} H_{SS}(K)(K-S)^+ dK.$$

Under risk-neutral measure Q, the arbitrage-free price of the contingent claim with payoff $H(S)$ is

$$\begin{aligned} E^Q[e^{-r_f(T-t)}H(S)] = \left(H(\bar{S}) - \bar{S}H_S(\bar{S})\right) e^{-r_f(T-t)} + H_S(\bar{S})S_t \\ + \int_{\bar{S}}^{\infty} H_{SS}(K)C(t,T;K)dK + \int_0^{\bar{S}} H_{SS}(K)P(t,T;K)dK. \end{aligned} \tag{5.46}$$

Specifically, Kozhan et al. (2013) define the payoff function for the variance swap contract as $g^v(r(S)) = 2\left(e^r - 1 - r\right)$, with $r(S) = \ln \frac{S}{S_t}$. Referring to Equation (5.46), $\bar{S} = S(t)$ is set. Under the risk-neutral measure Q, value of the payoff function is

$$E^Q[H(S)] = \frac{1}{B_{t,T}} \int_{S_t}^{+\infty} \frac{2}{K^2} C_{t,T}(K)dK + \frac{1}{B_{t,T}} \int_0^{S_t} \frac{2}{K^2} P_{t,T}(K)dK. \tag{5.47}$$

where $B_{t,T}$ is the time-t price of zero-coupon bond with maturity T.

Based on the previous work, the payoff function for the upside variance swap contract is defined as

$$H^u(S) = \begin{cases} g^v(r(S)), & \text{if } S > S_t, \\ 0, & \text{otherwise.} \end{cases} \tag{5.48}$$

The first order derivative of $H^u(S)$ is

$$H^u_S(S) = \begin{cases} 2\left(\frac{1}{S_t} - \frac{1}{S}\right), & \text{if } S > S_t, \\ 0, & \text{otherwise,} \end{cases}$$

where $H^u_S(S)$ is continuous but not differentiable at $S = S_t$.

The second order derivative of $H^u(S)$ is

$$H^u_{SS}(S) = \begin{cases} \frac{2}{S^2}, & \text{if } S > S_t, \\ 0, & \text{otherwise,} \end{cases}$$

where $H^u_{SS}(S)$ is not continuous at $\bar{S} = S_t$, but it is continuous on $(-\infty, S_t)$ and (S_t, ∞) separately.

Even though $H^u(S)$ is not twice-continuously differentiable at $S = S_t$, it is well defined and the discontinuity will not result in an infinite integral. Therefore, for the upside variance swap, the expected value of the payoff function under risk-neutral measure Q is

$$E^Q[H^u(S)] = \frac{1}{B_{t,T}} \int_{S_t}^{+\infty} \frac{2}{K^2} C_{t,T}(K) dK. \tag{5.49}$$

Likewise, if the payoff function for the downside variance swap contract is defined as

$$H^d(S) = \begin{cases} 0, & \text{if } S > S_t, \\ g^v(r(S)), & \text{otherwise,} \end{cases} \tag{5.50}$$

by taking the second derivative of $H^d(S)$, the expected value of the payoff function is obtained under risk-neutral measure Q

$$E^Q[H^d(S)] = \frac{1}{B_{t,T}} \int_0^{S_t} \frac{2}{K^2} P_{t,T}(K) dK. \tag{5.51}$$

Considering Equation (5.47),

$$E^Q[H(S)] = E^Q[H^u(S)] + E^Q[H^d(S)] \tag{5.52}$$

is obtained.

Equation (5.52) demonstrates that the risk-neutral variance can be decomposed into upside and downside risk-neutral variance, respectively, with the former constructed upon a continuum of out-of-money calls and the latter constructed upon a continuum of out-of-money puts.

As to the decomposition of risk-neutral skew, the same methodology applies. The payoff function for the upside and downside skew swap is defined as

$$H^u(S) = \begin{cases} g^s(r(S)), & \text{if } S > S_t, \\ 0, & \text{otherwise.} \end{cases} \tag{5.53}$$

and

$$H^d(S) = \begin{cases} 0, & \text{if } S > S_t, \\ -g^s(r(S)), & \text{otherwise.} \end{cases} \tag{5.54}$$

By utilizing Equation (5.46), under risk-neutral measure Q, the expected value for $H^u(S)$ and $H^d(S)$ can be expressed by a continuum of out-of-money calls and puts, respectively

$$\begin{aligned} E^Q[H^u(S)] &= \frac{6}{B_{t,T}} \int_{S_t}^{\infty} \frac{K - S_t}{K^2 S_t} C_{t,T}(K) dK, \\ E^Q[H^d(S)] &= \frac{6}{B_{t,T}} \int_{0}^{S_t} \frac{S_t - K}{K^2 S_t} P_{t,T}(K) dK. \end{aligned} \tag{5.55}$$

Therefore, for skew swap contract, the following applies

$$E^Q[H(S)] = E^Q[H^u(S)] - E^Q[H^d(S)]. \tag{5.56}$$

■

Chapter 6

Concluding Remarks

The purpose of this thesis is to add to the understanding of the options market by focusing on three specific new option types. The thesis mainly concentrates on options written on LETFs, on the VIX and on the USO.

Chapter 2 provides an overview of the options markets. Firstly, LETFs and their options market are discussed, on which limited research has been carried out. Most of the studies focus on the dynamics of LETFs, while literature on LETF options is quite rare. Secondly, the specifics of volatility products are explained compared to the traditional assets such as equity. In Chapters 3 and 4, volatility options are analyzed.

In Chapter 3, a pricing framework is first developed for options on LETFs tracking S&P 500 by adopting the Heston (1993) stochastic volatility model and following the work of Zhang (2010). A calibration experiment is performed using different sets of options written on equity LETFs and the results are compared to assess whether they contain consistent information regarding the underlying dynamics. A pricing framework for options on volatility LETFs is developed based upon the work of Bao et al. (2012). Lastly, how to incorporate jump risk into the stochastic volatility models is shown and how option prices can be computed within this extended model, which has not been carried out in previous research. All the results contribute to a better understanding of the LETF option market.

Chapter 4 investigates the higher-order moment risk premiums for the volatility market. This chapter contributes to the literature in two aspects. Firstly, it extends the current literature by also considering the third order moment risk premium, as most of the research performed so far only analyzes the variance risk premium. The results rely heavily on the methodology proposed in Kozhan et al. (2013). Secondly, this chapter is the first to analyze higher moment risk premiums for the volatility market. This is very important as volatility-related products are now actively traded. The empirical findings for the volatility market are different from those of Kozhan et al. (2013), through using the equity index market, and confirm the specifics of the volatility market and the novelty of the results.

Chapter 5 extends the study of higher moment risk premiums to the crude oil market. Moreover, the risk premiums are further decomposed into upside and downside components conditional on the direction of market movement. It is one of the few works in this fast growing field. The decomposed variance and skew risk premiums are found to be more informative than their undecomposed counterparts in predicting future market returns. Especially for skew risk premiums, the decomposition extracts much more information.

This research leads to a few strands of future research. First, how do those higher moment risk premiums relate to each other? Can these risk premiums be decomposed into idiosyncratic components and a common component and their information content analyzed? With respect to the decomposed risk premiums performed in Chapter 5, one further research question is how they depend on the business cycle and, more precisely, to what extent does the explanatory power of these decomposed risk premiums depend on the business cycle.

Bibliography

A. Ahn, M. Haugh, and A. Jain. Consistent pricing of options on leveraged ETFs. *SIAM Journal on Financial Mathematics*, 6(1):559–593, 2015. doi: 10.1137/151003933.

M. Ammann and R. Buesser. Variance risk premiums in foreign exchange markets. *Journal of Empirical Finance*, 23:16–32, 2013. doi: 10.1016/j.jempfin.2013.04.006.

B. An, A. Ang, T. Bali, and N. Cakici. The joint cross section of stocks and options. *The Journal of Finance*, 69(5):22792337, 2014. doi: 10.1111/jofi.12181.

A. Ang, J. Chen, and Y. Xing. Downside Risk. *Review of Financial Studies*, 19(4): 1191–1239, 2006. doi: 10.1093/rfs/hhj035.

M. Avellaneda and S. Zhang. Path dependence of leveraged ETF returns. *SIAM Journal on Financial Mathematics*, 1(1):586–603, 2010. doi: 10.1137/090760805.

G. Bakshi and D. Madan. A theory of volatility spreads. *Management Science*, 52 (12):1945–1956, 2006. doi: 10.1287/mnsc.1060.0579.

G. Bakshi, C. Cao, and Z. Chen. Empirical performance of alternative option pricing models. *Journal of Finance*, 52(5):2003–2049, 1997. doi: 10.1111/j.1540-6261.1997.tb02749.x.

G. Bakshi, N. Kapadia, and D. Madan. Stock return characteristics, skew laws, and the differential pricing of individual equity options. *Review of Financial Studies*, 16(1):101–143, 2003. doi: 10.1093/rfs/16.1.0101.

Q. Bao, S. Li, and D. Gong. Pricing VXX Option with Default Risk and Positive Volatility Skew. *European Journal of Operational Research*, 223:246–255, 2012. doi: 10.1016/j.ejor.2012.06.006.

C. Bardgett, E. Gourier, and M. Leippold. Inferring Volatility Dynamics and Risk Premia from the S&P 500 and VIX Markets. *Working Paper-SSRN.2296826*, 2017.

O. E. Barndorff-Nielsen, S. Kinnebrock, and N. Shephard. Measuring downside risk-realised semivariance. *CREATES Research Paper*, (2008-42), 2008.

D. Bates. Jumps and Stochastic Volatility: Exchange Rate Processes Implicit in Deutsche Mark Options. *Review of Financial Studies*, 1(9):69–107, 1996.

D. Bates. Post-'87 Crash Fears in the S&P 500 Futures Option Market. *Journal of Econometrics*, 94:181–238, 2000. doi: 10.3386/w5894.

P. Bertrand and J. Prigent. Portfolio Insurance Strategies: A Comparison of Standard Methods When the Volatility of the Stock is Stochastic. *International Journal of Business*, 8(4):461–472, 2003.

F. Black and A. Perold. Theory of constant proportion portfolio insurance. *Journal of Economic Dynamics & Control*, 16(3):403–426, 1992.

T. Bollerslev, G. Tauchen, and H. Zhou. Expected stock returns and variance risk premia. *Review of Financial Studies*, 22(11):4463–4492, 2009. doi: 10.1093/rfs/hhp008.

T. Bollerslev, V. Todorov, and L. Xu. Tail risk premia and return predictability. *Journal of Financial Economics*, 118:113–134, 2015. doi: 10.1016/j.jfineco.2015.02.010.

N. Branger, A. Kraftschik, and C. Völkert. The Affine Structure of Variance: Pricing VIX Derivatives in Consistent and Log-VIX Models. *Working Paper-SSRN.2028285*, 2016.

M. Broadie, M. Chernov, and M. Johannes. Model Specification and Risk Premia: Evidence from Futures Options. *The Journal of Finance*, 62(3):1453–1490, 2007. doi: 10.1111/j.1540-6261.2007.01241.x.

S. J. Byun and J. S. Kim. The information content of risk-neutral skewness for volatility forecasting. *Journal of Empirical Finance*, 23:142–161, 2013. doi: 10.1016/j.jempfin.2013.05.006.

P. Carr and D. Madan. Towards a theory of volatility trading. *in R. Jarrow (ed.), Risk Book on Volatility*, pages 417–427, 1998.

P. Carr and D. Madan. Option valuation using the Fast Fourier Transform. *Journal of Computational Finance*, 2(4):61–73, 1999.

P. Carr and L. Wu. Variance Risk Premiums. *Review of Financial Studies*, 22(3):1131–41, 2009. doi: 10.1093/rfs/hhn038.

J. Chevallier and B. Sévi. On the volatility-volume relationship in energy futures markets using intraday data. *Energy Economics*, 34(6):1896–1909, 2012. doi: http://dx.doi.org/10.1016/j.eneco.2012.08.024.

J. Chevallier and B. Sévi. A fear index to predict oil futures returns. *Energy Studies Review*, 20(3):1–17, 2013. doi: 10.15173/esr.v20i3.552.

J. Da Fonseca and M. Grasselli. Riding on the Smiles. *Quantitative Finance*, 11:1609–1632, 2011. doi: 10.1080/14697688.2011.615218.

G. Deng, T. Dulaney, C. McCann, and M. Yan. Crooked Volatility Smiles: Evidence from Leveraged and Inverse ETF Options. *Journal of Derivatives and Hedge Funds*, 19:278–294, 2014. doi: 10.1057/jdhf.2014.3.

E. Derman, I. Kani, and M. Kamal. Trading and hedging local volatility. *Journal of Financial Engineering*, 6(3):233–268, 1997.

J. Detemple and C. Osakwe. The valuation of volatility options. *European Finance Review*, 4(1):21–50, 2000. doi: 10.1023/A:1009814324980.

J.-C. Duan and W. Zhang. Forward-looking market risk premium. *Management Science*, 60(2):521–538, 2014. doi: 10.1287/mnsc.2013.1758.

D. Duffie, J. Pan, and K. Singleton. Transform Analysis and Asset Pricing for Affine Jump-Diffusion. *Econometrica*, 68(6):1343–1376, 2000. doi: 10.1111/1468-0262.00164.

B. Eraker. Do Stock Prices and Volatility Jump? Reconciling Evidence from Spot and Option Prices. *The Journal of Finance*, 59(3):1367–1404, 2004. doi: 10.1111/j.1540-6261.2004.00666.x.

B. Eraker, M. Johannes, and N. Polson. The Impact of Jumps in Volatility and Returns. *The Journal of Finance*, 58(3):1269–1300, 2003. doi: 10.1111/1540-6261.00566.

J. Fleming. The quality of market volatility forecasts implied by S&P 100 index option prices. *Journal of Empirical Finance*, 5:317–345, 1998. doi: 10.1016/S0927-5398(98)00002-4.

M. Forde and A. Jacquier. Small-time Asymptotic s for Implied Volatility under the Heston Model. *International Journal of Theoretical and Applied Finance*, 12(6): 861–876, 2009.

S. Gehricke and J. Zhang. Modeling VXX. *forthcoming Journal of Futures Markets*, 2014.

A. Grünbichler and F. Longstaff. Valuing futures and options on volatility. *Journal of Banking and Finance*, 20:985–1001, 1996. doi: 10.1016/0378-4266(95)00034-8.

M. Haugh. A Note on Constant Proportion Trading Strategies. *Operations Research Letters*, 39:172–179, 2011. doi: 10.1016/j.orl.2011.03.005.

S. Heston. A closed-form solution for options with stochastic volatility with applications to bond and currency options. *Review of Financial Studies*, 6(2):327–343, 1993. doi: 10.1093/rfs/6.2.327.

D. Huang and I. Shaliastovich. Volatility-of-volatility risk. *WorkingPaper SSRN-2497759*, 2014.

J. Hull and A. White. The Pricing of Options on Assets with Stochastic Volatilities. *The Journal of Finance*, 42(2):281–300, 1987. doi: 10.1111/j.1540-6261.1987.tb02568.x.

R. Jarrow. Understanding the risk of leveraged ETFs. *Finance Research Letters*, 7: 135–139, 2010. doi: 10.1016/j.frl.2010.04.001.

T. Johnson and E. So. The option to stock volume ratio and future returns. *Journal of Financial Economics*, 106(2):262–286, 2012. doi: 10.1016/j.jfineco.2012.05.008.

J. W. Jurek and Z. K. Xu. Option-implied currency risk premia. *WorkingPaper SSRN-2338585*, 2014. doi: 10.2139/ssrn.2338585.

A. Kaeck and C. Alexander. VIX Dynamics with Stochastic Volatility of Volatility. *Working Paper*, 2010.

M. Kilic and I. Shaliastovich. Good and bad variance premia and expected returns. *Working Paper*, 2015.

E. Konstantinidi and G. Skiadopoulos. How does the market variance risk premium vary over time? Evidence from S&P 500 variance swap investment returns. *Journal of Banking & Finance*, 62:6275, 2016. doi: 10.1016/j.jbankfin.2015.10.006.

A. Kostakis, N. Panigirtzoglou, and G. Skiadopoulos. Market timing with option-implied distributions: A forward-looking approach. *Management Science*, 57(7): 1231–1249, 2011. doi: 10.1287/mnsc.1110.1346.

R. Kozhan, A. Neuberger, and P. Schneider. The Skew Risk Premium in the Equity Index Market. *Review of Financial Studies*, 26(9):2174–2203, 2013. doi: 10.1093/rfs/hht039.

M. Lettau, M. Maggiori, and M. Weber. Conditional risk premia in currency markets and other asset classes. *Journal of Financial Economics*, 114(2):197–225, 2014. doi: http://dx.doi.org/10.1016/j.jfineco.2014.07.001.

T. Leung and R. Sircar. Implied Volatility of Leveraged ETF Options. *Applied Mathematical Finance*, 22(2):162–188, 2015. doi: 10.1080/1350486X.2014.975825.

T. Leung, M. Lorig, and A. Pascucci. Leveraged ETF Implied Volatilities from ETF Dynamics. *Working Paper*, 2014.

G.-H. Lian and S.-P. Zhu. Pricing VIX options with stochastic volatility and random jumps. *Decisions in Economics and Finance*, 36(1):71–88, 2013. doi: 10.1007/s10203-011-0124-0.

L. Lu, J. Wang, and G. Zhang. Long Term Performance of Leveraged ETFs. *SSRN Electronic Journal*, 2009. doi: 10.2139/ssrn.1344133.

H. Lustig, N. Roussanov, and A. Verdelhan. Common risk factors in currency markets. *The Review of Financial Studies*, 24(11):3731–3777, 2011. doi: 10.1093/rfs/hhr068.

J. Mencía and E. Sentana. Valuation of VIX derivatives. *Journal of Financial Economics*, 108:367–391, 2013. doi: 10.1016/j.jfineco.2012.12.003.

A. Neuberger. Realized Skewness. *Review of Financial Studies*, 25(11):3423–3455, 2012. doi: 10.1093/rfs/hhs101.

M. Neumann and G. Skiadopoulos. Predictable dynamics in higher order risk-neutral moments: Evidence from the S&P 500 options. *Journal of Financial and Quantitative Analysis*, 48(3):947–977, 2013. doi: 10.1017/S002210901300032X.

W. Newey and K. West. A simple positive semidefinite, heteroscedasticity and autocorrelation consistent covariance matrix. *Econometrica*, 55(3):703–708, 1987. doi: 10.2307/1913610.

Y.-H. Park. The effects of asymmetric volatility and jumps on the pricing of VIX derivatives. *Journal of Econometrics*, 192(1):313–328, 2016. doi: 10.1016/j.jeconom.2016.01.001.

A. Patton and K. Sheppard. Good volatility, bad volatility: Signed jumps and the persistence of volatility. *Review of Economics and Statistics*, 97:683–697, 2015. doi: 10.1162/REST_a_00503.

M. Prokopczuk and C. Wese Simen. Variance risk premia in commodity markets. *WorkingPaper SSRN-2195691*, 2014. doi: 10.2139/ssrn.2195691.

A. Sepp. VIX option pricing in a jump-diffusion model. *Risk Magazine*, 2:84–89, 2008.

B. Sévi. Forecasting the volatility of crude oil futures using intraday data. *European Journal of Operational Research*, 235(3):643 – 659, 2014. ISSN 0377-2217. doi: 10.1016/j.ejor.2014.01.019.

A. Trolle and E. Schwartz. Variance risk premia in energy commodities. *Journal of Derivatives*, 17(3):15–32, 2010.

R. E. Whaley. Derivatives on market volatility: Hedging tools long overdue. *The Journal of Derivatives*, 1:71–84, 1993.

B. Yang, P. Christoffersen, and K. Jacobs. Market skewness risk and the cross section of stock returns. *Journal of Financial Economics*, 107(1):46–68, 2013. doi: 10.1016/j.jfineco.2012.07.002.

J. Zhang. Path-Dependence Properties of Leveraged Exchange-Traded Funds: Compounding, Volatility and Options Pricing. *PhD thesis, New York University*, 2010.

J. E. Zhang and Y. Zhu. VIX futures. *Journal of Futures Markets*, 26(6):521–531, 2006. doi: 10.1002/fut.20209.

J. E. Zhang, J. Shu, and M. Brenner. The new market for volatility trading. *Journal of Futures Markets*, 30(9):809–833, 2010. doi: 10.1002/fut.20448.

H. M. Zhao, J. E. Zhang, and E. C. Chang. The relation between physical and risk-neutral cumulants. *International Review of Finance*, 13(3):345–381, 2013. doi: 10.1111/irfi.12013.

Y. Zhu and J. E. Zhang. Variance term structure and VIX futures pricing. *International Journal of Theoretical and Applied Finance*, 10(1):111–127, 2007. doi: 10.1142/S0219024907004123.